

**Id4 functions downstream of Bmp signaling to restrict
TCF function in endocardial cells during atrioventricular
valve development**



MAX-PLANCK-GESELLSCHAFT

Dissertation
zur Erlangung des Doktorgrades
der Naturwissenschaften

vorgelegt beim Fachbereich 15
der Johann Wolfgang Goethe-Universität
in Frankfurt am Main

Von
Suchit Ahuja
aus Neu Delhi, Indien

Frankfurt 2016
(D30)

Vom Fachbereich der

Goethe Universität als Dissertation angenommen.

Dekan:

Gutachter:

Datum der Disputation:

SUPERVISED BY

Dr. Sven Reischauer, Ph.D.
Department of Developmental Genetics
Max Planck Institute for Heart and Lung Research
Bad Nauheim, Germany

REVIEWER

Prof. Dr. Didier Stainier, Ph.D.
Department of Developmental Genetics
Max Planck Institute for Heart and Lung Research
Bad Nauheim, Germany

and

Prof. Dr. Anna Starzinski-Powitz, Ph.D.
Department of Molecular Cell Biology and Human Genetics
Institute of Cell Biology and Neuroscience
Johann Wolfgang Goethe University
Frankfurt am Main, Germany

ERKLÄRUNG

Ich erkläre hiermit, dass ich mich bisher keiner Doktorprüfung im Mathematisch-Naturwissenschaftlichen Bereich unterzogen habe.

Frankfurt am Main, den

.....

(Unterschrift)

Versicherung

Ich erkläre hiermit, dass ich die vorgelegte Dissertation über

Id4 functions downstream of Bmp signaling to restrict TCF function in endocardial cells during atrioventricular valve development

selbständig angefertigt und mich anderer Hilfsmittel als der in ihr angegebenen nicht bedient habe, insbesondere, dass alle Entlehnungen aus anderen Schriften mit Angabe der betreffenden Schrift gekennzeichnet sind.

Ich versichere, die Grundsätze der guten wissenschaftlichen Praxis beachtet, und nicht die Hilfe einer kommerziellen Promotionsvermittlung in Anspruch genommen zu haben.

Vorliegende Ergebnisse der Arbeit sind in folgendem Publikationsorgan veröffentlicht:

Ahuja S, et al. Dev. Biol. 2016; 412(1): 71-82. Id4 functions downstream of Bmp signaling to restrict TCF function in endocardial cells during atrioventricular valve development.

Frankfurt am Main, den

.....

(Unterschrift)

You have to dream before your dreams can come true.

Man needs his difficulties because they are necessary to enjoy success.

Great dreams of great dreamers are always transcended.

A.P.J. Abdul Kalam
Aerospace Scientist
1931-2015

Table of Contents

Abbreviations	11
1. Introduction	14
1.1 Congenital Heart Disease	14
1.2 Heart Valve Development	16
1.2.1 Origin Of Valvular Cells: Contribution From Different Heart Layers.....	17
1.2.2 Endocardial Cushion Formation: Signaling Molecules Involved.....	17
1.3 Zebrafish Heart Development	22
1.4 Zebrafish Atrioventricular Canal/Valve Development.....	25
1.5 Inhibitor of DNA Binding 4 (Id4)	27
1.6 AIM of the Project	29
2. Materials	30
2.1 Antibiotics	30
2.2 Antibodies	30
2.3 Bacterial Culture medium.....	31
2.4 Bacterial Strains.....	31
2.5 Buffers/Solutions	31
2.6 Centrifuges	33
2.7 Chemicals.....	34
2.8 Enzymes	36
2.9 Kits	37
2.10 Microscopes	37
2.11 Miscellaneous Equipment.....	38
2.12 Oligonucleotides	40
2.13 PCR enzymes and mastermix	41
2.14 Plasmids	42
2.15 Softwares.....	43

2.16	Tubes and containers.....	43
2.17	Zebrafish Food.....	44
2.18	Zebrafish Lines	44
3.	Methods	45
3.1	Zebrafish Husbandry	45
3.1.1	Zebrafish Maintenance	45
3.1.2	Zebrafish Breeding	45
3.2	Zebrafish Microinjection	45
3.2.1	Preparation of Injection plates.....	45
3.2.2	Preparation of Injection Needles	46
3.2.3	Microinjection	46
3.3	RNA Isolation.....	46
3.4	Reverse Transcription or cDNA Synthesis	46
3.5	PCR amplification from cDNA.....	47
3.6	Agarose Gel Electrophoresis.....	47
3.7	PCR Product Elution From Agarose Gel	48
3.8	E.Coli Competent Cells Preparation.....	48
3.9	Transformation of Competent E.Coli	48
3.10	DNA Restriction Digestion.....	48
3.11	Cloning	49
3.11.1	TA Cloning.....	49
3.11.2	Cold Fusion	49
3.11.3	Cloning <i>id4</i> Overexpression Constructs	50
3.12	Plasmid DNA Isolation	50
3.13	In situ Hybridisation.....	50
3.13.1	Probe Synthesis	50
3.13.2	Embryo/Adult Heart preparation for in situ hybridization	51
3.13.3	In situ Hybridization Day 1: Probe Hybridization.....	51
3.13.4	In situ Hybridization Day 2: Unbound Probe Removal.....	52
3.13.5	In situ Hybridization Day 3: Unbound Antibody Removal and Staining.....	53
3.13.6	In situ Hybridization: Microscopy and Imaging	53

3.14	TALEN (Transcription Activator-Like Effector Nucleases) Induced Mutagenesis	53
3.14.1	TALEN Designing.....	53
3.14.2	TALEN Assembly Day 1	54
3.14.3	TALEN Assembly Day 2	54
3.14.4	TALEN Assembly Day 3	55
3.14.5	TALEN Assembly Day 4	56
3.14.6	Talen Assembly Day 5	56
3.14.7	TALEN mRNA Synthesis	56
3.15	Heat Shock Experiments	57
3.15.1	Heat Stress of <i>id4</i> ^{-/-}	57
3.15.2	Heat Shock of <i>Tg(hsp70l:bmp2b)</i> or <i>id4</i> ^{-/-} / <i>Tg(hsp70l:bmp2b)</i>	57
3.16	Whole mount Immunohistochemistry	57
3.17	High Resolution Melt (HRM) Analysis	58
3.18	Statistical analysis	59
3.19	Imaging	59
3.19.1	Live Imaging Spinning Disk Microscopy	59
3.19.2	Imaging with confocal microscope LSM 700/780	59
3.20	Image Processing	59
3.21	Bmp signaling inhibition	60
4.	Results.....	61
4.1	<i>id4</i> is expressed in the developing AVC endocardium and the adult atrium..	61
4.2	Generation of <i>id4</i> mutants using TALEN Technology	63
4.3	<i>id4</i> mutants are susceptible to stress induced retrograde blood flow at the AV canal.	64
4.4	<i>id4</i> mutants exhibit reduction and mis-regulation of developmental markers of the atrioventricular canal and cardiac valve.....	66
4.5	<i>id4</i> mutants show expanded Alcam expression	67
4.6	Id4 is a mediator of Bmp signaling leading to <i>spp1</i> expression.....	69
4.7	<i>id4</i> mutants have higher Wnt/ β -Catenin activity in the AV Canal.	72
4.8	Higher Wnt/ β -Catenin activity leads to impaired AV canal development.	73
4.9	Id4 negatively regulates Wnt/TCF function in endocardial cells.	74

4.10	Endothelial re-expression of <i>id4</i> in <i>id4</i> mutants can partially rescue their valve developmental defects.....	76
4.11	Notch signaling appears unaffected in <i>id4</i> mutants.	78
5.	Discussion.....	79
5.1	Previously reported knowledge on AV Canal development and significance of this study.....	79
5.2	<i>id4</i> : current state of knowledge	80
5.3	<i>id4</i> mutants are phenotypically indistinguishable from their siblings but respond abnormally to cardiac stress	81
5.4	<i>id4</i> mutants have mis-regulated cardiac valve developmental markers.....	81
5.5	Id4 mediates Bmp signaling leading to <i>spp1</i> expression.....	82
5.6	Id4 restricts Wnt signaling in the developing AVC endocardium.....	83
6.	Conclusion.....	85
6.1	Proposed Model.....	85
I	GERMAN SUMMARY.....	86
	Einführung.....	86
	Ergebnisse und Diskussion.....	89
	Zusammenfassung und Ausblick.....	92
II	ENGLISH SUMMARY.....	93
	Introduction	93
	Results and Discussion	94
	Conclusion.....	96
III	REFERENCES.....	97
	ACKNOWLEDGEMENTS.....	108
	Curriculum Vitae.....	109

Abbreviations

ALPM	Anterior lateral plate mesoderm
AMP	Adenosine monophosphate
AP	Alkaline phosphatase
AS	Aortic Stenosis
ASD	Atrial Septal Defect
ATP	Adenosine triphosphate
AV	Atrioventricular
AVC	Atrioventricular Canal
AVSD	Atrioventricular Septal defect
bHLH	Basic Helix loop Helix
BMP	Bone morphogenetic protein
BSA	Bovine serum albumin
CaCl ₂	Calcium Chloride
cDNA	Complementary DNA
cds	Coding sequence
CHD	Congenital Heart Disease
<i>clo</i>	Cloche
CoA	Coarctation of Aorta
dH ₂ O	Distilled Water
DEPC	Diethylpyrocarbonate
DMSO	Dimethyl sulfoxide
DNA	Deoxyribonucleic acid
dNTP	Deoxyribonucleotide triphosphate
dpf	Days post fertilization
E	Embryonic day
EC	Endocardial Cushion
ECM	Extracellular Matrix
E.Coli	Escherichia coli
EDTA	Ethylenediaminetetraacetic acid
EGFP	Enhanced Green fluorescent protein
EMT	Epithelial-Mesenchymal Transition
ERK	Extracellular receptor kinase
EST	Expressed sequence tag
EtBr	Ethidium Bromide
FCS	Fetal Calf Serum
<i>g</i>	Acceleration of gravity
g	Gram
GFP	Green Fluorescent Protein
GSK	Glycogen Synthase Kinase
HA	Hyaluronic Acid
Has	Hyaluronan Synthase
HCl	Hydrochloric Acid
hpf	Hours post fertilization
HRM	High Resolution Melt
HRP	Horse Raddish peroxidase
IPTG	Isopropyl-D-1thiogalactopyranoside
KDa	Kilodalton

Abbreviations

KCl	Potassium Chloride
KH ₂ PO ₄	Potassium dihydrogen phosphate
l	Liter
LB	Luria Broth
ICC	Immunocytochemistry
IFT	Inflow Tract
IHC	Immunohistochemistry
m	Molar
mg	Milligram
MHC	Myosin Heavy chain
mins	Minutes
ml	Milliliter
mM	Millimol
MMLV	Moloney murine leukemia virus
mRNA	Messenger RNA
MgCl ₂	Magnesium Chloride
mpf	months post fertilization
<i>myh6</i>	myosin heavy chain 6, cardiac muscle, alpha
<i>myl7</i>	cardiac myosin light chain 7
NaCl	Sodium Chloride
NaN ₃	Sodium azide
Na ₂ HPO ₄	Disodium hydrogen phosphate
NaOH	Sodium Hydroxide
ng	Nanogram
NICD	Notch intracellular domain
nls	nuclear localization signal
OD	Optical Density
OFT	Outflow Tract
P	Postnatal Day
PBS	Phosphate Buffered Saline
PCR	Polymerase Chain Reaction
PDA	Patent Ductus Arteriosus
PKA	Protein Kinase A
PTU	N-Phenylthiourea
pH	Negative log of hydrogen ion concentration
q.s.	quantum sufficit
RNA	Ribonucleic Acid
RNase	Ribonuclease
rpm	Revolutions per minute
RT	Room temperature
RT-PCR	Reverse Transcription – PCR
RVD	Repeat-variable di-residue
secs	seconds
sem	Standard error of mean
Taq	<i>Thermus aqaticus</i>
TAE	Tris-acetate-EDTA
TALLEN	Transcription Activator-Like Effector Nucleases
TBE	Tris-borate-EDTA
TBS	Tris buffered saline

Abbreviations

TE	Tris-EDTA
TOF	Tetralogy of Fallot
TGF β	Transforming Growth Factor β
TGA	Transposition of the Great Arteries
Tricane	Ethyl-m-aminobenzoate methanesulfonate
tRNA	Transfer RNA
U	Unit
UTR	Untranslated Region
UV	Ultraviolet
V	Volt
<i>vmhc</i>	Ventricular myosin heavy chain
VSD	Ventricular Septal Defect
W	Watt
Wt	wild-type
X-gal	5-bromo-4-chloro-3-indolyl-D-galactopyranoside
μ l	microliter
μ m	micromolar

1. Introduction

1.1 Congenital Heart Disease

Congenital Heart Disease (CHD) refers to defects in the heart of the new born. It is one of the major causes of infant morbidity and mortality. Approximately 1.3 million children are born annually with CHD worldwide (Hoffman, 2013). Based on the type of defect it leads to, CHDs can be classified (Bruneau, 2008) as follows:

- a. **Acyanotic heart anomalies:** This category includes atrial septal defects, ventricular septal defects and atrioventricular septal defects. Defective septum formation leads to mixing of oxygenated and de-oxygenated blood, which results in pressure overload on the ventricles leading to heart failure. Patent Ductus Arteriosus (PDA) is another defect of this category. This also results in mixing of oxygenated and de-oxygenated blood between aorta and pulmonary artery respectively.
- b. **Cyanotic Heart Anomalies:** In this category, the deoxygenated blood enters the systemic circulation bypassing the lungs. Such a condition leads to cyanosis, i.e appearance of bluish coloration on the skin of affected individual. Defects contributing to such a condition are tricuspid atresia, tetralogy of Fallot, transposition of the great arteries, pulmonary atresia, Ebstein's anomaly of the tricuspid valve, persistent truncus arteriosus, double outlet right ventricle, and total anomalous pulmonary venous connection.
- c. **Left Sided Heart Obstructive lesions:** These defects lead to obstruction in the systemic outflow of blood from the left ventricle. Deformities leading to such condition include hypoplastic left heart syndrome, coarctation of the aorta and aortic stenosis.

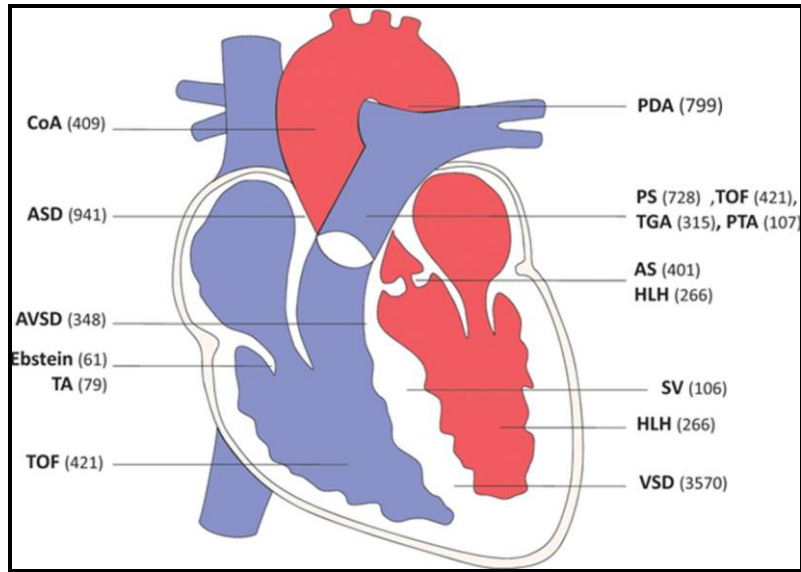


Figure 1.1: (adapted from (Fahed et al., 2013)) Locations of various congenital heart malformations and their approximate incidence. Numbers are indicative of birth prevalence per million live births. AS (Aortic Stenosis), ASD (Atrial Septal Defect), AVSD (AtrioVentricular Septal Defect), CoA (Coarctation of Aorta), Ebstein (Ebstein anomaly), HLH (Hypoplastic Left Heart), MA (Mitral Atresia), PDA (Patent Ductus Arteriosus), PS (Pulmonary Stenosis), PTA (Persistent Truncus Arteriosus), TA (Tricuspid Atresia), TGA (Transposition of the Great Arteries), SV (Single Ventricle), TOF (Tetralogy of Fallot) and VSD (Ventricular Septal Defect).

The AVC/Valve associated congenital malformations account for approximately 10% of total CHDs reported in live births (Fahed et al., 2013). Several genetic mutations have been reported to be contributing to congenital valve malformations. *Notch1* is an endocardial gene which critically regulates valve formation (Timmerman et al., 2004). Mutations in *Notch1* have been reported to cause disease conditions like Bicuspid Aortic Valve (Garg et al., 2005). Marfan's syndrome is another example in which valve abnormality is reported. It is caused by mutations in *Fibrillin-1* gene and the clinical manifestations include mitral valve prolapse and valvular regurgitation (Robinson et al., 2002; Ramachandra et al., 2015). Abnormalities of valve development have also been reported in case of noonan's syndrome, which is caused by mutations in *PTPN11* (Tartaglia et al., 2001; Bruneau, 2008). Mitral valve prolapse and pulmonary valve stenosis are typical valvular defects seen in case of noonan's syndrome (Tartaglia and Gelb, 2005).

Genetic Mutation	Syndrome Name	Cardiac Disease
Nonsyndromic		
NKX2-5	—	Atrial septal defect, ventricular septal defect, electrical conduction defect
GATA4	—	Atrial septal defect, ventricular septal defect
MYH6	—	Atrial septal defect
NOTCH1	—	Aortic valve disease
Syndromic		
TBX5	Holt-Oram	Atrial septal defect, ventricular septal defect, electrical conduction defect
TBX1	DiGeorge	Cardiac outflow tract defect
TFAP2 β	Char	Patent ductus arteriosus
JAG1	Alagille	Pulmonary artery stenosis, tetralogy of Fallot
PTPN11	Noonan	Pulmonary valve stenosis
Elastin	William	Supravalvar aortic stenosis
Fibrillin	Marfan	Aortic aneurysm

Table 1.1: (adapted from (Srivastava, 2006)) Summarizing the list of genes contributing to congenital heart defects

Thus there is quite a bit of evidence suggesting that abnormalities in valve development are also genetically manifested. However, the underlying mechanisms involved in these disorders remain largely unknown. So, it is important to study valve development carefully and find out novel genes that contribute to this process. Here, I describe an unreported expression and function of *id4*, inhibitor of DNA Binding 4 in AV Canal/ Valve and the possible mechanism by which it regulates valve function.

1.2 Heart Valve Development

The Atrioventricular Canal (AVC) acts as a bridge between atrium and ventricle in the vertebrate heart. It harbors the valves to maintain uni-directional flow of blood from atrium to ventricle. To regulate the blood flow, the heart valves open and close approximately 3 billion times in an average human life span (Schoen, 2008). The onset of valve development is marked by appearance of endocardial cushions in the primitive heart tube (Schroeder et al., 2003). During the course of development the valves continue to grow into fibrous leaflets with increased ECM deposition and remodeling (Hinton et al., 2006). In the developmental phase, the valve progenitor cells in the endocardial cushions are highly proliferative as compared to mature valves which show little to no cell proliferation (Hinton et al., 2006; Lincoln et al., 2004).

1.2.1 Origin Of Valvular Cells: Contribution From Different Heart Layers

The organization and stratification of adult valve leaflets is conserved between humans, mice sheep, rabbits and chickens (Hinton et al., 2006). The cell lineage studies done in mammals based on *alphaMHC-Cre* (myocardial), *Tie2-Cre* (endocardial) and *Wnt1-Cre* (neural crest) expressing cells during development, reveal that majority of cells contributing to heart valves are of endothelial/endocardial origin (de Lange et al., 2004). However, there are some evidence based on experiments based on *Wt1-Cre* and *Tbx18-Cre* suggesting that cells of epicardial origin are also present cardiac valves (Cai et al., 2008; Zhou et al., 2008).

1.2.2 Endocardial Cushion Formation: Signaling Molecules Involved

Swellings in the AVC are the first sign of the development of endocardial cushions in the looping heart in chick, mouse and human (Fishman and Chien, 1997; Moorman, 2003; Martinsen, 2005). Signaling from the myocardium causes inhibition of chamber specific gene expression in the AVC and also leads to increased production of ECM proteins in the region of cardiac jelly (Lyons et al., 1990; Harrelson et al., 2004; Plageman and Yutzey, 2004; Ma et al., 2005). This increase in ECM proteins causes the endocardial tissue to swell and protrude in the lumen of developing heart (Henderson and Copp, 1998; Camenisch et al., 2000).

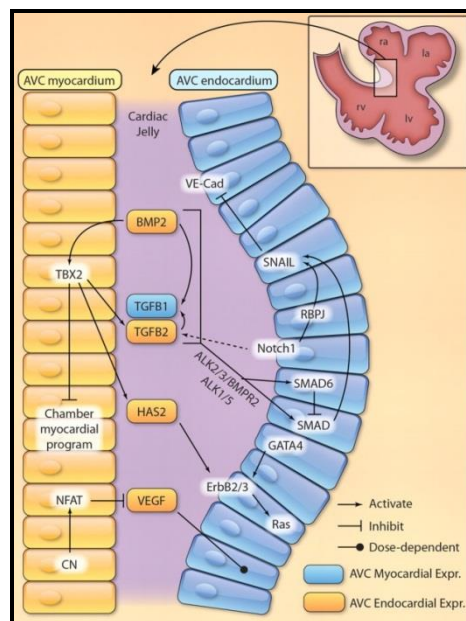


Figure 1.2: (adapted from (von Gise and Pu, 2012)) Molecular signals involved in endocardial cushion EMT. Complex signaling interplay between AVC myocardium, endocardium and cardiac jelly during endocardial cushion EMT and valve formation.

Endocardial cushion formation and EMT (Epithelial - Mesenchymal Transition) occurs due to the signals from both endocardium and myocardium. During EMT, the endocardial cells break the cell junctions with neighboring cells and migrate to populate the cushions with the mesenchymal cells (von Gise and Pu, 2012). The signaling events leading to cushion formation in OFT are nearly similar to those in AVC, with the only difference that OFT cushions are formed 1 day later than AVC cushions (Camenisch et al., 2002; Délot, 2003).

Role Of TGF β /BMP Signaling

BMPs belong to the TGF- β super family and are indispensable for cardiac valve development. BMP2, 4, 5, 6 and 7 have been shown to be crucial for EMT in AVC or OFT (Nakajima et al., 2000; Somi et al., 2004). BMP2 is expressed in AVC myocardium at the onset of EMT after which the expression shifts to cushion mesenchyme. BMP2 null mice fail to express *Tbx2* in the AVC, which is required to inhibit the activation of chamber specific gene program in the AVC (Harrelson et al., 2004; Kokubo et al., 2007; Ma et al., 2005). BMP2 has also been shown previously to induce endocardial EMT in ventricular explants where it is not required, so it is important that *Bmp2* expression remains restricted to AVC myocardium (Luna-Zurita et al., 2010). This can be due the expansion of *Tbx2* expression which is a direct target of BMP2 and can direct the expression of EMT inducing genes (*Tgfb2* and *Has2*) in ventricular explants (Shirai et al., 2009). *Bmp4* in mice is not expressed at the onset of AV endocardial cushion development but at the later stages of valve development (Jiao et al., 2003; McCulley et al., 2008). Its expression in OFT myocardium is more prominent than AV myocardium (Jiao et al., 2003; McCulley et al., 2008). Mice lacking *Bmp4* show AVC and atrial septal defects, in addition to, defect in OFT cushion formation (Jiao et al., 2003; McCulley et al., 2008). BMP5, 6 and 7 null hearts have normal development, however the double mutants have problems in OFT endocardial cushion formation (Kim et al., 2001; Yamagishi et al., 2009). Some of them also show defective valve morphogenesis and chamber septation (Kim et al., 2001; Yamagishi et al., 2009). The data generated from endothelial specific deletion of Bmp receptors also supports the argument that BMP signaling is crucial for AVC development. Targeted deletion of *Bmp receptor-1a* in the mice endocardium leads to defective EMT, failed cushion formation and reduced to no phospho-Smad1/5/8 activity in the AVC of mutant mice (Ma et al., 2005). Similar consequences of impaired AV cushion

development were also observed in mice with endothelial specific deletion of receptors *Alk2* and *Alk3* (Song et al., 2007; Wang et al., 2005).

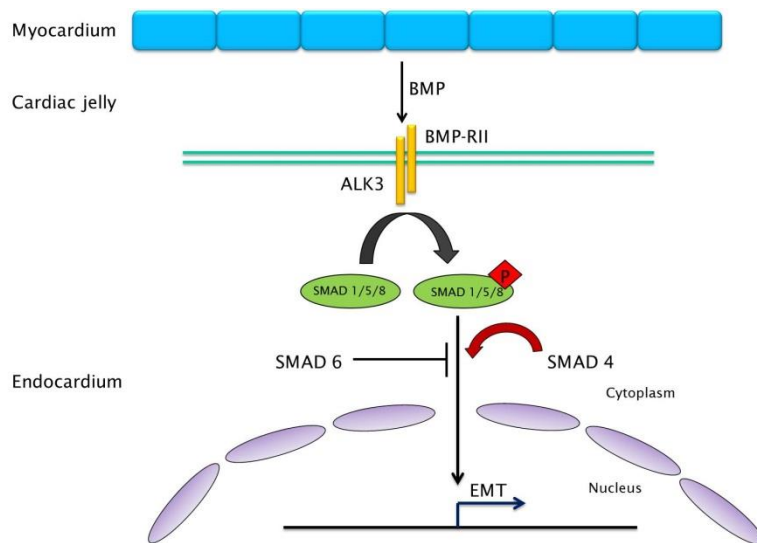


Figure 1.3: BMP Signaling in Valve Development. BMP ligands are secreted from the myocardium and bind to ALK3/BMPRII heterodimeric receptors on the endocardium. Binding of BMP leads to phosphorylation of SMAD1/5/8. This phospho-SMAD1/5/8 forms a complex with SMAD4 and translocate into nucleus to activate gene transcription important for EMT. SMAD4 also aids a cross-talk between BMP and TGF- β signal transduction pathways. SMAD6, on the contrary, prevents the interaction between phospho-SMAD1/5/8 and SMAD4, therefore decreases BMP signaling.

Defective *Bmp* signaling results in downregulation of various transcription factors involved in AVC cushion development like *Snai1*, *Twist1* and *Msx1* (Ma et al., 2005; Wang et al., 2005). SMADs are downstream effectors and crucial mediators of TGF β /BMP signaling. SMADs mediate BMP signals leading to activation of *Tbx2* critical for AVC specification (Shirai et al., 2009). SMAD4 physically interacts with GATA4 and regulates EMT and cushion formation in AVC development (Moskowitz et al., 2011). In contrast to SMAD4 disrupted mice which display absence of valve forming activities, the SMAD6 mutant mice show heart valve hyperplasia and excessive mesenchymal cells (Galvin et al., 2000; Moskowitz et al., 2011). In the light of all the aforementioned data, it can be concluded that, BMP signaling is crucial for cardiac valve development.

Role Of NOTCH Signaling

Notch signaling plays an important role in heart valve development. NOTCH is a transmembrane receptor (NOTCH1-NOTCH4) with a single-pass transmembrane domain, an extracellular domain and a Notch intracellular domain (NICD). Signaling takes place when Notch ligands (*Jagged1/2* or *Delta1/3/4*) expressed on the surface of another cell interact with Notch receptor, leading to cleavage and nuclear translocation of NICD (MacGrogan et al., 2011). In the nucleus, NICD binds to RBPJ converting it from repressor to activator (Fortini

and Artavanis-Tsakonas, 1994). The bHLH transcription factors HES and HEY are established Notch targets (MacGrogan et al., 2011).

In situ hybridization and immunostaining experiments have revealed that, during EMT *Notch1* and *Delta4* are expressed in the endocardial cushions of AVC and OFT (Del Monte et al., 2007; Timmerman et al., 2004). *Notch1* or *RBPJ* null mice have reduced expression of pro-EMT genes like *Snail1* and *Tgfb2*. Reduced *Snail1* expression prevents downregulation of VE-Cadherin (endothelial cell adhesion molecule) thereby inhibiting endocardial EMT (Timmerman et al., 2004). The experiments done with *Notch1* gain of function further confirm the importance of notch signaling during EMT. The ventricular explants from *Notch1* overexpressing mice show the expression of EMT inducing genes like *Tgfb2*, *Snail1* and *Snail2* but fail to invade the gel matrix in collagen gel assays (Luna-Zurita et al., 2010). However upon addition of BMP2, these cells show complete EMT, suggesting that a potential cross-talk between NOTCH and BMP pathways is critical in AVC valve formation (Luna-Zurita et al., 2010). Taken together, these data suggest an important role of Notch signaling in heart valve development.

Role Of Wnt Signaling

The developing endocardial cushions in AVC and OFT have active canonical wnt signaling (Gitler et al., 2003; Hurlstone et al., 2003; Liebner et al., 2004). Multiple Wnt ligands like *Wnt2*, *Wnt4*, *Wnt 9b*, *Wnt3a* and *Wnt7b* are expressed during the course of mice AVC development (Alfieri et al., 2010). Studies done in chicken show that *Wnt9a* is expressed in the AV endocardial cells where it promotes the proliferation of AV endocardial cushions during valve development (Person et al., 2005). Upon treatment of chicken AVC explants with Wnt inhibitor *Frzb*, this proliferation is inhibited (Person et al., 2005). The field of zebrafish has also contributed significantly towards our understanding of Wnt signaling in AVC development. The evidence provided by various Wnt reporting zebrafish lines clearly highlights the presence of Wnt signals in the AVC of developing zebrafish embryo (Kashiwada et al., 2015; Moro et al., 2012). Wnt signaling is endogenously regulated by a β -catenin destruction complex consisting of proteins like APC, GSK3 β (Glycogen Synthase Kinase 3 β), AXIN and CK1 (Casein Kinase 1). The zebrafish *apc* mutant which has unregulated Wnt signaling shows hyperproliferative endocardial cushions and upregulated valve markers (Hurlstone et al., 2003). Additionally, overexpression of *apc* or Wnt inhibitor

dkk1 inhibits cardiac cushion formation. Thus, from the given data it can be concluded that Wnt signaling is indispensable for cardiac valve formation.

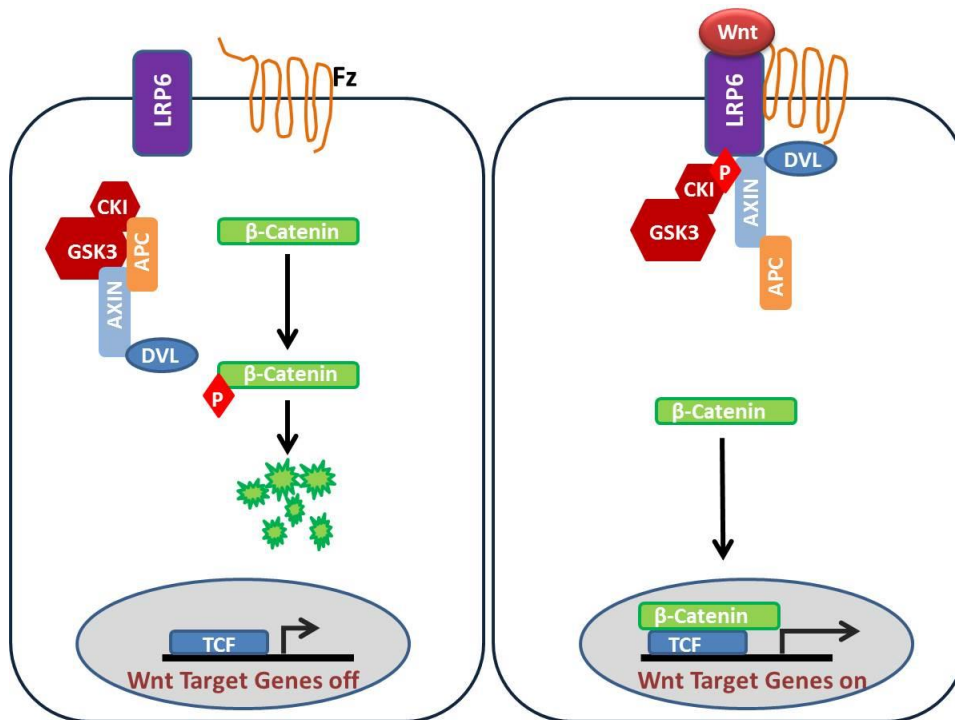


Figure 1.4: Canonical Wnt Signaling Pathway. In the absence of Wnt ligand, β -Catenin is degraded by a destruction complex comprising of proteins like CK1, GSK3 β , AXIN and APC. However, binding of Wnt to receptors Frizzled and LRP6 leads to inhibition of β -Catenin degradation and its nuclear translocation where it dimerizes with TCF/Lef-1 transcription factors to activate gene expression.

Role Of Extracellular Matrix

The initial steps of heart valve formation involve accumulation of ECM in the developing AV Canal that leads to formation of localized swelling which gives rise to the AV endocardial cushions followed by EMT leading to formation of functional heart valves (Lockhart et al., 2011). The Extracellular Matrix of the endocardial cushions provides support for cell migration and promotes invasion of mesenchymal cells. The AVC myocardium secretes a number of ECM components like fibronectin, transferrin, hLAMP1, ES130 which are involved in crucial regulations of EMT (Krug et al., 1995; Sinning, 1997).

Hyaluronic Acid (HA) is one of the most abundant glycosaminoglycan found in the ECM of the AV, OFT cushions and valve leaflets of the developing heart. It is synthesized by the enzyme HAS2 and is exported directly into the extracellular space. The expression of *Has2* begins in the embryonic myocardium and endocardium from around E8.5 and at E9.5 the

expression gets refined to atrial and ventricular endocardium with only little expression in AV myocardium (Camenisch et al., 2000). By E9.5, the cardiac jelly is also rich in HA and another ECM protein Versican. In the extracellular space, HA interacts with other ECM proteins like aggrecan, versican to maintain proper functional architecture of Extracellular Matrix (Camenisch et al., 2000; Kohda et al., 1996). The *Has2*^{-/-} mutant mice do not have AV endocardial cushions thus there is no event of EMT. Additionally, these mice lack HA and die around E9.5. Interestingly it was also shown that, AVC morphogenesis can be rescued in AV explants from *Has2*^{-/-} by addition of exogenous HA or ErbB ligand, heregulin-1 (neuregulin-1) (Camenisch et al., 2002, 2002). The fact that addition of neuregulin-1 rescues EMT shows ErbB receptor activation is coupled to hyaluronan function in endocardial cushion EMT and both these molecular events are crucial for AVC morphogenesis.

Versican encoded by *CSPG2* is a chondroitin sulfate proteoglycan. Versican has the ability to interact with HA, cartilage link protein and fibulin in the extracellular matrix to make a firm architecture of the matrix (Lockhart et al., 2011). In addition it also interacts with ECM cell surface receptors like integrin (Kern et al., 2006, 2007). Upon interaction with β 1-Integrin, it can activate focal adhesion kinase which promotes cell adhesion and prevents cell apoptosis (Wight, 2002) . During valve development, Versican has similar expression pattern and crucial role like HA (Camenisch et al., 2000; Kern et al., 2006). Versican mutant mice lack endocardial cushions and die around E10.5 which further confirms its crucial role in valve development (Mjaatvedt et al., 1998).

Thus, the given data clearly indicates that Extracellular Matrix proteins are extremely important for valve development.

1.3 Zebrafish Heart Development

Due to its advantages like external fertilization and transparency of the embryo, zebrafish was used as the model system for this work. The following section will highlight the morphogenetic movements and underlying molecular networks involved in zebrafish heart development.

The heart development in zebrafish proceeds through a series of morphogenetic movements and by 48 hpf a looped and functional heart with two discrete chambers, bulbous arteriosus and an AV Canal is formed.

Fate mapping techniques have revealed that, at blastula stage (5 hpf) the atrial myocardial progenitors are positioned more ventrally as compared to their ventricular counterparts at lateral marginal zone (Keegan et al., 2004; Stainier et al., 1993). The endocardial progenitors, unlike the myocardial ones, are not segregated as per the respective chambers and are present throughout the marginal zone (Lee et al., 1994). By 6-9 somites (12-13 hpf), the myocardial progenitors are found in the anterior lateral plate mesoderm which expresses *nkx2.5*. In this region, transcription factors like *hand2* and *gata4* are also expressed (Figure 1.5) (Schoenebeck et al., 2007; Yelon et al., 2000). Whereas the expression of *gata4* is present throughout antero-posterior axis of the ALPM, the *hand2* expression is restricted to the posterior region of ALPM and *nkx2.5* is expressed in the posterior ALPM as well but in medial portion (Schoenebeck et al., 2007).

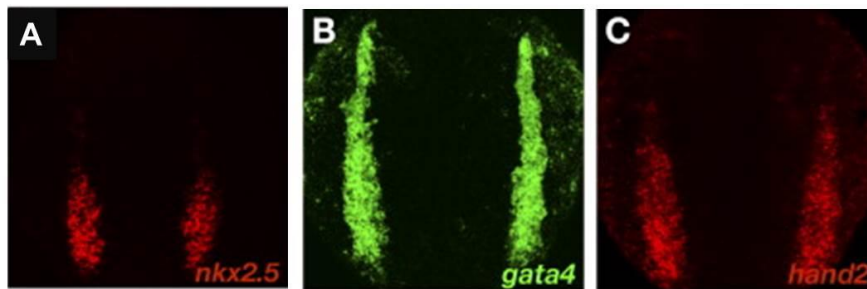


Figure 1.5: Gene expression patterns at ALPM . At 6-9 somite stages, *nkx2.5*(A) and *hand2*(C) are expressed in the posterior region of ALPM but *nkx2.5* is expressed in a more medial region. *gata4* on the other hand is expressed throughout the antero-posterior axis of the ALPM. Modified images are adapted from (Schoenebeck et al., 2007).

Cardiac differentiation program begins at 13-14 somite stage (16 hpf), when these bilateral population of cells start to express myocardial genes like *myl7* and *vmhc*. At this stage, and later as well, there is a posterior sub population of *nkx2.5* expressing cells which never initiate *myl7* expression and hence do not contribute to the myocardium (Yelon et al., 1999). *vmhc* is expressed only in a subset of *myl7* expressing cells, which lie in medial portion of *myl7* expressing region (Figure 1.6) (Yelon et al., 1999; Yelon, 2001). Atrium specific gene expression marked by *myh6* takes place later than *vmhc*, at 19 somites stage (18 hpf) (Berdougo et al., 2003). Unlike *vmhc* expressing cells, the *myh6* expressing cells are placed more laterally (Berdougo et al., 2003). The bilateral myocardial precursors migrate towards the midline and at around 18 somites come in contact with each other (Yelon et al., 1999; Yelon, 2001). After this initial contact, the bilateral cell populations begin to fuse. Upon completion of this fusion, at around 21 somites (19.5 hpf), a cardiac cone is formed which appears as a ring like structure of cardiac cells when viewed dorsally. By 20.5 hpf, the cone

starts transforming into a tube like structure. The ventricular part of the tube is formed first followed by the atrial domain. Around 26 hpf, the cardiac tube is completely formed.

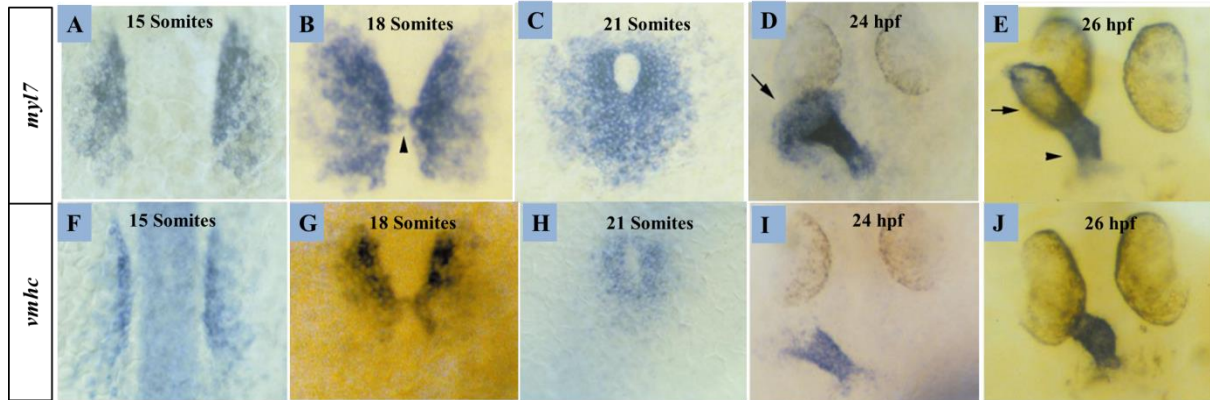


Figure 1.6: Tracking cardiac tube assembly by studying *myl7* (cardiac myosin light chain) and expression patterns. (A, F) Bilateral fields of cardiac progenitors at ALPM. (B, G) Migrating cardiac progenitors fuse at the midline around 18 somites. (C, H) At 21 somites, cardiac cone is formed by fusion of the migrating cardiac precursors. (D, I) Formation of cardiac tube at 24 hpf. (E, J) Completely formed cardiac tube at 26 hpf. Modified images are adapted from (Yelon et al., 1999).

This linear heart tube undergoes a series of complex morphogenetic movements leading to the formation of an asymmetrical heart, which has a more anteriorly placed/right sided ventricle and a dorsally placed/left sided atrium. The transition from a linear heart tube to a heart with properly shaped chambers, involves ballooning, a process which creates bulges in the linear heart tube (Christoffels et al., 2000; Auman et al., 2007). These bulges give rise to two types of surfaces within the chambers (with distinct molecular and morphological characteristics): a convex Outer Curvature (OC) and concave Inner Curvature (IC). At molecular level, the expression of *nppa* (natriuretic peptide a) only in the outer curvature of the ventricle, distinguishes it from the inner curvature. At morphological level, only the cells of the outer curvature elongate as opposed to the inner curvature cells which retain their initial morphology during chamber growth and expansion (Auman et al., 2007). The cells of cardiac ventricle OC in *wea* or the *weak atrium* mutants as well as in BDM (a drug to reduce cardiac contractility) treated embryos are small and fail to elongate, implying that proper fluid flow is also important for chamber morphogenesis (Auman et al., 2007).

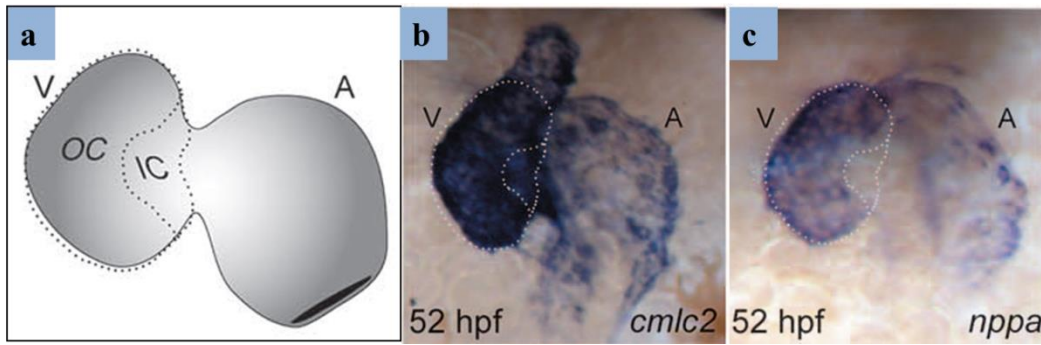


Figure 1.7: Cardiac Chambers post ballooning and expansion. (a) scheme showing the Outer Curvature (OC) and Inner Curvature (IC) in cardiac ventricle. (b) in situ hybridization with *cmlc2* or *myl7* showing a properly formed, 2 chambered heart at 52 hpf. (c) *nppa* expression is enriched in outer curvature of the cardiac ventricle. Modified images are adapted from (Auman et al., 2007). A: Atrium, V: Ventricle.

1.4 Zebrafish Atrioventricular Canal/Valve Development

The heart chambers are separated by an Atrioventricular (AV) canal, which harbors the valves, important for maintaining unidirectional flow of blood from atrium to ventricle.

The AV canal formation begins in the embryonic heart at around 37 hpf, when the myocardial AV canal marker genes like *bmp4*, *cspg2a* (*versican*) and *tbx2b* which are previously expressed in the whole ventricle start getting restricted to the AVC myocardium (Walsh and Stainier, 2001; Chi et al., 2008). They become restricted to the AV boundary by 48 hpf. During the same period, the endocardial AVC marker genes like *has2* and *notch1b* also get restricted to the AV boundary (Walsh and Stainier, 2001; Chi et al., 2008). At morphological level, the formation of AV canal can be observed when a constriction starts to appear between the future atrium and the ventricle at 37 hpf (Beis et al., 2005), eventually leading to the formation a looped heart by 48 hpf, with a distinct AV canal separating these chambers. Another hallmark of AV canal development is expression of cell adhesion molecule Alcam by AV canal endocardial cells (Beis et al., 2005). The Alcam expression starts at 36 hpf with a single cuboidal cell in the AV Canal endocardium. At this point, all the other endocardial cells are squamous and Alcam negative. By 55 hpf, the Alcam expression is observed in all of the myocardium but only in the AV canal endocardial cells that have turned cuboidal as compared to squamous and Alcam negative chamber endocardial cells. Around 60 hpf, the superior AVC endocardial cells send protrusions into the ECM (between AVC myocardium and endocardium) and a primitive valve leaflet of the superior AVC becomes apparent by 85 hpf (Beis et al., 2005; Scherz et al., 2008). The cells in the inferior AVC send protrusions into ECM by 80 hpf and a primitive leaflet is formed there around 102 hpf (Beis et al., 2005;

Scherz et al., 2008). This also goes to show that the two valve leaflets are formed asynchronously and the superior aspect of AVC leads in development. Eventually, the two valve leaflets are properly formed by 7 dpf.

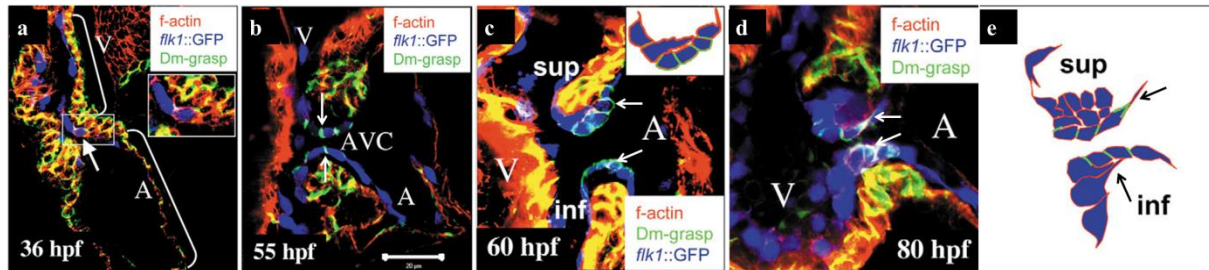


Figure 1.8: Alcarn (Dm-grasp) expression during AVC development. (a) Alcarn expression starts in AV canal at 36 hpf with one endocardial cell expressing Alcarn. (b) At 55hpf, Alcarn expression is present throughout the AVC endocardium and myocardium. (c, d) Alcarn expression in AVC at 60 and 80 hpf respectively. (e) Schematic representation of AVC endocardial cells at 80 hpf as shown in (d). Arrows (a-d) highlight Alcarn expression. Arrows in (e) show protrusions from AVC endocardial cells. A: Atrium, V: Ventricle, AVC: Atrioventricular canal, sup: Superior AVC, inf: Inferior AVC. Green: Alcarn or Dm-grasp (according to old nomenclature), Blue: endocardium. Modified images are adapted from (Beis et al., 2005).

As in the mouse, a number of signaling pathways like Notch, TGF- β , Wnt/ β -Catenin, ErbB and Calcineurin/NFAT are shown to be of great significance in zebrafish AVC development as well. Inhibition of Notch signaling starting from 24 hpf results in aberrant appearance of Alcarn expressing cuboidal endocardial cells in the ventricle at 60 hpf, whereas constitutively active Notch signaling restricts the Alcarn expression in the AV Canal (Beis et al., 2005). This indicates that the Notch signaling inhibits ectopic expression of AVC markers in the ventricle. However, inhibition of Notch signaling at the later stages from 36 hpf results in improper AVC development and reduced Alcarn expression, suggesting a role of Notch signaling in maintaining AVC characteristics at later time points in development (Beis et al., 2005). Inhibition of ErbB and TGF- β results in retrograde blood flow around 3 dpf and obstruction in calcineurin signaling starting from 48 hpf results in the formation of improper AVC endocardium (Beis et al., 2005; Scherz et al., 2008). Constitutively active Wnt/ β -Catenin signaling, present in zebrafish *apc* mutant, results in hyper-proliferative valvular endocardium and misregulated valve markers, thus implying that a controlled Wnt signaling is important for AVC development and maturation (Hurlstone et al., 2003).

Taken together, these data highlight the importance of various signaling cascades in AV Canal development, but possible cross-talk between them and its probable role in AVC development is largely unknown.

1.5 Inhibitor of DNA Binding 4 (Id4)

Id4 belongs to Id family of proteins (Id1-4), which are dominant negative regulators of bHLH (Basic Helix Loop Helix) transcription factors. Id proteins lack a classical DNA binding domain but have a HLH domain with which they bind to other bHLH transcription factors, thus inhibiting their DNA binding (Benezra et al., 1990; Massari and Murre, 2000).

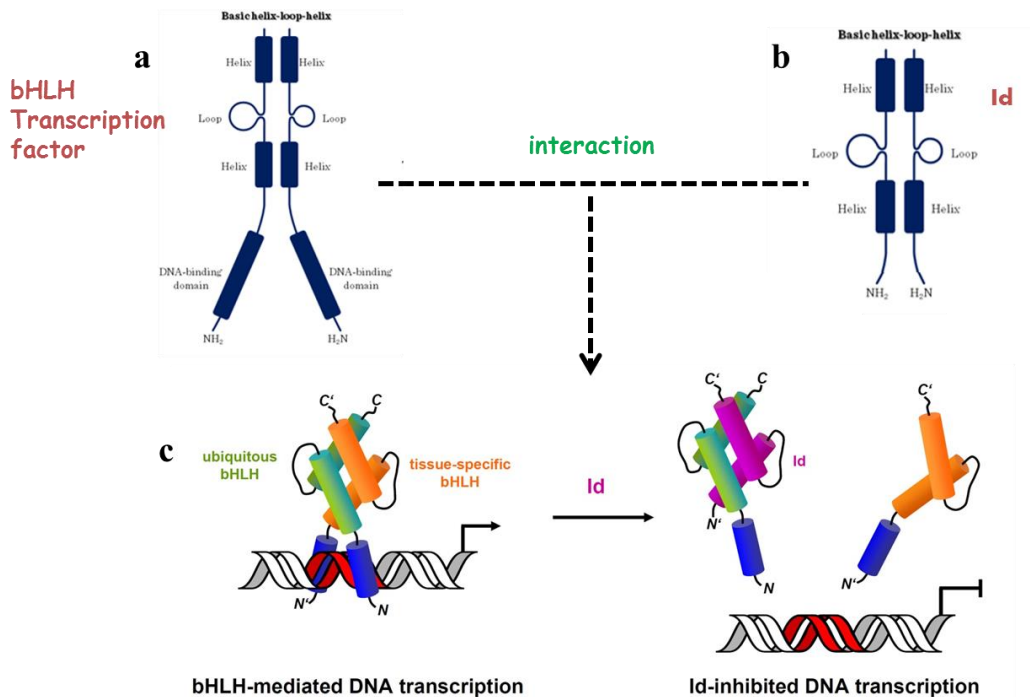


Figure 1.8: Id inhibited DNA transcription. (a) bHLH transcription factor with bHLH and DNA binding domain. (b) Id protein with bHLH domain and without DNA binding domain. (c) Normally bHLH proteins dimerize for DNA binding. However, in presence of an Id protein this interaction is inhibited that leads to inhibition of gene transcription. Modified Images are adapted from (<http://www.uni-salzburg.at/index.php?id=25633> and http://www.tankonyvtar.hu/en/tartalom/tamop425/0011_1A_Jelatvitel_en_book/ch02s04.html).

Previously reported expression studies in the mice suggest that ID4 is expressed in neurons (Yun et al., 2004), adipocytes (Murad et al., 2010), osteoblasts (Tokuzawa et al., 2010), mammary gland cells (Dong et al., 2011), prostate epithelial cells (Sharma et al., 2013) and sertoli cells (Chaudhary et al., 2001). Depending on the tissue of expression, different functional roles have been proposed for ID4. In mammary gland, ID4 has been shown to regulate branching morphogenesis and cell proliferation of mouse mammary cells by suppressing p38/MAPK activity (Dong et al., 2011). Furthermore, it has been reported that ID4 can drive mesenchymal stem cell differentiation towards osteoblasts instead of adipocytes (Tokuzawa et al., 2010). For doing so, ID4 releases HES1 from HES1-HEY2 complex leading to RUNX2 stabilization, thus increasing its transcriptional activity. ID4 has also been shown

to have a critical role in nervous system. In the *Id4* null mice, neural precursor cells show slower proliferation and smaller brain size compared to wildtype littermates (Yun et al., 2004). Additionally, the *Id4* null mice also have malformed prostates with fewer tubules and loss of NKX3.1 expression (Sharma et al., 2013). Taken together, these studies have contributed significantly to our knowledge on ID4 function, however its role in cardiac development still remains unclear.

1.6 AIM of the Project

I became interested in Id4 because of the following reasons:

- Its ability to control crucial biological processes in different tissues.
- Its potential to interact with different molecules in various signaling pathways.
- In spite of being an important protein, no reported function to date in heart development.

The main goal of this project was to find out if Id4 can be a novel player in cardiac development. Due to advantages like external fertilization, optical transparency of the early stage embryo/larvae, the Zebrafish was chosen as the model system for this study. To achieve the main goal of the project, a roadmap of following specific aims was designed:

- **AIM 1:** Determine the spatio-temporal expression pattern of *id4* during heart development.
- **AIM 2:** Understand the function of Id4 by creating its loss-of-function mutant using TALEN technology.
- **AIM 3:** Determine the signaling cascade that it can be part of, and a potential cross-talk with molecules of other cascades that it might have, during cardiac development.

2. Materials

2.1 Antibiotics

Table: 2.1: List of antibiotics used in this thesis work along with their respective working concentrations.

Antibiotics	Working Concentration
Ampicillin	100 µg/ml
Spectinomycin	50 µg/ml
Tetracycline	10 µg/ml

2.2 Antibodies

Table: 2.2: List of antibodies used in this thesis work along with their respective dilutions, supplier details.

Antibodies	Dilution	Supplier
Alcam Antibody (Zn8)	1:10	Developmental Studies Hybridoma Bank
Anti-Digoxigenin-AP, Fab fragments	1:10,000	Roche
DsRed Polyclonal Antibody	1:300	Clontech
Goat Anti Mouse Alexa Fluor 488	1:300	Invitrogen
Goat Anti Rabbit Alexa Fluor 568	1:300	Invitrogen

2.3 Bacterial Culture medium

Table: 2.3: List of bacterial culture mediums in this thesis work along with their preparation recipes

Bacterial Strain	Composition/Supplier
LB agar	Roth
LB medium	Roth
SOC medium	Dissolve following in distilled water : Tryptone 2% Yeast Extract 0.5% NaCl 0.05% KCl 0.0186% adjust to pH 7 and add MgCl ₂ 10mM D-glucose 20mM followed by autoclaving.

2.4 Bacterial Strains

Table: 2.4: List of bacterial strains used in this thesis work along with its purpose of use.

Bacterial Strain	Purpose of Use
Dh5 α	Competent cells for cloning

2.5 Buffers/Solutions

Table: 2.5: List of buffers/solutions used in this thesis work along with their respective compositions.

Buffers/Solutions	Composition
Alkaline Tris Buffer	100mM Tris HCl pH 9.5 100mM NaCl 50mM MgCl ₂

Materials

	0.1% Tween 20 Dissolved in distilled water
Blocking Buffer (<i>in situ</i> hybridization)	2mg/ml BSA 2% Sheep Serum Dissolved in PBT
Blocking Buffer (Immunohistochemistry)	1% DMSO 2% FCS 1% BSA 0.1% Tween 20 Dissolved in PBS
DEPC Water	0.01% DEPC dissolved in distilled water, followed by autoclaving
E3 embryo medium	3g Instant Ocean 0.75g Calcium sulphate Dissolved in 10 Litres of Distilled water
Fish Fix	Dissolve 4g PFA in 80 ml of fish fix buffer by heating to 60 °C. Cool and adjust pH to 7.4. Make up volume to 100 ml using fish fix buffer.
Fish Fix Buffer	For 100 ml of buffer : 77 ml 0.1M Na ₂ HPO ₄ 23 ml 0.1M NaH ₂ PO ₄ 12 µl 1M CaCl ₂ 4g sucrose
PBS	8g NaCl 0.2g KCl 1.44g Na ₂ HPO ₄ 0.24g KH ₂ PO ₄ Dissolved in 900 ml of distilled water, adjust pH 7.4, makeup volume to 1000 ml with distilled water
4 % PFA	Add 4g PFA in 70 ml PBS, heat the solution to 60°C until PFA gets dissolved. Cool and

Materials

	adjust to pH 7, make up volume to 100 ml.
PBT	0.1% Tween 20 in PBS
Permeabilization Solution (Immunohistochemistry)	0.3% Triton X-100 1% DMSO 1% BSA 0.1% Tween 20 Dissolved in PBS
Pre hybridization solution (HM-)	50% Formamide 5X SSC 0.1% Tween 20 Adjust to pH 6 with 1M Citric Acid
HM+	HM- Heparin 50 µg/ml tRNA 500 µg/ml
20x SSC	175.3g NaCl 88.2g Sodium Citrate Dissolve in 800 ml distilled water. Adjust pH to 7. Make up volume to 1000 ml with distilled water.
10x TBE	121g Tris 62g Boric Acid 7.4g EDTA Dissolve in 1000 ml distilled water.
Wash Buffer (Immunohistochemistry)	0.1% Tween 20 in PBS

2.6 Centrifuges

Table: 2.6: List of centrifuges used in this thesis work along with their respective model/supplier details.

Centrifuges	Supplier
Centrifuge (1.5-2 ml tubes) 5415 D	Eppendorf
Centrifuge (1.5-2 ml tubes) 5418	Eppendorf

Centrifuge (200 µl tubes) 5417 R	Eppendorf
Centrifuge (15-50 ml tubes) 5810 R	Eppendorf
Centrifuge (slow speed, 1.5-2ml tubes)	Qualitron
Centrifuge (slow speed, 200 µl tubes)	Qualitron
Refrigerated Centrifuge 5424 R (1.5-2 ml tubes)	Eppendorf

2.7 Chemicals

Table: 2.7: List of chemicals used in this thesis work along with their respective model/supplier details.

Chemical	Supplier
1-Phenyl-2-thiourea (PTU)	Sigma
Agarose	Peqlab
Agarose, Low Gelling Temperature	Sigma
Blocking Reagent	Roche
Bovine Serum Albumin (BSA)	Sigma
Chloroform	Merck
Citric Acid	Sigma
DEPC	Sigma
D Glucose	Sigma
DIG labelling mix	Roche
Dimethyl Sulfoxide	Sigma
DMH1	Sigma
DNA Away	Molecular Bioproducts
DNA ladder	Thermo Scientific
dNTP	Thermo Scientific
Ethanol	Roth
Ethidium Bromide	Sigma
Ethylenediaminetetraacetic acid (EDTA)	Roth
Fetal Calf Serum	Biochrom
Formaldehyde	Santacruz
Formamide	Applichem

Materials

Gel loading dye	Thermo Scientific
Glycerol	Roth
Heparin	Sigma
Isopropanol	Roth
Magnesium Chloride	Fluka
Magnesium Sulphate	Fluka
Methanol	Roth
Methylene Blue	Sigma
Mineral Oil	Sigma
NBT/BCIP stock solution	Roche
Nuclease free water	Thermo Scientific
Paraformaldehyde	Sigma
PBS	Sigma
Potassium Chloride	Merck
Potassium dihydrogen phosphate	Merck
Phenol Red	Sigma
RNase ZAP	Sigma
Sheep serum	Sigma
Sodium Chloride	Roth
Sodium Citrate	Sigma
Sodium hydroxide	Sigma
Sodium phosphate monobasic monohydrate	Sigma
Sodium phosphate dibasic dodecahydrate	Sigma
Sucrose	Roth
SYBR Safe	Invitrogen
Tricaine	Pharmaq
TRIS	Sigma
Tris-EDTA (TE 10x)	Cayman Chemicals
Triton X-100	Sigma
TRIzol Reagent	Ambion
tRNA	Sigma
Tryptone	Fluka
Tween-20	Sigma

X-gal	Sigma
Yeast Extract	Fluka

2.8 Enzymes

Table: 2.8: List of enzymes used in this thesis work along with their respective model/supplier details.

Enzymes	Supplier
AgeI	NEB
BamHI	NEB
BsaI	NEB
ClaI	NEB
EcoRI	NEB
Esp3I	Thermo Scientific
Plasmid Safe DNase	Epicentre
Pronase	Roche
Proteinase K	Roche
RNasein	Promega
RQ1 RNase-Free DNase	Promega
SP6 RNA polymerase	Promega
T4 DNA Ligase	NEB
T3 RNA Polymerase	Promega
T7 RNA polymerase	Promega
NotI	NEB
XbaI	NEB
XhoI	NEB

2.9 Kits

Table: 2.9: List of kits used in this thesis work along with their respective model/supplier details.

Kits	Supplier
Cold Fusion Cloning Kit	System Biosciences
Gel extraction Kit	Thermo Scientific
Maxima cDNA synthesis	Thermo Scientific
Mini Prep Plasmid isolation kit	Thermo Scientific
mMessage mMachin kit (SP6)	Ambion
mMessage mMachin Kit (T7)	Ambion
PCR product cleanup (ExoSAP)	Jena Bioscience
PCR purification kit	Thermo Scientific
pGEM-T Easy Cloning Kit	Promega
RNA clean and concentrator - 5	Zymo Research
Superscript III First strand synthesis	Invitrogen

2.10 Microscopes

Table: 2.10: List of microscopes used in this thesis work along with their respective model/supplier details.

Microscopes	Supplier
Confocal Microscope, LSM 700	Zeiss
Confocal Microscope LSM 780	Zeiss
Embryo Microinjection, Stereomicroscope Stemi 2000	Zeiss
Stereomicroscope, Stereodiscovery V8	Zeiss
Stereomicroscope, MZ 16 F	Leica
Stereomicroscope, SMZ18	Nikon
Stereomicroscope, with camera SMZ25	Nikon
Stereomicroscope Stereodiscovery V8, with camera AxioCam MRc5	Zeiss

Spinning Disk Microscope, Cell observer SD	Zeiss
--	-------

2.11 Miscellaneous Equipment

Table: 2.11: List of Miscellaneous equipments used in this thesis work along with their respective model/supplier details.

Equipment	Supplier
Agarose Gel Electrophoresis Chamber	Peqlab
Bacterial Incubator	Heraeus
Bacterial Incubator Shaker	Infors HAT
Combitips	Eppendorf
Dark Reader Transilluminator	Clare Chemical Research
Forceps	Dumont
Fumehood	Bense
Gel DOC EZ Imager	BIORAD
Gel Electrophoresis Power supply	Peqlab
Heating Block	VWR
Homogenizer	Bibby Scientific
Hot Plate	Janke & Kunkel Gmbh
Hot Plate Magnetic Stirrer	VWR
HRMA Machine, Eco	Illumina
Hybridization oven	VWR
Immedge pen	Vector Laboratories
Injection Micromanipulator	World Precision Instruments
Injection Needles	Harvard Apparatus
Injection Needle Puller	Sutter Instruments
Injection Pump, PicoPump	World Precision Instruments
Latex Gloves	Roth
Magnetic Stir Bar	VWR
Microdish	ibidi
Microloader Pipette Tips	Eppendorf
Magnetic Stirrer	HANNA Instruments

Materials

Microscale	Novex
Microwave	Bosch
Mineral Oil	Sigma
Multipette Plus	Eppendorf
Laboratory Film	Parafilm
Pasteur pipette	Greiner bio-one
PCR cycler	MJ Research
PCR cycler, Mastercycler Pro	Eppendorf
pH meter	Mettler Toledo
pH strips	Merck
Petri dish (90 mm, 60 mm, 35mm)	Greiner bio-one
PICOSPRITZER III	Parker
Pipetteman (1000 μ l, 200 μ l, 100 μ l, 20 μ l, 10 μ l, 2 μ l)	Gilson
Pipetboy	Integra
Pipette pump	Bel-Art Products
Pipette filter tips	Greiner bio-one
Pipette tips	Greiner bio-one
qPCR adhesive seals	illumina
qPCR machine	BIORAD
qPCR plates, 48 well	illumina
Rocker	Grant Instruments
Rotator	Stuart
Scalpel	Braun
Surgery Scissors	Fine Science Tools
Serological pipette	Greiner bio-one
Serum pipette	Greiner bio-one
Spectrophotometer, NANODROP 2000C	Thermo Scientific
Vortex	Scientific Industries
Water bath	Julabo
Weighing Balance	Sartorius
Zebrafish incubator	Binder
Zebrafish aquatic housing system	Tecniplast

2.12 Oligonucleotides

Table: 2.12: List of oligonucleotides used in this thesis work along with their purpose of use.

Gene	Oligonucleotides	Purpose
<i>bmp4</i>	<i>bmp4</i> fw: GACTATCCTGAAAGATCCACCA <i>bmp4</i> rev: TGAGATGATCGGCTAATGGA	Primers used for amplification and cloning of <i>bmp4</i> <i>in situ</i> hybridization probe
<i>cspg2a</i>	Same <i>in situ</i> hybridization probe used as published in (Walsh and Stainier, 2001)	
<i>has2</i>	<i>has2</i> fw: GAGTGGCTTTACAACCTCCTGTG <i>has2</i> rev: TATCCCAAACACTCACACAATGC	Primers used for amplification and cloning of <i>has2</i> <i>in situ</i> hybridization probe
<i>id4</i>	<i>id4</i> Fw: TCCGCAGGATAAGAAAGTCAG <i>id4</i> Rev: CTGCAGGTCCAGAATATAGTC	Primers used for identification of TALEN induced lesion by HRMA in TALEN injected F0 embryos.
<i>id4</i>	<i>id4</i> Δ5hrmfw: AGTAAAGTGGAAATCCTCCAG <i>id4</i> Δ5hrmrev: AGGTCCAGAATATAGTCAATG	Specific primers used for segregating mutants with 5bp deletion allele (<i>id4</i> ^{bns18}) by HRMA
<i>id4</i>	<i>id4</i> fw_ish: GTGTGACCAACAATAACTCATCC <i>id4</i> rev_ish : CATAAGTTATAGAACATCGCGCA	Primers used for amplification and cloning of <i>id4</i> <i>in situ</i> hybridization probe
<i>id4</i>	<i>id4</i> qf1: ACACAAATCAACACAGAGCA <i>id4</i> qr1: CACATGAGAAATCGGACTGG	qPCR primers used for <i>id4</i>
<i>id4</i>	Id4 ov ex gfp new fw: CCGCTCGAGGGATCCACCGGTATGGTGAGCA AGGGCGAGGA Id4 ov ex gfp new rev :	Primers used for making <i>id4</i> overexpression construct <i>fli1:id4-2A-</i>

	CATGTCTGGATCATCATCGATTACTTGTACA GCTCGTCCA	GFP by cold fusion cloning
<i>id4</i>	Id4 ovex id4cds F: CATCATTTTGGCAAAGAATTCGCCACCATGAAGGC CAGCGTGCCGGT Id4 ovex id4cds R: AGTAGCACCAGAACCGGATCCGCGACACAAAAAA AGTGAGT	Primers used to amplify <i>id4</i> cds for making <i>id4</i> overexpression construct <i>fli1:id4-2A-mCherry</i> by cold fusion cloning
<i>id4</i>	Id4 ovex 2Amcherry F: CTTTTTTTGTGTCGCGGATCCGGTTCTGGTGCTACT AATTT Id4 ovex 2Amcherry R: CATGTCTGGATCATCATCGATTACTTGTACAGCT CGTCCA	Primers used to amplify 2A-mCherry for making <i>id4</i> overexpression construct <i>fli1:id4-2A-mCherry</i> by cold fusion cloning
<i>rpl13</i>	<i>rpl13</i> qf1: TAAGGACGGAGTGAACAACCA <i>rpl13</i> qr1: CTTACGTCTGCGGATCTTTCTG	qPCR primers used for <i>rpl13</i>
<i>spp1</i>	<i>spp1</i> fw: AGCGACTACAAAAAATCCATCGTCT <i>spp1</i> rev: CTGAACAAGTTTGGCAGCAGTTCGA	Primers used for amplification and cloning of <i>spp1</i> <i>in situ</i> hybridization probe
<i>tbx2b</i>	<i>tbx2b</i> fw: GAGATAGTTACAGTTGTACAGTGG <i>tbx2b</i> rev: TGTGAACTTGTAGCGGCAGTCGT	Primers used for amplification and cloning of <i>tbx2b</i> <i>in situ</i> hybridization probe

2.13 PCR enzymes and mastermix

Table: 2.13: List of PCR enzymes/mastermix used in this thesis work along with their respective model/supplier details.

PCR enzyme/Master Mix	Supplier
2x Dynamo Color Flash	ThermoFisher Scientific

KAPA2G 2x	KAPABIOSYSTEMS
Maxima Sybr Green qPCR Master Mix	ThermoFisher Scientific
PCR Master Mix	ThermoFisher Scientific
Phusion DNA Polymerase	NEB

2.14 Plasmids

Table: 2.14: List of plasmids used in this thesis work along with their respective details.

Plasmids	Source	Antibiotic resistance	Purpose
fli1:GFP	Published in (Covassin et al., 2006)	Ampicillin	Used the plasmid backbone with promoter for making endothelial specific <i>id4</i> overexpression constructs
pCS2TAL3DD	Grunwald Lab (Utah)	Ampicillin	Expression vector to clone final TALEN arm
pCS2TAL3RR	Grunwald Lab (Utah)	Ampicillin	Expression vector to clone final TALEN arm
pGEM-T	Promega	Ampicillin	in situ probe synthesis, as a sub cloning vector to generate sticky ends
pHD(1-10), pNG(1-10), pNI(1-10), pNN(1-10)	Addgene	Tetracycline	TALEN RVDs corresponding a particular nucleobase : HD – C (Cytosine) NG – T (Thymine) NI – A (Adenine)

			NN – G (Guanine)
pLR-HD, pLR-NG, pLR-NI, pLR-NN	Addgene	Spectinomycin	Last half repeat used for cloning TALEN arms
pFUS_A	Addgene	Spectinomycin	Used to assemble first 10 RVDs for each TALEN arm
pFUS_B(N-1)	Addgene	Spectinomycin	Used to assemble 11 th to (N-1) RVDs for each TALEN arm (N : Total number of RVDs)

2.15 Softwares

Table: 2.15: List of softwares used in this thesis work along with their respective purpose of use.

Software	Purpose
Adobe Photoshop, illustrator	Image formatting
GraphPad Prism, Microsoft Excel	Data Analysis
Image J, Imaris, Zen	Image Processing

2.16 Tubes and containers

Table: 2.16: List of tubes and containers used in this thesis work along with their respective model/supplier details.

Tubes and Containers	Supplier
Bacterial culture tubes	Sarstedt
Beakers (100 ml, 600 ml, 1000 ml)	VWR

Centrifuge tubes (500 µl)	Sarstedt
Centrifuge tubes (1.5 ml, 2 ml)	Sarstedt
Centrifuge tubes (15 ml, 50 ml)	Greiner bio-one
Conical Flasks (100 ml, 500 ml)	VWR
Glass bottles (100 ml, 250 ml, 500 ml, 1000 ml)	Duran
PCR tubes (200 µl)	Sarstedt
PCR tube strips	Sarstedt

2.17 Zebrafish Food

Table: 2.17: List of zebrafish food used during different developmental time points.

Food	Fish Age	Supplier
Brine Shrimp	5 dpf – 12dpf	Special diets services
SDS 100	>12dpf – 1 month	Special diets services
SDS 200	>1 month – 2 months	Special diets services
SDS 300	>2months – 3 months	Special diets services
Topical Breeder mix and SDS 400	Adult fish (\geq 3months)	Special diets services

2.18 Zebrafish Lines

Table: 2.18: List of zebrafish lines used in this thesis work along with their details of use and publications in which they were described.

Zebrafish Lines	Details	Publications
AB	Wild-type	
<i>apc</i> ^{mcr/mcr}	Mutant with high Wnt activity	(Hurlstone et al., 2003)
<i>Tg(7xTCF-Xla.Siam:nlsmCherry)</i> ^{ia5}	Wnt reporter	(Moro et al., 2012)
<i>Tg(hsp70l:bmp2b)</i> ^{fr13}	Bmp2b overexpression	(Chocron et al., 2007)
<i>Tg(kdrl:ras-mcherry)</i> ^{s896}	Endothelial specific reporter	(Chi et al., 2008)
<i>Tg(TP1bglob:VenusPEST)</i> ^{s940}	Notch reporter	(Ninov et al., 2012)

3. Methods

3.1 Zebrafish Husbandry

3.1.1 Zebrafish Maintenance

The zebrafish were kept and maintained as described (Westerfield, 2000) in a fish culture system from Tecniplast. Briefly, the adult zebrafish was kept in following condition:

Parameter	Conditions used
Temperature in fish tank	28°C
Temperature of fish Room	29°C
Light/Dark Cycle	14hours/10 hours

Table 3.1: Temperature and light conditions used for zebrafish maintenance

The zebrafish embryos were kept in Egg water in B.O.D incubator at 28°C. At 24 hpf, PTU was added to the embryos to prevent pigment formation until required. Also, at this stage 50µl of 10mg/ml pronase was added to 40 ml egg water to dechorionate the embryos for 3 hours after which the egg water was changed to remove the pronase.

3.1.2 Zebrafish Breeding

For breeding purposes, male and female zebrafish were put together in special mating tanks with egg permeable insets in the evening, separated by a transparent divider. The next morning divider was removed. After about 15 minutes, females laid eggs which were immediately fertilized by the males. Fertilized eggs accumulated at the bottom of the tanks and were collected by filtering the contents of the tank through a sieve. These eggs were then washed with E3 medium and transferred to 10 cm dish with approximately 40 ml E3 medium.

3.2 Zebrafish Microinjection

3.2.1 Preparation of Injection plates

2% Agarose solution was prepared in E3 medium by heating the solution in the microwave. After agarose was dissolved, approximately 20 ml of solution was poured in 10 cm petri dish. Next, a special mold with lanes was kept on the poured agarose solution until the solution got

solidified. After solidification, the mold was carefully removed and an injection plate with lane cavities was obtained.

3.2.2 Preparation of Injection Needles

The injection needles were prepared from glass capillaries using an injection needle puller. The glass capillary was fixed in the needle puller from its two ends under tension. The center of the capillary was melted with the heat. As a result two fine needles were pulled apart, which were further used for injection purposes.

3.2.3 Microinjection

The injection needle with 5 μ l of injection mix (having DNA/RNA to be injected) was fixed into injection micromanipulator. The pressure conditions for injection including duration of the pulse were then adjusted in the injection pump (picospritzer) to allow the injection droplets to come out of the needle tip. The droplet size was calibrated with microscale to inject the requisite amount of injection mix. Finally, the fertilized eggs were aligned on injection plates and injected at no later than one-celled stage. The plasmids were injected always into the cell whereas mRNA injections were done in the yolk.

3.3 RNA Isolation

RNA extraction was performed from around 25 zebrafish embryos (of required developmental stage), adult heart atrium or ventricle as required, using trizol reagent (Ambion) as per manufacturer's instructions. The adult heart tissue was homogenized with an automated homogenizer and manual homogenization by pestle was done for embryos. Finally the RNA was eluted in 50 μ l of RNase free water.

3.4 Reverse Transcription or cDNA Synthesis

cDNA was synthesized from RNA using maxima cDNA synthesis kit. 500ng of RNA was incubated with 5X reaction mix and maxima enzyme mix as per manufacturer's instructions. The incubation cycle used for synthesis was:

Step	Temperature	Duration
1	25°C	5 mins
2	50°C	30 mins

3	85°C	10 mins
----------	------	---------

Table 3.2: Temperature conditions used for cDNA synthesis.

The cDNA thus obtained was diluted to working concentration of 150ng/μl for further downstream applications.

3.5 PCR amplification from cDNA

The PCR reactions were carried out in Eppendorf Mastercycler Pro thermal cyclers. Primers were designed according to region of interest and usually amplified with kappa 2G Fast Ready mix or Phusion HF DNA Polymerase. Standard PCR reactions with both the enzymes were setup according to manufacturer’s instructions with 1μl of cDNA and 1μl each of forward and reverse primers (10 μm) in a 20 μl reaction. The PCR cycle parameters used were:

Step	Temperature	Duration	Step Description
1	95°C	7 minutes	Initial Denaturation
2	95°C	20 seconds	PCR Cycling, 35 cycles
	58-65°C Primer specific annealing temperature	25 seconds	
	72°C	20 seconds	
3	72°C	7 minutes	Final Extension

Table 3.3: Standard PCR conditions used.

After the final extension, the reaction was stopped by gradually getting the cycler to 4°C.

3.6 Agarose Gel Electrophoresis

The DNA samples were resolved on 1-1.5% agarose gel containing sybr safe reagent to stain the DNA. The time duration for electrophoresis was 30 – 45 minutes depending on the size of DNA to be resolved and appropriate DNA ladder was also used to assess the size of DNA sample. After electrophoresis, the gel was viewed with UV light in a gel doc imager system.

3.7 PCR Product Elution From Agarose Gel

The PCR Products resolved on agarose gel were purified from the gel using GeneJET Gel Extraction Kit (Thermo Scientific), according to manufacturer's instructions. Final elution was done with autoclaved water in 20 μ l volume.

3.8 E.Coli Competent Cells Preparation

A DH5 α colony from a sterile culture was inoculated in 6 ml LB medium at 37°C for overnight culture. Next day morning, 1 ml of this overnight culture was added to 200ml of LB medium and kept in shaker incubator for at least 4 hours at 37°C. After this, the bacterial culture was chilled on ice for 20 mins followed by centrifugation for 10 mins at 4000rpm and 4°C. The supernatant was then discarded and pellet was allowed to dry. The dried pellet was then resuspended with 5 ml of cold 0.1M CaCl₂ and kept on ice 5 mins. This chilled homogenate was centrifuged for 5 mins at 4000 rpm and 4°C. The cell pellet thus obtained was again resuspended in 0.1M CaCl₂ and all the steps till getting the cell pellet again were followed in the same order. The supernatant was now discarded and the pellet was allowed to dry. The dried pellet was now resuspended with 0.1M CaCl₂ / 15% Glycerol and 20 μ l of this suspension was aliquoted in prechilled 1.5ml centrifuge tubes and stored at -80°C.

3.9 Transformation of Competent E.Coli

Competent E.Coli cells stored at -80°C were thawed on ice for 5 minutes. 5 μ l of ligation mix prepared from ligation of desired combination of vector and cDNA/PCR Product was incubated with competent cells on ice for 20 minutes. Next, these E.Coli cells were given a heat shock at 42°C for 45 seconds followed by incubation on ice for 2 minutes. After this, E.Coli cells were incubated with 800 μ l of LB medium at 37°C for 1 hour with vigorous shaking. Finally the cells were centrifuged at 11000rpm for 2 minutes and cell pellet was plated on LB-agar plate made with requisite antibiotic.

3.10 DNA Restriction Digestion

DNA restriction digestion was performed for cloning purposes. The required DNA was digested with restriction endonucleases under temperature conditions as specified by the manufacturer. Following reaction mix was prepared for the 30 μ l digestion reactions:

3 μ l	10X Buffer
1 μ g-2 μ g	DNA

2U/ μ l	Restriction Endonuclease (20U/ μ l)
q.s.	H ₂ O

3.11 Cloning

3.11.1 TA Cloning

TA cloning was done in pGEMT Easy Vector, mostly for In Situ Hybridization Probe synthesis. The desired PCR products/cDNA were first ligated into pGEMT Easy vector as follows:

5 μ l 2X Rapid Ligation Buffer
3 μ l purified PCR Product/cDNA
1 μ l pGEMT Easy Vector
1 μ l T4 DNA Ligase

This ligation mix was kept at room temperature for 1 hour or overnight. Subsequently, the ligation mix was transformed into competent cells to get bacterial clones with desired plasmid.

3.11.2 Cold Fusion

The desired vector was linearized by appropriate restriction enzymes. More than one insert (or as required) was amplified by PCR. For PCR amplification of the insert, both forward and reverse primers were designed such that their respective 5' ends have 15 base pair homology with neighboring sequence (in the final construct). A restriction enzyme site was also inserted in the primer next to homology sequence, so that the insert can be digested out for another application. A typical primer sequence was: 5'--vector sequence (15bp) -- restriction enzyme site -- insert specific sequence (20bp) -- 3'. Finally the reaction mix with vector and inserts was prepared as follows:

1 μ l linearized vector (50-100ng)
1 μ l PCR inserts/cDNA (50-100ng)
0.4 μ l 5X master mix

This reaction mix was then incubated for 5 minutes at room temperature followed by 10 minutes on ice. Lastly, the competent E.Coli cells were transformed with reaction mix and cultured overnight on LB-agar plate.

3.11.3 Cloning *id4* Overexpression Constructs

Full length cds of *id4* was PCR amplified and fused to viral 2A self-cleaving peptide along with a fluorescent reporter GFP or mCherry with cold fusion technology under the control of endothelial specific *fli1a* promoter (Covassin et al., 2006) to obtain *Tg(fli1:id4-2A-mCherry)* or *Tg(fli1:id4-2A-GFP)*. 12pg of plasmid along with 15pg Tol2 (Transposase) RNA was injected into the one cell staged embryos. Mosaic embryos having the transgene were used for experiment at requisite stage (*id4* overexpression in *Tg(7xTCF-Xla.Siam:nlsmCherry)^{ia5}*) or raised to obtain the F0 carriers for the rescue experiments.

3.12 Plasmid DNA Isolation

Mini-Prep plasmid isolation method was used to obtain concentrated and purified plasmid DNA for various downstream processes. Briefly, one bacterial colony was inoculated per tube containing 4ml LB medium with appropriate anti-biotic, overnight in a shaker incubator at 37°C. The following day bacterial culture was precipitated by centrifuging it at 4000 rpm for 10 minutes using a table top centrifuge. Following this, plasmid DNA was isolated from the bacterial pellet using GeneJET Plasmid Miniprep kit (Thermo Scientific), according to manufacturer's instructions. Finally, plasmid was eluted in 30µl of sterile/autoclaved water.

3.13 In situ Hybridisation

3.13.1 Probe Synthesis

The PCR product of the gene of interest was cloned in pGem-T Easy vector. This vector was then linearized with the appropriate restriction enzyme to obtain templates for probe synthesis. 10µl Reaction mixtures including linearized plasmid (1µg), 5x Transcription Buffer (2µl), DTT 0.1M (1µl), DIG 10x(1µl), RNase inhibitor (0.5 µl) and (Sp6/T7) RNA Polymerase (0.5 µl) were kept at 37°C for 2 hours for probe synthesis. After this, the reaction mixture was incubated with 1µl of DNase for 15 minutes at 37°C to digest the DNA template from reaction. The probe synthesis was stopped and probe RNA was eluted in 30 µl of nuclease free water from a cleanup column of RNA Clean and Concentrator-5 kit according to

manufacturer's instructions. Finally, the eluted RNA probe was diluted in HM+ at a concentration of 10ng/μl and stored at -80°C.

3.13.2 Embryo/Adult Heart preparation for in situ hybridization

Embryo Fixation

PTU was added in the egg water of developing embryos to stop the pigmentation at 24 hpf till the embryos were harvested for fixation. 30 μl of 10 mg/ml pronase was also added to dechorionate the embryos. At the requisite stage, the embryos were harvested and washed twice for 5 minutes with PBS. After this, the embryos were fixed with 4% PFA overnight at 4°C. Next day the fixed embryos were washed again with PBS twice for 5 mins and dehydrated by series of 5 mins washes in methanol dilutions (diluted in PBS) i.e 25%, 50%, 75% methanol and were eventually brought in 100% methanol. The dehydrated embryos were then kept at -20°C for long term storage.

Adult Heart Fixation

The adult fish was sacrificed by tricaine over dose to harvest the heart. The heart was then rinsed quickly in PBS followed by overnight fixation in 4%PFA. Next day the fixed heart was processed and dehydrated in the same way as mentioned for the embryos and stored at -20°C in 100% methanol until required for in situ hybridization.

3.13.3 In situ Hybridization Day 1: Probe Hybridization

The dehydrated embryos/adult heart samples stored in 100% methanol were rehydrated to PBS by a series of 5 minute washes in 75%, 50%, 25% Methanol/PBS dilutions and eventually in PBS. This was followed by four washes of 5 minutes each in PBT. The embryos/adult heart tissue were then permeabilized in Proteinase K. For permeabilization, 10μg/ml Proteinase K was prepared in 0.1% PBT and samples were incubated in it for following time periods:

Adult Hearts: 50 minutes at 37°C

Embryos 24 hpf : 10-15 minutes at RT

 48-60 hpf : 25 minutes at RT

 72 hpf : 30minutes at RT

The permeabilization reaction was stopped by fixing the sample in 4%PFA for 20 minutes at RT. This was followed by four PBT washes of 5 minutes each and then the embryos/adult heart were incubated in pre-hybridization buffer (HM+) for 2-5 hours at 70°C. After pre-hybridization, the embryos/adult hearts were incubated with RNA probe overnight at 70°C.

3.13.4 In situ Hybridization Day 2: Unbound Probe Removal

Prior to start of day 2, the following solutions of HM- and its dilutions in 2xSSC were warmed at 70°C: 100%HM-, 75%HM-/2xSSC, 50%HM-/2xSSC, 25%HM-/2xSSC, 2xSSC, 0.2xSSC.

After these solutions were warmed, the RNA probe was removed and hybridized embryos/adult hearts were washed with these solutions for 10 minutes at each step in the following order at 70°C:

1. 100%HM-
2. 75%HM-/2xSSC
3. 50%HM-/2xSSC
4. 25%HM-/2xSSC
5. 2xSSC (2 times)
6. 0.2xSSC (2 times 30 minutes each)

Next, the embryos were transferred to 100% PBT from 0.2xSSC by a series of washes at room temperature. These were 10 minute washes with various dilutions of 0.2xSSC/PBT solutions in the following order:

1. 75% 0.2xSSC/PBT
2. 50% 0.2xSSC/PBT
3. 25% 0.2xSSC/PBT
4. 100% PBT (2 times)

The washed embryos were now incubated in blocking buffer for 3 hours at room temperature. After blocking, the embryos were kept overnight in 1:10,000 dilution of anti-DIG antibody in blocking buffer at 4°C.

3.13.5 In situ Hybridization Day 3: Unbound Antibody Removal and Staining

The unbound antibody was removed by six PBT washes of 15 minutes each. This was followed by 3 washes of 5 minutes each in alkaline tris buffer. Finally, the washed embryos were kept for staining in staining solution in dark at room temperature. The staining duration was probe specific ranging from several hours to a couple of overnights. The over-night incubation were done at 4°C. The staining was stopped by washing the embryo/hearts with PBT 3 times for 5 minutes each. This was followed by fixing the stained embryos/hearts in 4%PFA for 2 hours at room temperature. After this, the PFA was removed by 3 washes of 5 minutes each with PBT. The embryos/adult hearts were then dehydrated by a series of washes in methanol/PBS dilutions in the following order :

1. 25%MeOH/PBS (5 mins)
2. 50%MeOH/PBS (5 mins)
3. 75%MeOH/PBS (5 mins)
4. 100%MeOH/PBS (5 mins)

Finally, the dehydrated embryos/adult hearts were stored in 100%MeOH overnight at -20°C.

3.13.6 In situ Hybridization: Microscopy and Imaging

Next morning, the embryos/adult hearts were rehydrated back to PBS by following the dehydration steps in reverse order. These embryos were then soaked in 25% and 50% glycerol for at least 2 hours on each step and eventually were brought to 100% glycerol for imaging. Alternatively, the rehydrated embryos/hearts were mounted in 2% agarose as well for imaging.

3.14 TALEN (Transcription Activator-Like Effector Nucleases) Induced Mutagenesis

3.14.1 TALEN Designing

id4 TALEN was targeted against its bHLH domain, which is the main functional domain. To design the TALEN, the genomic region coding for bHLH domain was pasted on the TALEN targetor page <https://tale-nt.cac.cornell.edu/node/add/talen>. The TALEN was then cloned into destination vectors according to the following 5 day protocol:

3.14.2 TALEN Assembly Day 1

First 10 TALEN RVD plasmids for both left and right arm were cloned in pFUS_A vector and the remaining RVDs from 11 to N-1 (N is total no. of RVDs in a particular arm) were cloned in pFUS_B vector. 20µl ligation reaction was prepared for each of the destination vectors separately as follows:

150ng (each RVD plasmid)
 150ng (pFUS_A or pFUS_B)
 1µl BsaI
 1µl T4 DNA Ligase
 2µl 10X T4 DNA Ligase Buffer
 Nuclease Free H₂O upto 20µl

This ligation mix was kept in a PCR cycler under following temperature conditions:

Step	Temperature	Duration
1	37°C	5 mins
2	16°C	10 mins
Repeat steps (1-2) 10 times		
3	50°C	5 mins
4	80°C	5 mins

Table 3.4: Temperature conditions used for TALEN assembly day1 ligation reaction.

After this, the ligation mix was treated with Plasmid-Safe Nuclease to remove all the unligated fragments of DNA. For this purpose, 1µl Plasmid-Safe Nuclease and 1µl 10mM ATP was added to ligation mix which was incubated at 37°C for 1 hour.

5µl of the ligation mix thus obtained was used for bacterial transformation. The transformed bacteria were cultured on spectinomycin plates (treated with 40µl of 20mg/ml X-Gal 20 mins before plating bacteria) overnight at 37°C.

3.14.3 TALEN Assembly Day 2

Atleast 4 white colonies were screened for each of destination vectors of each arm by colony PCR. The tip with which the bacterial colony was added in PCR mix was also put in the bacterial medium for overnight culture later on. The PCR conditions used for colony PCR with pCR8_F1 and pCR8_R1 primers as follows:

Step	Temperature	Duration
1	95°C	5 mins
2	95°C	15 secs
3	55°C	30 secs
4	72°C	30 secs
Repeat steps (2 - 4) 35 times		
5	72°C	5 mins

Table 3.5: Temperature conditions used for colony PCR on day2 of TALEN assembly.

After PCR, all the amplified PCR products were resolved on a 1% agarose gel. A bacterial clone was selected for overnight culture, if on the gel, a laddering of its PCR products was seen with the highest band on ~1.2Kb (for destination vector with 10RVDs i.e pFUS_A) or ~800bp (for destination vector with 5-6RVDs i.e pFUS_B).

3.14.4 TALEN Assembly Day 3

Mini-Prep plasmid isolation was done on the bacterial cultures incubated overnight to obtain the destination vectors for both arms of TALEN. The pFUS_A and pFUS_B plasmids with RVDs thus obtained were then ligated into bigger destination vectors pTAL_DD (for left arm) and pTAL_RR(for right arm) along with the last repeat of each arm. 20µl ligation reaction was prepared for each of the pTAL vectors separately as follows:

- 150ng pFUS_A
- 150ng pFUS_B
- 80ng of pTAL_DD or pTAL_RR
- 150ng of pLR (vector containing last half-repeat of each arm)
- 1µl Esp3I
- 1µl T4 Ligase
- 2µl 10X T4ligase buffer
- Nuclease Free H₂O upto 20µl

The ligation mix was kept in PCR cycler under following temperature conditions:

Step	Temperature	Duration
1	37°C	5 mins
2	16°C	10 mins
Repeat steps (1-2) 10 times		

3	37°C	15 mins
4	80°C	5 mins

Table 3.6: Temperature conditions used for TALEN assembly day3 ligation reaction.

5µl of this ligation was used to transform bacteria, which was cultured on ampicillin plates overnight (these plates were also pre-treated with X-Gal like spectinomycin plates on day1).

3.14.5 TALEN Assembly Day 4

At least 4 white bacterial colonies were screened from the plates cultured overnight. The method for screening was colony PCR and similar PCR conditions as Day2 were followed, only primers used were different (TAL_F1 and TAL_R2). A bacterial clone was considered to be correct, if on the agarose a faint band around 2-3KB was observed and bands of the lower size showed a smearing effect. These correct clones were cultured overnight to obtain final talen vectors for left and right arm.

3.14.6 Talen Assembly Day 5

Mini prep plasmid isolation was done to obtain full length TALEN vectors from overnight cultures.

3.14.7 TALEN mRNA Synthesis

For mRNA synthesis, the TALEN vectors were first linearized as follows:

- 3-4µg of TALEN plasmid
- 5µl 10X CutSmart Buffer (NEB)
- 0.3µl 100X BSA
- 2µl NotI-HF
- Nuclease Free H₂O upto 50µl

This linearization reaction mix was kept at 37°C for 4 hours. After 4 hours, the linearized and unlinearized vectors were run on a 1% agarose to check if vector digestion worked. The linearized vector was then eluted from the gel by using GeneJET Gel Extraction Kit (Thermo Scientific), according to manufacturer's instructions.

To prepare mRNA from linearized TALEN vectors, mMMESSAGE mMACHINE SP6 Kit (Ambion), was used for invitro mRNA transcription and following reaction was prepared:

- Nuclease Free H₂O upto 30µl
- 15µl 2X NTP/CAP

3µl 10X Reaction Buffer
1µg Linearised TALEN Vector
2µl SP6 Enzyme mix

This reaction mix was kept at 37°C for 2 hours. After this, the reaction mix was incubated with 1µl of TURBO DNase for 15 minutes at 37°C to remove template DNA. Finally, the TALEN mRNA was retrieved by column purification of the reaction mix using RNA Clean & Concentrator-5 Kit, according to manufacturer's instructions.

3.15 Heat Shock Experiments

3.15.1 Heat Stress of *id4*^{-/-}

The embryos from incross of *id4*^{+/-} or cross between *id4*^{+/-} and *id4*^{-/-} were heat stressed for 1 hour at 37°C on a heat block in petridish, from 48 hpf to 49 hpf. After heat shock, the embryos were brought back to normal zebrafish raising temperature of 28°C and were analyzed at 77 hpf.

3.15.2 Heat Shock of *Tg(hsp70l:bmp2b)* or *id4*^{-/-} / *Tg(hsp70l:bmp2b)*

The embryos were heat shocked for 30 mins at 37°C in a B.O.D incubator at 26 and 48 hpf. At 52 hpf, the heat shocked embryos were sorted for ectopic vasculature growth as previously described (Wiley et al., 2011) and fixed for further experiments.

3.16 Whole mount Immunohistochemistry

Whole mount immunohistochemistry was performed on embryos from an incross of *id4*^{+/-} or cross between *id4*^{+/-} and *id4*^{-/-} at 52 hpf and 77 hpf for Alcam staining. These fish were in *Tg(kdrl:ras-mcherry)*^{s896} background to visualize the endocardium.

Embryos at the requisite stage were briefly washed with PBS and fixed with 4% PFA for 1 hour at room temperature. After this, the embryos were washed 3 times with PBT with each wash being 10 minutes long. Next, the washed embryos were permeabilized for 3 hours at room temperature in permeabilization solution. The permeabilized embryos were then incubated with blocking buffer for 1 hour at room temperature. After blocking, the embryos were incubated with following primary antibodies (diluted in blocking buffer) overnight at 4°C:

Primary Antibody	Dilution	For staining
Zn8	1:10	Alcam
DsRed Polyclonal Antibody	1:300	mCherry, to image endocardium

Table 3.7: List of primary antibodies used, along their respective dilutions and protein targets.

Next day, the embryos were washed thrice for 10 minutes each time with PBT to remove the unbound primary antibody. Then the embryos were incubated in dark with following fluorescent secondary antibodies diluted 1:300 in PBT for 2 hours at room temperature:

Secondary Antibody	For staining
Goat Anti Mouse Alexa Fluor 488	Zn8(Alcam)
Goat Anti Rabbit Alexa Fluor 568	DsRed (endocardium)

Table 3.8: List of secondary antibodies used, and their target primary antibodies.

Finally, the stained embryos were washed thrice in PBT for 10 minutes each time and imaged using LSM 700 confocal microscope.

3.17 High Resolution Melt (HRM) Analysis

HRM Analysis was done on PCR products for genotyping purposes. PCR was performed on the genomic DNA using the primers flanking the region of mutation. The following reaction mix was prepared for PCR:

- 5 µl 2x Maxima Sybr Green qPCR Master Mix
- 1 µl 10 µM forward primer
- 1 µl 10 µM reverse primer
- 1 µl genomic DNA
- 2 µl Nuclease free water

After the PCR, HRM analysis was performed on the PCR products to segregate them on the basis of melting temperature and thus identify the different genotypes. Following temperature conditions were used for PCR and HRM analysis:

Step	Temperature	Duration	Step Description
1	95°C	10 minutes	Polymerase activation

2	95°C	10 seconds	PCR Cycling, 35 cycles
	60°C	15 seconds	
3	95°C	15 seconds	High Resolution Melt Analysis
	55°C	15 seconds	
	95°C	15 seconds	

Table 3.9: Temperature conditions used for PCR followed by HRM Analysis.

3.18 Statistical analysis

Statistical analysis was performed using GraphPad software. Data are presented as mean \pm sem. p-values were calculated by Student's t test. $p < 0.05$ was considered as statistically significant.

3.19 Imaging

3.19.1 Live Imaging Spinning Disk Microscopy

Live Imaging with Spinning Disk microscope was performed to assess the blood flow in the larvae.

At 77 hpf, the heat stressed larvae were anaesthetized in 0.004% tricaine and embedded with 1.5% low melt agarose with 0.004% tricaine in glass bottom dishes. The embedded larvae were then washed in E3 medium for 15 mins to remove remaining tricaine. Afterwards, brightfield live imaging was performed at the AV canal to observe the blood flow using Cell Observer SD, Spinning disk microscope.

3.19.2 Imaging with confocal microscope LSM 700/780

Confocal microscopy was performed for imaging Wnt reporter and Alcam antibody stained embryos. The requisite embryos were mounted in 1.5% low melt agarose and imaged in Z planes. The optical sections were 1.5 μm thick.

3.20 Image Processing

The images obtained from LSM 700/Spinning Disc microscopes were processed using softwares like Zen, ImageJ and Imaris.

3.21 Bmp signaling inhibition

Previously established Bmp signaling inhibitor, Dmh1 (sigma) (Wiley et al., 2011; Neely et al., 2012) was used to inhibit Bmp signaling in the embryos. 10 μ m Dmh1 was added to the embryos in egg water from 25 or 35 hpf until 52 hpf. After this, the embryos were washed with PBS and fixed with 4% PFA for in situ hybridization.

4. Results

4.1 *id4* is expressed in the developing AVC endocardium and the adult atrium.

I was interested to unravel the role of *id4* in cardiac development, for which the first step was to understand its expression pattern. To determine the spatio-temporal expression pattern of *id4*, I performed whole mount in situ hybridization in the embryo as well as in the adult heart. At 52 hours post fertilization (hpf), *id4* is highly expressed in the brain and eye of the zebrafish embryo (Fig. 4.1A) which is consistent with previously reported expression data on mouse development (Mouse Genome Informatics, MGI). In addition to this, I observed the expression of *id4* in the embryonic heart (Fig. 4.1A, C), which has not been reported previously (result independently validated by collaborator Dogra, D.). Around 2 days post fertilization (dpf), the cardiac expression of *id4* is concentrated in the AVC of the embryonic heart and little expression can be observed at the inflow tract as well (Fig 4.1C).

Next, I wanted to check if cardiac expression of *id4* is maintained until the adulthood, for which I performed whole mount in situ hybridization on adult hearts. Interestingly, in adult zebrafish hearts 5 months post fertilization (mpf) its expression in addition to the AVC gets highly enriched in the atrial chamber (Fig. 4.1D') as opposed to embryonic heart, where only low level of expression can be detected at the atrial inflow tract (Fig. 4.1C). To validate the adult cardiac chamber specific expression pattern, I performed quantitative RT PCR analysis on samples of atrial and ventricular RNA individually, which confirmed that *id4* is indeed an atrial exclusive gene with an average fold change of 125 (Fig. 4.1E). Further on, I wanted to find out the layer of heart in which *id4* is expressed. For this purpose I performed in situ hybridization on *clo* mutant, which lacks endocardium (Stainier et al., 1995). At 52 hpf, *clo* mutant embryos did not show any *id4* expression (Fig. 4.1B) in their heart, further indicating that *id4* expression is restricted to the endocardial layer during early development.

To validate the *id4* layer of expression in the adult heart, I sectioned the in situ hybridization stained hearts. Interestingly, in these sections I observed a fine layer of expression at the luminal side of the atrial tissue and the cardiac valve (Fig. 4.1F). This indicates that *id4* is expressed in the endocardium of the adult heart as well. (Certain lines in this section 4.1 have been quoted verbatim from Ahuja et. al, Dev. Biol. 2016; 412(1): 71-82).

Taken together, this data indicates *id4* as a novel gene expressed during cardiac development.

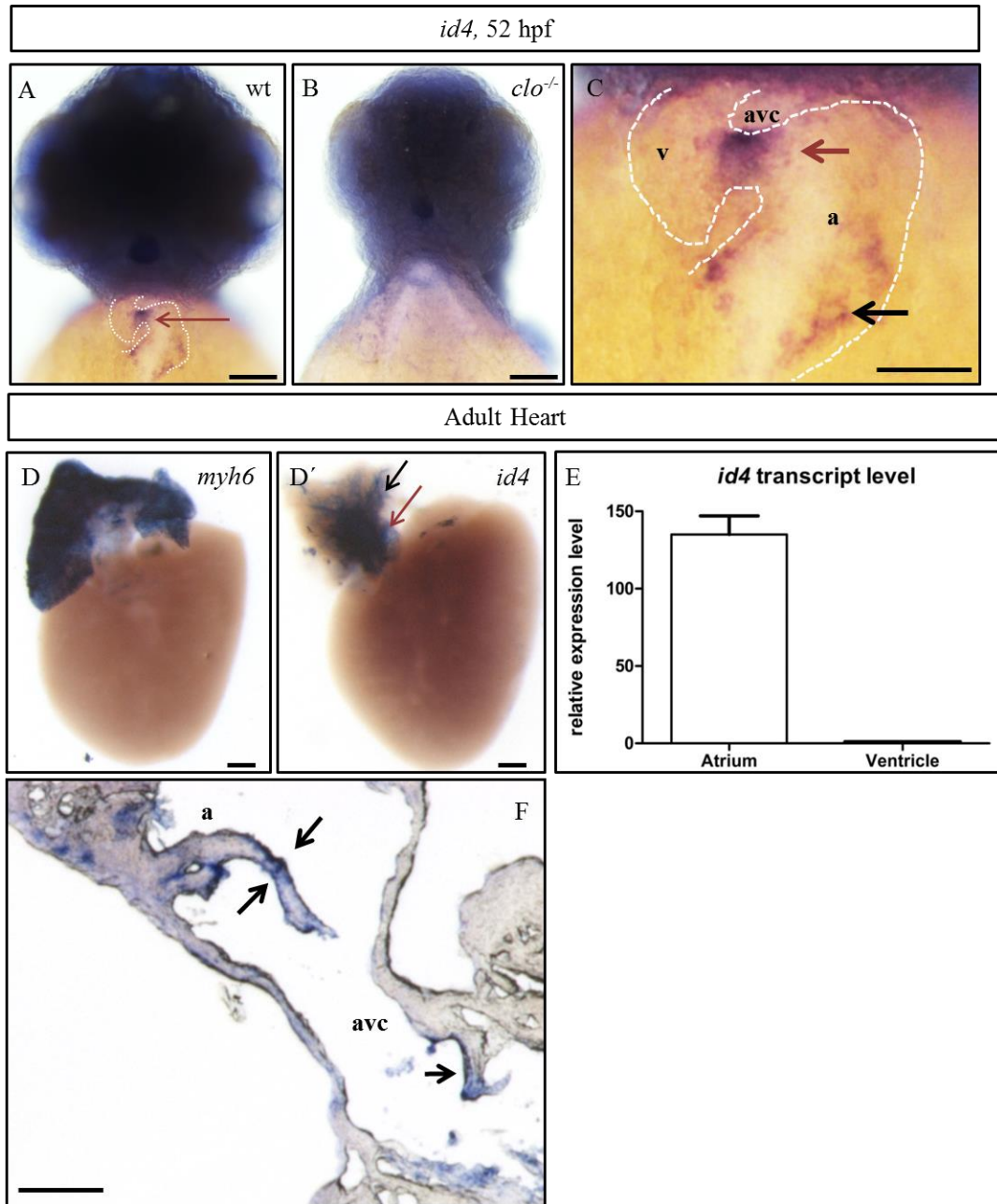


Figure 4.1. Expression analysis of *id4* in development and adult heart by whole mount in situ hybridization. (A) At 52 hpf *id4* is expressed in brain and heart of zebrafish embryos. In the heart, its expression is enriched at the AVC and little expression is present at the inflow tract as well. (B) Lack of *id4* expression in *clo* mutants, suggests that it is expressed in the endocardium. (C) Higher Magnification image of *id4* expression in the embryonic heart clearly shows its expression at the AVC (red arrow) and inflow tract (black arrow). (D') In the adult heart, *id4* is expressed in the atrium (black arrow) and AV canal (red arrow). (D) *myh6* (atrial MHC) was used as positive control for atrium. (E) qPCR confirmation of *id4* expression in the atrium of the adult zebrafish heart. (F) A section through whole mount in situ hybridization stained adult heart. Arrow heads indicate endocardial expression of *id4* in adult atrium and avc. Scale bar for Fig. 1A, B, D, D', F 100 μ m and Scale bar for Fig. 4.1C, 50

μ m. a, atrium; avc, atrioventricular canal; v, ventricle. Figure reprinted with permission from Ahuja et. al, Dev. Biol. 2016; 412(1): 71-82. Result in Figure 4.1A was validated in an independent experiment by collaborator Dogra, D.

4.2 Generation of *id4* mutants using TALEN Technology

To unravel *id4* function, I made a mutation in *id4* using transcription activator-like effector nuclease (TALEN) technology (Cermak et al., 2011). The two TALEN arms were targeted to the genomic region encoding for Id4 HLH domain. These TALEN arms were composed of the following RVDs: HD NI NN NG NI NI NI NN NG NN NN NI NI NI NG HD HD NG HD and NN HD NI NN NN NG HD HD NI NN NI NI NG NI NG NI NN (Fig. 4.2A). The TALEN activity was tested by RNA injection followed by high resolution melt (HRM) analysis of the PCR amplicon spanning the target site in F0 animals (Fig. 4.2B). The altered melt profile of injected F0 animals indicated a possible genomic lesion, thus confirming that TALEN was working. In F1 animals, using the same method (Fig. 4.3C), I was able to isolate the allele *id4*^{bnsl8}, a 5 bp deletion (Fig. 4.3A) leading to premature stop codon and formation of truncated protein (Fig. 4.3B). The TALEN approach was found to be highly specific as no phenotypes segregating independently of the induced genomic lesion were observed in intercrossed F1 *id4*^{bnsl8} heterozygotes. Surprisingly, animals homozygous for *id4*^{bnsl8} are phenotypically indistinguishable from their siblings (Fig. 4.3D, E), grow normally and become fertile adults suggesting some functional redundancy of Id4 with other proteins of the Id family. (Certain lines in this section 4.2 have been quoted verbatim from Ahuja et. al, Dev. Biol. 2016; 412(1): 71-82).



Figure 4.2. TALEN design for targeting *id4*. (A) Left and right TALEN arms attached with FokI DD and FokI RR were targeted to the genomic region of *id4* in exon 1 corresponding to its bHLH domain. (B) The efficacy of TALEN was judged by the HRM analysis of the PCR product of targeted

region. Arrow indicates altered melt profile of TALEN injected embryos. RVD: repeat-variable diresidue, N: Nucleotide. Modified figure reprinted with permission from Ahuja et. al, Dev. Biol. 2016; 412(1): 71-82.

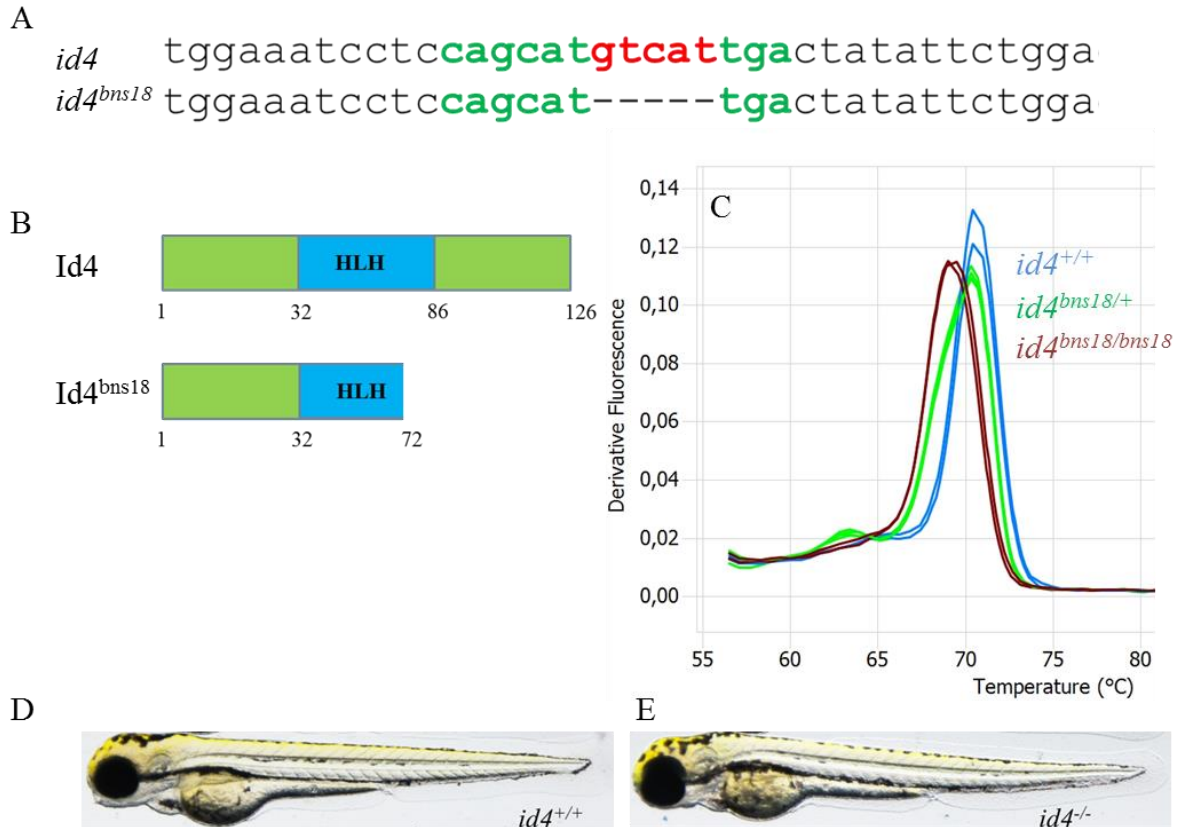


Figure 4.3. TALEN induced mutagenesis to generate an *id4* loss-of-function allele. (A) *id4^{bns18}* contains a 5 bp deletion in the first exon which encodes the bHLH domain. (B) This deletion is predicted to lead to the formation of a truncated protein. (C) High Resolution Melt analysis was used to distinguish the WT siblings from heterozygous and homozygous mutants. (D, E) Overall morphology of *id4^{-/-}* larvae is indistinguishable from their *id4^{+/+}* siblings at 72 hpf. Modified figure reprinted with permission from Ahuja et. al, Dev. Biol. 2016; 412(1): 71-82.

4.3 *id4* mutants are susceptible to stress induced retrograde blood flow at the AV canal.

As there were no observable abnormalities in homozygous mutant animals, I made use of a conditional heat stress system. In this strategy, the embryos from a heterozygous incross were exposed to 37°C for 1 hour starting at 48 hpf. It has been shown previously that exposure to high temperature can increase heart rate (Baker et al., 1997) and consequently cardiac load, a result I could reproduce (data not shown). Following this, I analyzed the blood flow at the

AVC at 77 hpf because by this time the zebrafish heart has fully established unidirectional blood flow. High resolution bright field spinning disk microscopy at this stage revealed that mutant hearts have a significantly higher susceptibility to show retrograde blood flow at the AV canal at the time of ventricular systole, as compared to siblings (Fig. 4.4c, *id4* wt video1, *id4* mut video2). This finding can be compared to mitral valve regurgitation, where ailing valves are unable to prevent retrograde blood flow. To incorporate the regurgitating blood, the atrium of *id4*^{-/-} hearts appears expanded at the end of ventricular systole (Fig. 4.4b), unlike the atrium in *id4*^{+/+} siblings (Fig. 4.4a). This expanded atrium clearly shows the extent of blood regurgitation in *id4*^{-/-} hearts as compared to their *id4*^{+/+} siblings. Taken together, these results suggest a crucial function of *id4* in the development of the atrioventricular valves. (Certain lines in this section 4.3 have been quoted verbatim from Ahuja et. al, Dev. Biol. 2016; 412(1): 71-82).

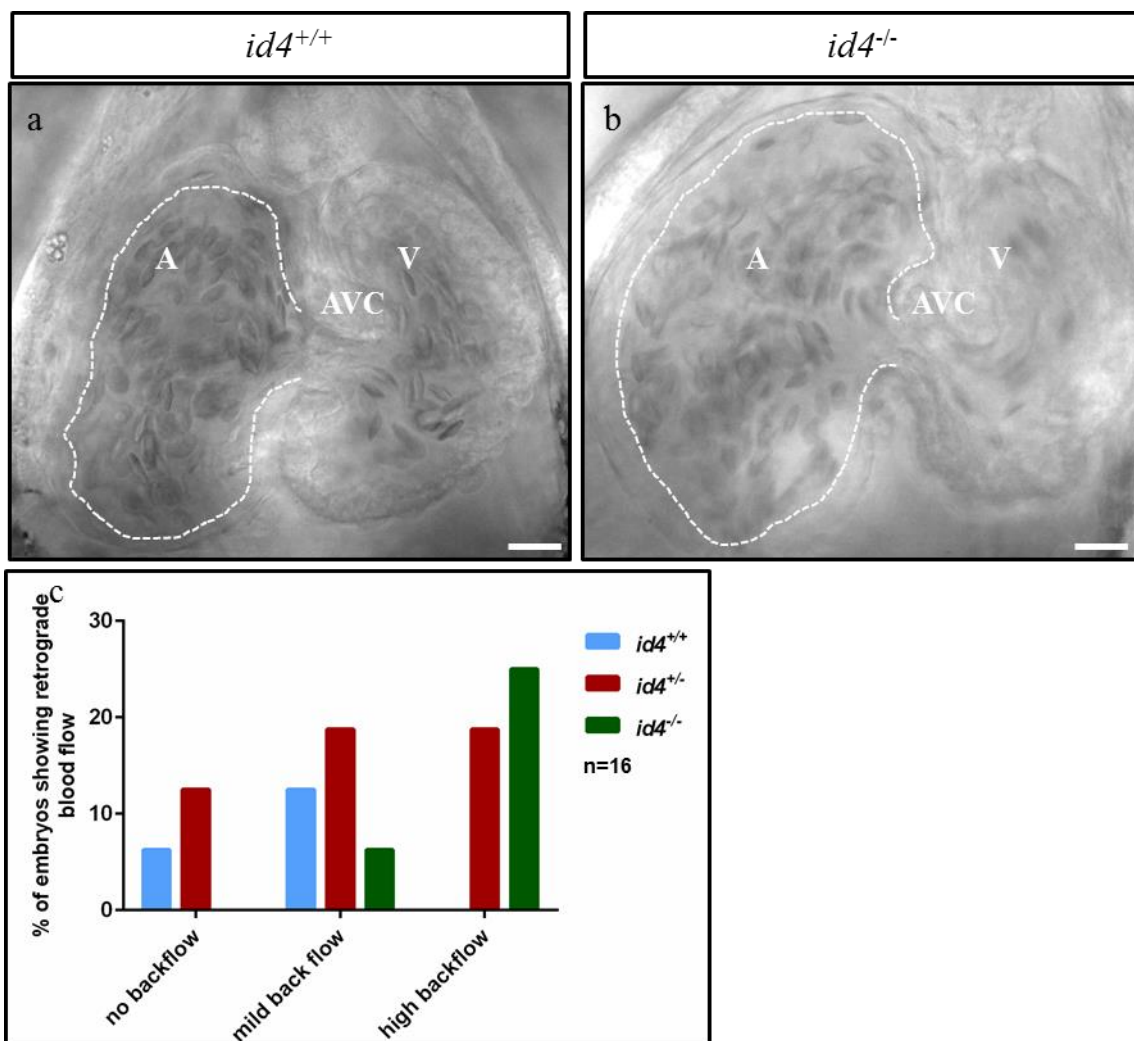


Figure 4.4. *id4* mutant larvae exhibit retrograde blood flow after heat stress conditions. Embryos from an incross of *id4* heterozygous animals were exposed to heat stress at 48 hpf for 1 hour at 37°C,

followed by bright field spinning disk microscopy. (a, b) Single frames (at end of ventricular systole) from blood flow movies of *id4*^{+/+} and *id4*^{-/-} siblings respectively. (c) Quantification of embryos showing retrograde flow. Scale bar, 20 μm (A, Atrium; AVC, Atrioventricular Canal; V, Ventricle). Figure reprinted with permission from Ahuja et. al, Dev. Biol. 2016; 412(1): 71-82.

4.4 *id4* mutants exhibit reduction and mis-regulation of developmental markers of the atrioventricular canal and cardiac valve.

For more than a decade now, the field of zebrafish heart development has used well established markers to analyze and characterize AV canal and valve development. These markers include myocardial genes like *bmp4*, *tbx2b*, *cspg2a* and endocardial genes like *spp1* and *has2* (Fig. 4.5, Table 4.1). I made use of whole mount in situ hybridization to analyze the expression pattern of these genes in *id4* mutants at 52 hpf. While the expression of some markers like *tbx2b* and *has2* appeared unchanged, others showed altered expression patterns in *id4* mutants. *bmp4* and *cspg2a* are initially expressed in the whole heart tube at around 37 hpf and become restricted to the AV boundary by 48 hpf (Walsh and Stainier, 2001). However in *id4* mutants, the *bmp4* expression domain was expanded to the entire ventricle in addition to the AVC. The *cspg2a* (*versican*) expression domain was also expanded at the AVC and its ectopic expression was detected in the atrium including the inflow tract as well. These mis-regulated AVC markers point towards a probable expansion of the AVC region. Interestingly, *spp1* (osteopontin) expression, contrary to other mis-regulated markers, was considerably reduced in *id4* mutants. The lack of *spp1* expression, which marks later stages of valve development (Peal et al., 2009), can be indicative of a problem in valve maturation. (This passage has been quoted verbatim from Ahuja et. al, Dev. Biol. 2016; 412(1): 71-82).

Taken together, the mis-regulated expression of these marker genes is suggestive of a crucial role of *id4* in AVC development.

Gene	Mutants with highly aberrant expression	Mutants with mildly aberrant expression	Mutants with wt expression
<i>bmp4</i>	9/20	8/20	3/20
<i>cspg2a</i>	12/20	6/20	2/20

<i>spp1</i>	12/20	8/20	0/20
-------------	-------	------	------

Table 4.1. Types of expression patterns observed in *id4*^{-/-} for the dysregulated genes shown in Figure 4.5. The numerators indicate the numbers of mutants with a particular type of expression pattern and denominators indicate the total number of embryos analyzed. Modified table reprinted with permission from Ahuja et. al, Dev. Biol. 2016; 412(1): 71-82.

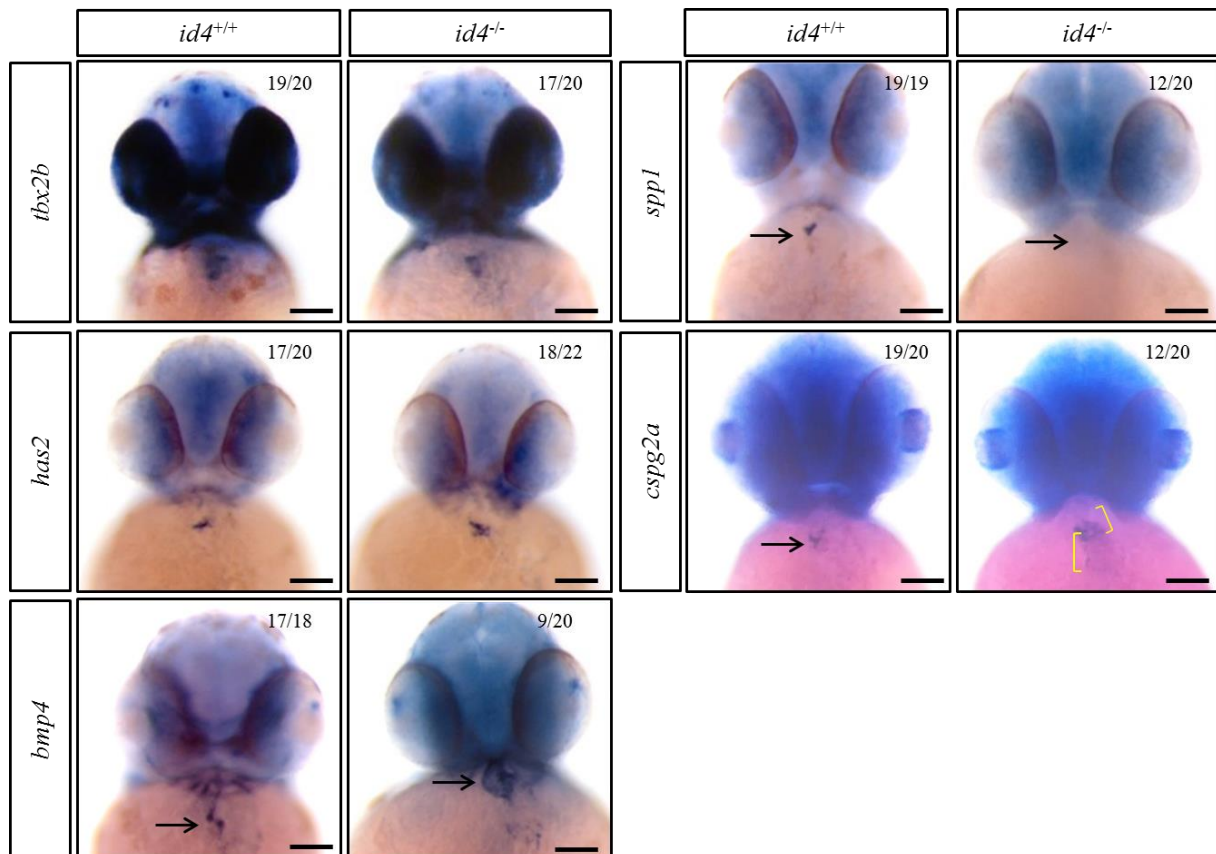


Figure 4.5. AV canal marker gene analysis in *id4* mutants at 52 hpf. Myocardial (*tbx2b*, *bmp4*, *cspg2a*) and endocardial (*has2*, *spp1*) AVC marker gene expression was analyzed in embryos from incrosses of *id4* heterozygous animals. After in situ hybridization, embryos were separated according to expression patterns and subsequently genotyped to test the associated genetic background. Amongst these markers, *tbx2b* and *has2* expression was found to be unchanged, *bmp4* and *cspg2a* were misexpressed and *spp1* expression was reduced in *id4* mutants. Scale bar, 100 μ m. Modified figure reprinted with permission from Ahuja et. al, Dev. Biol. 2016; 412(1): 71-82.

4.5 *id4* mutants show expanded Alcam expression

Another critical marker to track the valve development process is Alcam, a cell adhesion molecule of immunoglobulin superfamily, that is expressed in AVC endocardium. The

expression pattern of Alcam during zebrafish valve development has been reported previously (Beis et al., 2005). Alcam expression in the AVC endocardium during zebrafish heart development begins at 36 hpf, with one endocardial cell at the border between atrium and ventricle turning cuboidal from squamous and starting to express Alcam. Over the course of next 12 hours, the cells in the AV canal differentiate further and start showing stronger staining for Alcam. By 52 hpf, all the endocardial cells lining AV canal acquire the cuboidal shape and express Alcam as compared to squamous and Alcam negative endocardial cells present in the heart chambers. This makes Alcam as a reliable marker to track AVC development. I analyzed the Alcam expression in *id4*^{-/-} embryos at 52 and 77 hpf. At 52 hpf, I found that Alcam positive AV endocardial cells were significantly increased in both the superior and inferior AVC of the *id4* mutants by approximately 22% and 26% respectively (Fig. 4.6a, b, c). Consistent with this observation, at 77 hpf also the Alcam positive cells were found to be increased by approximately 45% and 40% in both the superior and inferior AVC of *id4* mutants respectively (Fig. 4.7a, b, c).

Taken together these data indicate that *id4* is critically required during AVC development.

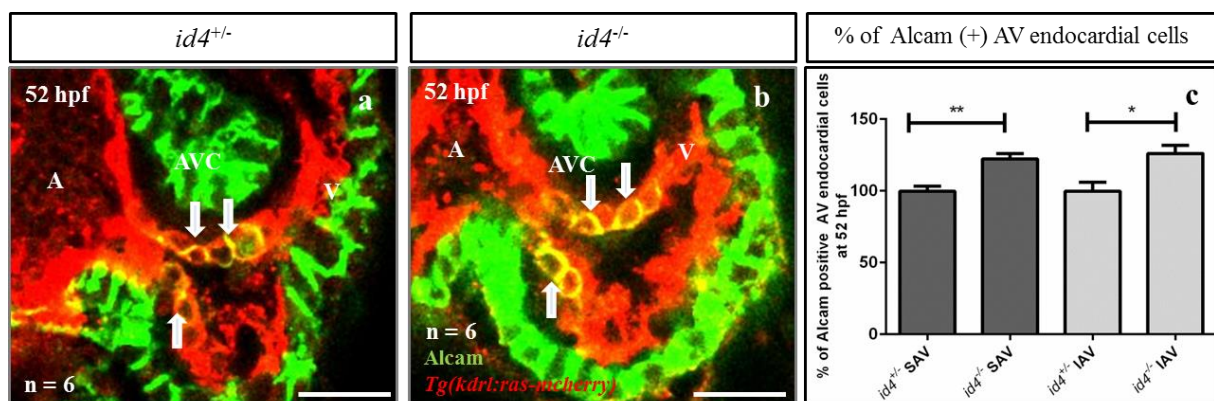


Figure 4.6. The number of Alcam positive AV endocardial cells appears to be increased in *id4* mutants. Alcam positive AV endocardial cells at 52 hpf in *id4* mutants (b) and their siblings (a). (c) Quantification of Alcam positive AV endocardial cells. (A, Atrium; AVC, Atrioventricular Canal; V, Ventricle; SAV, Superior AVC; IAV, Inferior AVC). Scale bar, 20 μ m. p-value ** - 0.0016, * - 0.0114. Figure reprinted with permission from Ahuja et. al, Dev. Biol. 2016; 412(1): 71-82.

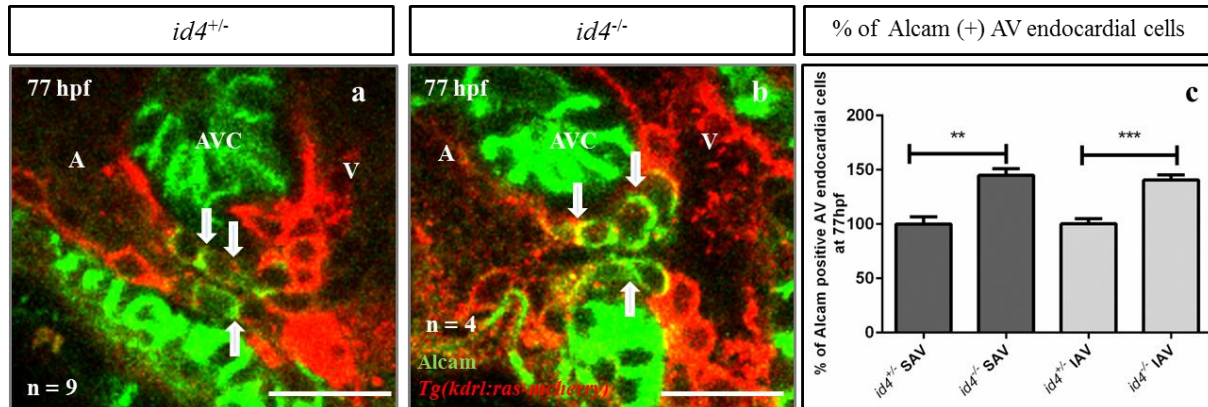


Figure 4.7. Alcam positive AV endocardial cells appear to be increased in *id4* mutants. At 77 hpf Alcam positive AV endocardial cells increase in *id4* mutants (b) as compared to their siblings (a). (c) Quantification of Alcam positive AV endocardial cells. (A, Atrium; AVC, Atrio-Ventricular Canal; V, Ventricle; SAV, Superior AVC; IAV, Inferior AVC) Scale bar, 20 μ m. p-value ** - 0.0016, *** - 0.0003. Figure reprinted with permission from Ahuja et. al, Dev. Biol. 2016; 412(1): 71-82.

4.6 *Id4* is a mediator of Bmp signaling leading to *spp1* expression.

It was clearly evident by now that the AVC development in *id4* mutants is affected, however the signaling pathway affected remained to be explored. To answer this question, I focused on two signaling molecules which showed extreme and contrasting changes with respect to each other. These were *spp1* as it was reduced, and *bmp4* which showed a clear expanded expression domain. In order to explore the Bmp signaling axis, I made use of a conditional Bmp overexpression approach. I used the previously reported Bmp overexpression line *Tg(hsp70l:bmp2b)^{fr13}* (Chocron et al., 2007) that expresses Bmp2b under heat shock promoter *hsp70*. The fact that Bmp2 and Bmp4 signal through the same receptors by mobilizing Smad1/5/8 (Hager-Theodorides et al., 2002; Miyazono et al., 2010), supported the notion of using this line to explore Bmp signaling. Stimulation of Bmp2b expression by heat shock lead to an increase in the expression of both *id4* (Fig. 4.8A, B) and *spp1* (Fig. 4.8C, D) in the brain and heart of the embryo as compared to non-transgenic siblings. These data indicate that both *id4* and *spp1* are downstream of Bmp2/4 signaling. To validate this result, I also made use of Dmh1, a previously reported inhibitor of Bmp signaling (Wiley et al., 2011; Neely et al., 2012). Embryos were incubated with 10 μ m Dmh1 in two treatment regimens: either from 25 or 35 hpf until 52 hpf, which was followed by expression analysis of *id4* and *spp1*. Indeed the expression of both *id4* and *spp1* was found to be significantly downregulated in Dmh1 treated embryos (Fig. 4.9B, C, E, F) as compared to DMSO treated

control embryos (Fig. 4.9A, D). This further confirmed that both *id4* and *spp1* are downstream of Bmp signaling.

I further tested whether Id4 can mediate Bmp signals to induce *spp1* expression. I checked this by stimulating Bmp overexpression in the *id4*^{-/-} background. Interestingly, *Tg(hsp70l:bmp2b)*^{fr13}/*id4*^{-/-} embryos did not show increased *spp1* expression (Fig. 4.10B, Table 4.2) unlike its *Tg(hsp70l:bmp2b)*^{fr13}/*id4*^{+/+} siblings (Fig. 4.10A).

This implies that Id4 is indeed a crucial mediator of Bmp signaling leading to *spp1* expression.

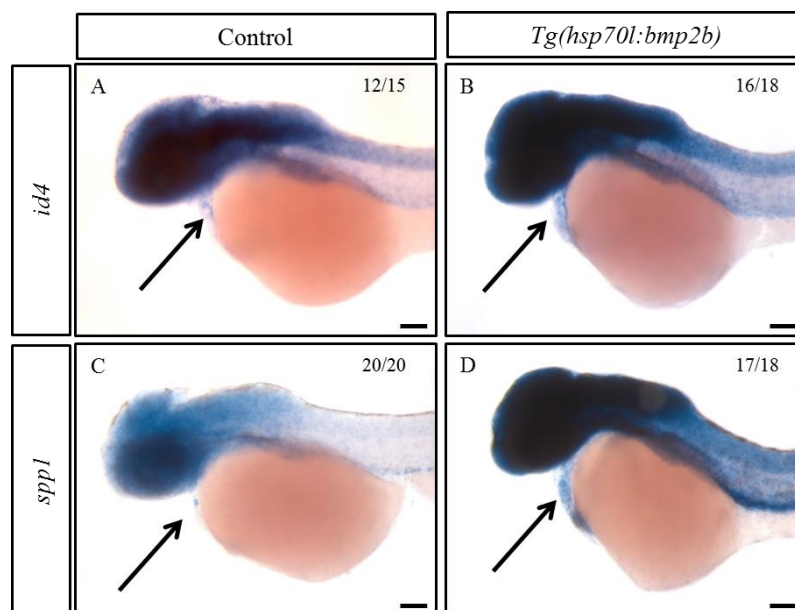


Figure 4.8. *id4* and *spp1* are downstream of Bmp Signaling. Increased expression of *id4* (A, B) and *spp1* (C, D) was observed at 52 hpf in *Tg(hsp70l:bmp2b)* embryos after heat shock at 26 and 48 hpf for 30 minutes at 37°C. Scale bar, 100 μ m. Modified figure reprinted with permission from Ahuja et. al, Dev. Biol. 2016; 412(1): 71-82.

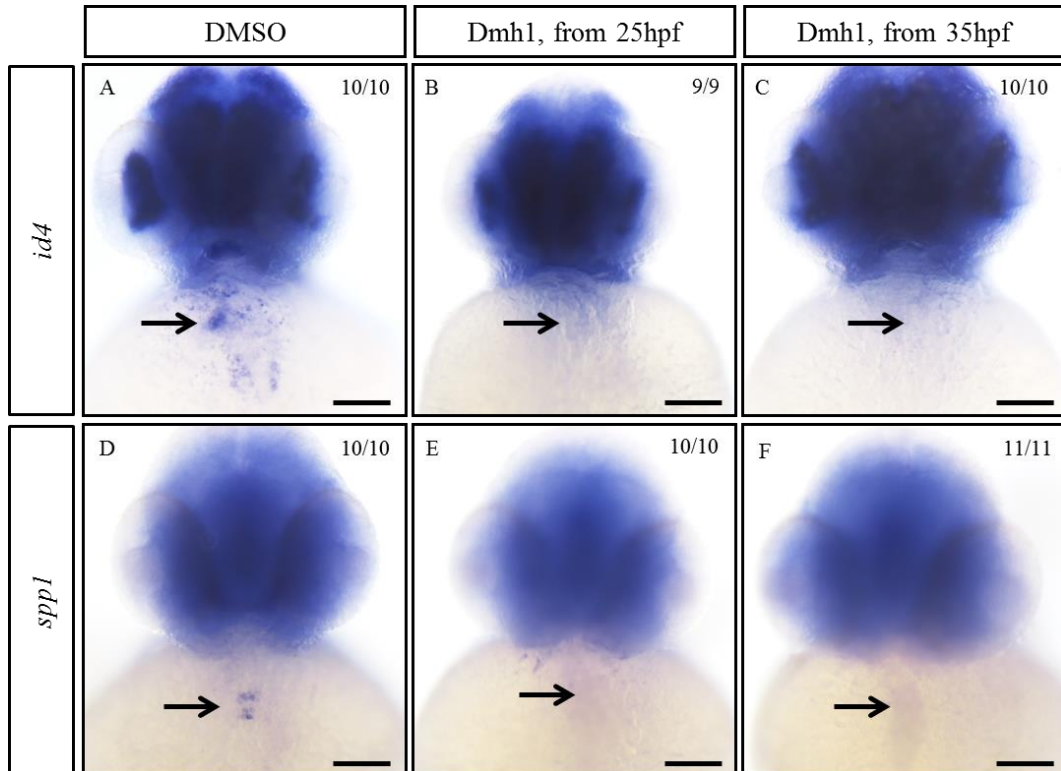


Figure 4.9. Bmp inhibitor Dmh1 treatment leads to reduction of *id4* and *spp1* expression. Wt embryos were treated with 10 μ m of Dmh1 from 25 or 35 hpf until 52 hpf. Decreased expression of *id4* (B,C) and *spp1* (E,F) was observed at 52 hpf in Dmh1 treated embryos as compared DMSO treatment where expression pattern of *id4* (A) and *spp1* (D) was unchanged. Scale bar, 100 μ m. Figure reprinted with permission from Ahuja et. al, Dev. Biol. 2016; 412(1): 71-82.

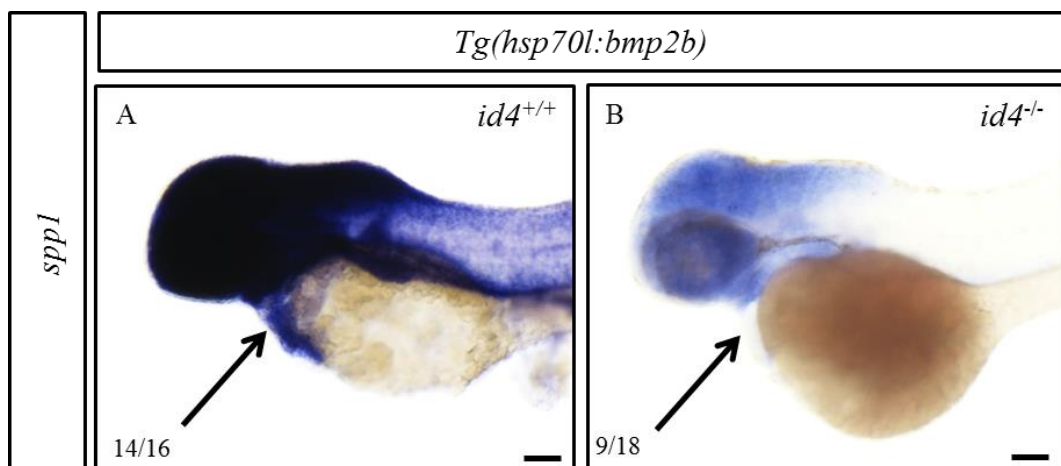


Figure 4.10. Id4 mediates Bmp Signaling leading to *spp1* expression. (A, B) *spp1* expression was examined in *id4* siblings and mutants in the *Tg(hsp70l:bmp2b)* background at 52 hpf after heat shock mediated induction of Bmp2b expression. Unlike their *id4*^{+/+} *Tg(hsp70l:bmp2b)* siblings (A), most of

the *id4^{-/-}/Tg(hsp70l:bmp2b)* (B) did not show an increase in *spp1* expression. Scale bar, 100 μ m. Modified figure reprinted with permission from Ahuja et. al, Dev. Biol. 2016; 412(1): 71-82.

Gene	Mutants with highly aberrant expression	Mutants with mildly aberrant expression	Mutants with wt expression
<i>spp1</i>	9/18	7/18	2/18

Table 4.2. Types of *spp1* expression pattern observed in *id4^{-/-}/Tg(hsp70l:bmp2b)* shown in Figure 4.10B. The numerators indicate the numbers of mutants with a particular type of expression pattern and denominators indicate the total number of embryos analyzed. Modified table reprinted with permission from Ahuja et. al, Dev. Biol. 2016; 412(1): 71-82.

4.7 *id4* mutants have higher Wnt/ β -Catenin activity in the AV Canal.

Previous data suggests that cardiac Bmp signaling functions downstream of Wnt/ β -Catenin signaling (Verhoeven et al., 2011) indicating that there might be some kind of molecular interaction also possible between Id4 and Wnt/ β -Catenin signaling. To check this hypothesis, I analyzed the level of Wnt/ β -Catenin signaling in *id4* mutants by using the previously established Wnt reporter line *Tg(7xTCF-Xla.Siam:nlsmCherry)^{ia5}* (Moro et al., 2012), which reports Wnt/ β -Catenin signaling by expressing mCherry in the nucleus of the cell. The red fluorescence can be appreciated in the developing endocardial cushions starting around 3 dpf, suggesting active Wnt/ β -Catenin signaling by this time point. At 77 hpf, I observed a significant increase in TCF reporting nuclei in both the superior and inferior cushions of *id4^{-/-}* (Fig. 4.11A, B, C, D) larvae as compared to their wild-type siblings suggesting that Id4 can negatively regulate Wnt/ β -Catenin activity.

Thus, these data suggest that *id4* mutants have elevated levels of Wnt/ β -Catenin signaling.

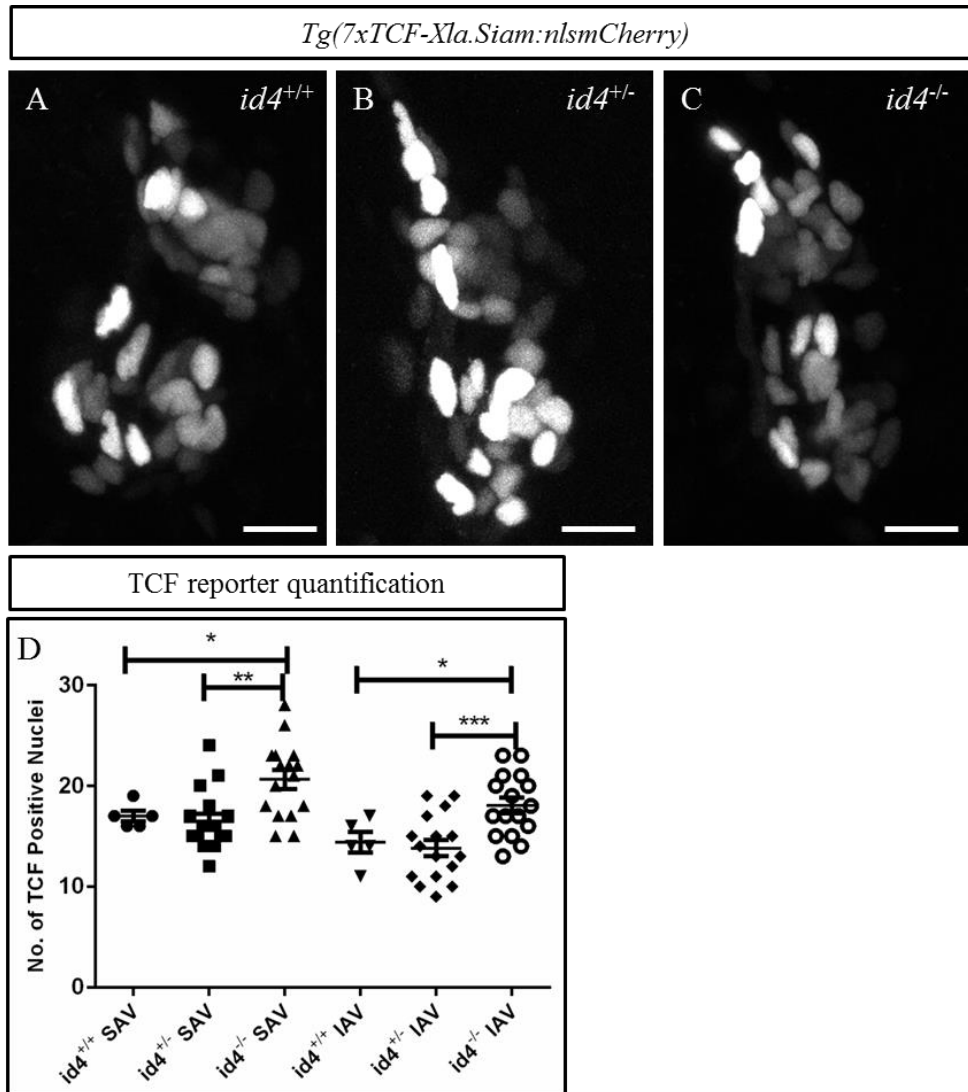


Figure 4.11. *id4* mutants show higher Wnt activity in the AV Canal. (A, B, C) Embryos from either heterozygous incross of *id4*^{+/+} or a maternal zygotic cross between *id4*^{+/+} and *id4*^{-/-} in *Tg(7xTCF-Xla.Siam:nlsMCherry)* background were imaged at 77 hpf followed by quantification (D) of TCF positive nuclei. There was significant increase observed in TCF positive nuclei in *id4* mutants as compared to siblings. Scale bars, 10 μ m (SAV, Superior AV Canal; IAV, Inferior AV Canal.) p value SAV ** - 0.0016, * - 0.0493; IAV * - 0.0251, *** - 0.0007. Modified figure reprinted with permission from Ahuja et. al, Dev. Biol. 2016; 412(1): 71-82.

4.8 Higher Wnt/ β -Catenin activity leads to impaired AV canal development.

As it was clear that *id4* mutants have higher Wnt/ β -Catenin activity, I wanted to study the effect of increased Wnt/ β -Catenin signaling on the AV Canal development. To answer this question, I made use of the zebrafish *apc*^{mcr/mcr} mutant which has elevated levels of Wnt/ β -Catenin signaling due to lack of a functional beta-catenin destruction complex. Using whole

mount in situ hybridization, I studied the expression of valve maturation marker *spp1* in *apc* mutants.

At 52 hpf, *apc* mutant embryos showed downregulated *spp1* expression (Fig. 4.12A, B), similar to my previous observation in *id4* mutants. This data clearly indicated that higher Wnt/ β -Catenin signaling interferes with valve development by preventing the expression of important valve differentiation markers.

Thus, higher Wnt/ β -Catenin signaling is inhibitory for cardiac valve development.

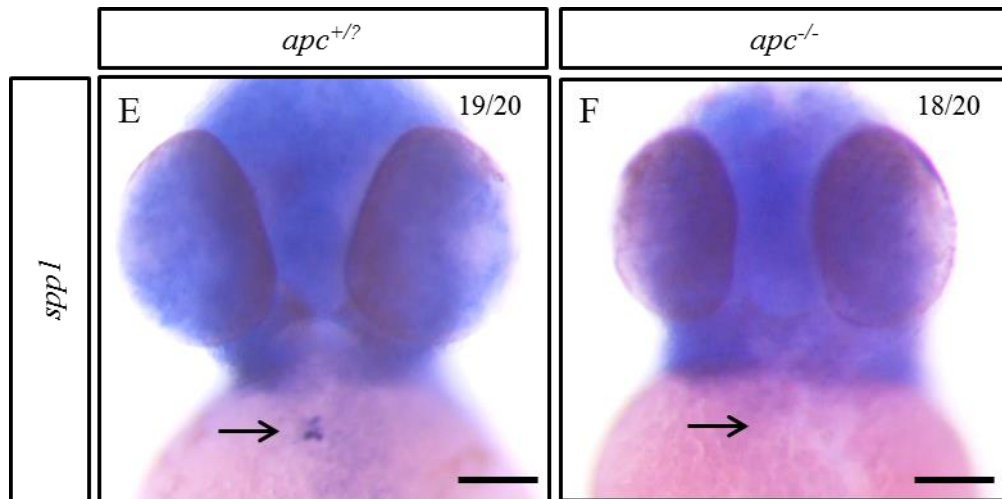


Figure 4.12. Elevated Wnt signaling leads to impaired cardiac valve development. (A, B) To assess the significance of higher Wnt activity in AV canal, *spp1* expression was analyzed in *apc* mutants. At 52 hpf, *apc* mutants show reduced *spp1* expression as compared to siblings. Scale bars, 100 μ m. Modified figure reprinted with permission from Ahuja et. al, Dev. Biol. 2016; 412(1): 71-82.

4.9 Id4 negatively regulates Wnt/TCF function in endocardial cells.

My previous results highlighted that *id4* mutants have higher Wnt/ β -Catenin activity which can negatively affect valve development. From this I hypothesized that Id4 might negatively regulate Wnt/ β -Catenin signaling in the developing AV canal. To test this idea, I designed a plasmid encoding Id4-2A-GFP under the endothelial specific promoter *fli1* and analyzed its effect on Wnt signaling by injecting it in the line *Tg(7xTCF-Xla.Siam:nlsmCherry)^{ia5}*. As an experimental control, I used the expression of GFP under the same promoter *Tg(fli1:GFP)*. Next, I analyzed the intensities of both GFP and mCherry in AVC endocardial cells at 77 hpf.

Fluorophore intensities were compared in the cell where both the fluorophores were present at a noticeable level. ImageJ software was used for intensity comparison. Interestingly, the ectopic expression of *id4*, lead to reduced nlsmCherry fluorescence which meant inactivation of Wnt/TCF activity in these cells (Fig. 4.13B, C, D). Additionally, Id4 mediated reduction in Wnt/TCF reporter activity was also observed to be taking place in a dose dependent manner. However, the expression of GFP alone by *Tg(fli1:GFP)* did not have any effect on mCherry fluorescence (Fig. 4.13A, C, D) and the overall appearance of the cell was yellow due to presence of both the flurophores (Fig 4.13A).

These data highlight that Id4 can negatively regulate TCF activity in a cell autonomous way and thus establish it as a crucial player in valve development.

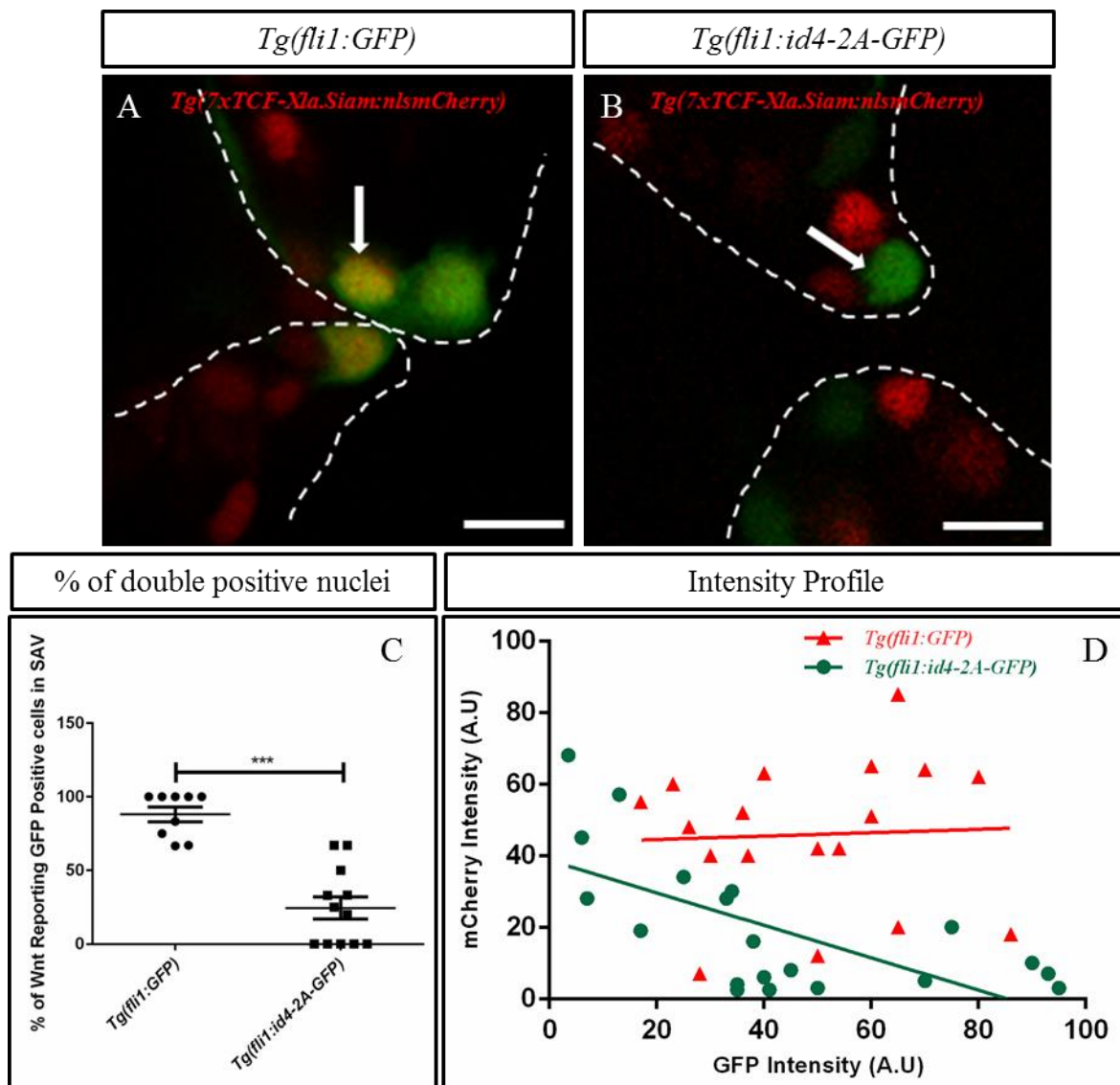


Figure 4.13. Id4 negatively regulates TCF function in endocardial cells. (A, B) Transient endothelial specific overexpression of *id4* leads to a dose dependent reduction of Wnt reporting signal

(B) in the AV Canal as compared to overexpression of GFP (A) in a similar manner, which did not have any effect. (C) Percentage of Wnt reporting cells in transient GFP and *id4* overexpression embryos and their intensity profile (D). p value *** - 0.0001. Scale bars, 10 μ m. SAV, Superior AV Canal. Modified figure reprinted with permission from Ahuja et. al, Dev. Biol. 2016; 412(1): 71-82.

4.10 Endothelial re-expression of *id4* in *id4* mutants can partially rescue their valve developmental defects.

To further validate its cell autonomous function, I wanted to check if exclusive re-expression of *id4* in the endocardium of *id4*^{-/-} animals can rescue their abnormal valve development. For this purpose, I generated *id4*^{-/-} animal carrying germ line clones of *Tg(fli1:id4-2A-mCherry)* and crossed it to a homozygous *id4* mutant. This cross gave two types of offspring on which further analysis was done: the *id4* mutants with endocardial re-expression of *id4* and pure *id4* mutants.

In these embryos, I performed expression analysis of *spp1* and *bmp4* as they showed altered expression patterns in *id4* mutants. At 52 hpf, I observed that most of the *id4*^{-/-} embryos re-expressing *id4* in their endocardium showed reappearance of *spp1* expression (Fig. 4.14B, Table 4.3) as compared to their *id4*^{-/-} siblings that did not show *spp1* expression (Fig. 4.14A). Furthermore, the *id4* mutants re-expressing *id4* also showed *bmp4* expression restricted to the AV boundary, unlike their *id4*^{-/-} siblings where *bmp4* expression was found to be expanded in the cardiac ventricle. (Fig. 4.14C, D).

These data clearly endorse that endocardium is the primary tissue of *id4* expression where its function is important for proper valve development and maturation.

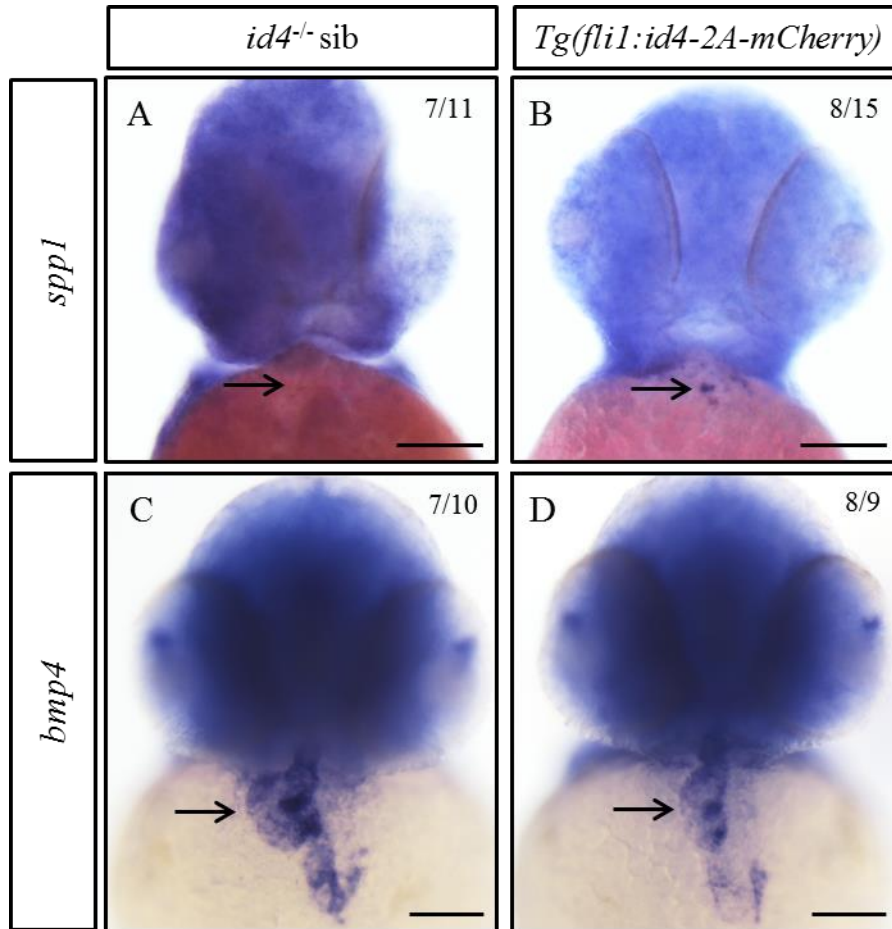


Figure 4.14. Endothelial re-expression of *id4* in *id4*^{-/-} can partially rescue *spp1* and *bmp4* expression patterns in *id4* mutants. Although *id4*^{-/-} generally lack *spp1* expression (A), a subset does exhibit *spp1* expression after endothelial specific *id4* re-expression (B). Similarly, as compared to *id4*^{-/-} which show ectopic *bmp4* expression (C), the *id4* mutants with endothelial specific re-expression of *id4* show less expanded *bmp4* expression (D). Scale bars, 100 μ m. Modified figure reprinted with permission from Ahuja et. al, Dev. Biol. 2016; 412(1): 71-82.

Gene	Mutants with highly aberrant expression	Mutants with mildly aberrant expression	Mutants with wt expression
<i>spp1</i> (Fig. 4.14 A)	7/11	4/11	0/11
<i>spp1</i> (Fig. 4.14 B)	4/15	3/15	8/15

Table 4.3. Types of *spp1* expression pattern observed in *id4*^{-/-} with endothelial over-expression of *id4* in Figure 4.14A, B. The numerators indicate the numbers of mutants with a particular type of expression pattern and denominators indicate the total number of embryos analyzed. Modified table reprinted with permission from Ahuja et. al, Dev. Biol. 2016; 412(1): 71-82.

4.11 Notch signaling appears unaffected in *id4* mutants.

To characterize the valve development phenotype better, I crossed the *id4* mutants to previously established Notch reporter line *Tg(TP1bglob:VenusPEST)^{s940}* (Ninov et al., 2012). At 77 hpf, I did not observe any apparent difference in the Notch reporter expression in *id4^{-/-}* as compared to their *id4^{+/+}* siblings (Fig. 4.15). This suggests that, *id4* does not seem to affect the Notch signaling in AVC development.

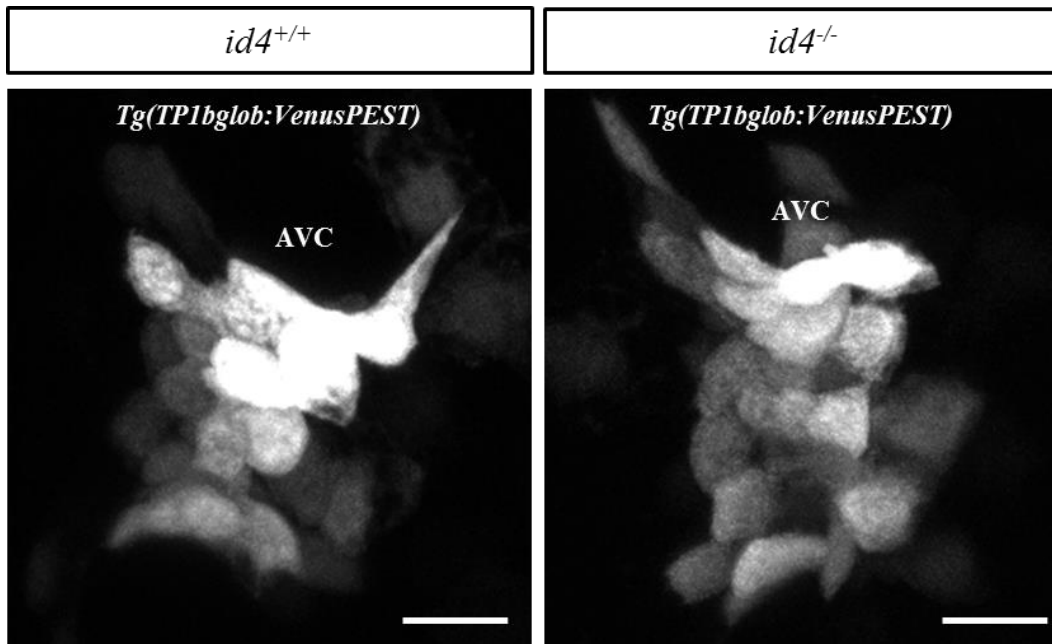


Figure 4.15. Notch signaling appears to be unaffected in *id4* mutants at the AVC. Representative maximum intensity projections of *id4^{+/+}* and *id4^{-/-}* AVC in notch signaling reporter background at 77 hpf. No significant difference was observed between them. Scale bar, 10 μ m. (AVC, Atrioventricular canal). Figure reprinted with permission from Ahuja et. al, Dev. Biol. 2016; 412(1): 71-82.

5. Discussion

5.1 Previously reported knowledge on AV Canal development and significance of this study

The developmental processes governing the morphogenesis of vertebrate heart are incompletely understood. Due to lack of comprehensive understanding of these processes, congenital heart disorders are the most common type of birth defects and a leading cause of morbidity in newborn children.

Correct patterning of the atrioventricular canal is one such complex process, which is important for cardiac looping and chamber septation during heart development. Previous studies have shown that several pathways including endocardial notch (Timmerman et al., 2004) and Wnt (Hurlstone et al., 2003; Ober et al., 2006) as well as myocardial Bmp expression (Ma et al., 2005) are essential for the proper patterning of the AVC and the formation of the cardiac valves. Intriguingly, components of these pathways are expressed broadly at early developmental stages of the heart but get refined to the AVC at later stages during AVC maturation (Walsh and Stainier, 2001) and valve development, implying a high level of crosstalk between the myocardium and the endocardium and a high level of integration of these pathways. There are studies that support this hypothesis in which it has been shown that Notch signaling acts upstream of Wnt/ β -Catenin signaling (Wang et al., 2013) during early valve development. Further loss and gain-of-function studies focusing on Wnt/ β -Catenin signaling in AVC formation revealed that myocardial Wnt/ β -Catenin activity is important for the development of the AVC conduction system (Gillers et al., 2015) and endocardial Wnt/ β -Catenin signals appear to trigger EMT and proliferation of the endocardium during cushion formation (Wang et al., 2013). Over activation of β -Catenin function in a zebrafish *apc* mutant further induces ectopic expression of myocardial *bmp4* (Verhoeven et al., 2011), suggesting that Wnt/ β -Catenin signaling acts upstream of Bmp signaling and highlighting its important function in the specification and patterning of the AVC and the valves. (This passage has been quoted verbatim from Ahuja et. al, Dev. Biol. 2016; 412(1): 71-82).

However, the importance of various pathways during valve development is relatively well established, a potential crosstalk between them or how they work in coordination during valve development still remains poorly understood.

In this regard, I identify *Id4* as a novel player that functions downstream of Bmp signaling to restrict Wnt/ β -Catenin signaling in the endocardium of developing valves and thus contribute to proper AVC development.

5.2 *id4*: current state of knowledge

Id4 belongs to *Id* family of proteins that function by dimerizing to bHLH proteins and prevent their DNA binding. Right from its discovery (Benezra et al., 1990), its function has been studied in various organ systems like brain/nervous system, bone, mammary gland and prostate.

ID4 has been shown to regulate G1-S transition in the cell cycle of neural stem cells, as a result the *Id4*^{-/-} mice have smaller brain size due to prolonged G1-S transition (Yun et al., 2004). In another elegant study on bone development, ID4 has been shown to be a crucial factor in promoting osteoblast differentiation (Tokuzawa et al., 2010). For doing so, ID4 facilitates the release of HES1 from HES1-HEY2 complexes, which increases the stability and activity of RUNX2, thus aiding osteoblast differentiation. ID4 also contributes to the regulation of branching morphogenesis and ductal expansion in the mammary gland. *Id4*^{-/-} mice show impaired mammary development due to increased p38MAPK activity which leads to escalated cell death and reduced proliferation in mammary gland cells (Dong et al., 2011). ID4 is also indispensable for proper development of prostate gland. Similar to aberrant mammary gland development, the prostate gland in *Id4*^{-/-} mice show small size, reduced branching morphogenesis and decreased expression of key differentiation markers like NKX3.1 (Sharma et al., 2013). Some reports also suggest that loss of *Id4* also initiates events responsible for prostate cancer progression (Sharma et al., 2012). In prostate cancer, the *Id4* promoter gets hypermethylated leading to its epigenetic silencing, eventually causing loss of *Id4* expression contrary to normal WT prostates which have high *Id4* expression. These data suggest a potential tumor suppressor function of ID4.

The prevalent state of experimental data increased our knowledge about *Id4*, however its function during cardiac development was still unknown.

Here I describe for the first time, the role of *Id4* in cardiac AVC development as a mediator of Bmp signaling and regulator of Wnt/ β -Catenin signaling.

5.3 *id4* mutants are phenotypically indistinguishable from their siblings but respond abnormally to cardiac stress

In the embryo, *id4* is expressed in the developing AV endocardial cushions, with very little expression present at the atrial inflow tract (Fig. 4.1A. Result in Fig. 4.1A was validated independently by collaborator Dogra, D.). However, in the adult heart its expression gets comprehensively enriched in the atrial chamber (Fig. 4.1D', E). To unravel the function of *id4* in the developing heart, I performed TALEN mutagenesis and retrieved a 5 bp deletion allele *id4^{bns18}* (Fig. 4.2, 4.3). This allele leads to the formation of truncated protein with incomplete HLH domain with presumably no function (Fig. 4.2, 4.3). Homozygous *id4^{-/-}* animals reach adulthood normally, however cardiac stress induced by increased heart rate causes retrograde flow in the larval heart at 77 hpf pointing to defective valve morphogenesis (Fig. 4.4, *id4* wt video1, *id4* mut video2). Upon a closer look at the heart of the 77 hpf larvae, I could also observe an inflated atrium at the end of ventricular systole in *id4* mutants to incorporate the back-flowing blood due to malformed AV canal (Fig 4.4). Aberrant valve function post stress served as a motivation to study various valve developmental markers to gain better molecular insight of the defect.

5.4 *id4* mutants have mis-regulated cardiac valve developmental markers

By performing in-situ hybridization, I analyzed the expression patterns of several genes known to be critical for different aspects of AVC development (Fig. 4.5, Table 4.1). These include myocardial developmental markers like *bmp4*, *cspg2a*, *tbx2b* and endocardial markers like *has2*, *spp1*. These markers apart from *spp1* are expressed throughout the antero-posterior axis of the developing heart tube at 37 hpf and become restricted to the AVC by 48 hpf (Bartman et al., 2004; Chi et al., 2008; Walsh and Stainier, 2001). In addition to these, the expression of Alcam starting 36 hpf in the endocardium of the developing AVC, makes it also a reliable marker to track AVC development (Beis et al., 2005). By 52 hpf, almost all the AV endocardial cells express Alcam.

At 52 hpf, I observed that most of these markers showed aberrant expression patterns in the *id4* mutants. Intriguingly, while the myocardial *tbx2b* expression at the AV boundary did not appear to be affected, the expression domain of another developmental marker versican (*cspg2a*) was expanded not just at the AVC but also slightly into the atrium. In addition to

this, *bmp4* was also found to be expressed ectopically in the cardiac ventricle, a phenotype that has been previously associated with high Wnt/ β -Catenin signaling (Verhoeven et al., 2011). Consistent with the expansion of *bmp4* and *cspg2a* expression, I further found that more number of endocardial cells express Alcam (Fig. 4.6, 4.7) in both the superior and the inferior AV canal indicative of a slight expansion of the AVC at 52 and 77 hpf. Surprisingly, in contrast to the expanded AVC markers, the terminal valvular differentiation marker *spp1* (osteopontin) showed a significantly downregulated expression and the other endocardial AVC marker *has2* did not show any apparent change in expression, in the *id4*^{-/-} animals. Taking clue from these mis-regulated valve developmental markers, I went ahead to investigate the signaling pathways affected in *id4* mutants.

5.5 Id4 mediates Bmp signaling leading to *spp1* expression

Previous studies on bone development suggest that Id4 acts downstream of Bmp signaling (Tokuzawa et al., 2010). I wanted to test if similar phenomenon is applicable in other tissues like the heart. For this purpose, I used a conditional transgenic line *Tg(hsp70l:bmp2b)*^{fr13} that expresses *bmp2b* under heat shock promoter, *hsp70*. Post heatshock, I found a significant upregulation of *id4* and *spp1* expression in the larval brain and heart (Fig. 4.8). This data suggested that both *id4* and *spp1* are downstream of Bmp signaling and from my previous finding I knew *id4*^{-/-} lack *spp1* expression, so I asked the question, whether Id4 could mediate Bmp signals leading to *spp1* expression. To answer this question, I conditionally overexpressed Bmp2b in the *id4*^{-/-} background. Interestingly, the lack of *spp1* expression in most of the *id4* mutants (Fig. 4.10), suggested that Bmp responsive induction of *spp1* is dependent on Id4 function. These findings indicate that *id4* expression is controlled by Bmp signaling. However, *bmp4* itself is transcriptionally upregulated in *id4* mutants. This increase could be attributed to a compensatory feedback loop that gets activated due to the downregulation of Bmp target genes in the absence of *id4*. The fact that Wnt/ β -catenin signaling can positively regulate *bmp4* expression in the heart (Verhoeven et al., 2011), could be another possible explanation for this phenomenon.

5.6 Id4 restricts Wnt signaling in the developing AVC endocardium

Previously published data associate ectopic *bmp4* expression (as seen in *id4* mutants as well) to higher Wnt/ β -catenin signaling (Verhoeven et al., 2011), which points towards a likelihood of some molecular interaction between Id4 and components of Wnt signaling pathway. To test this hypothesis, I crossed the *id4^{bns18}* allele into a previously established reporter line for Wnt/ β -catenin signaling *Tg(7xTCF-Xla.Siam:nlsMCherry)^{ia5}* (Moro et al., 2012). Analysis of *id4^{-/-}* larvae in this background revealed significantly high number of TCF reporter positive cells in the AVC (Fig. 4.11) indicating that Id4 might negatively influence Wnt/ β -catenin signaling to promote valve maturation. After establishing that *id4* mutants have higher Wnt reporter activity, I wanted to assess whether this increase could be causal to immature valves that lack *spp1* expression in *id4^{-/-}* animals. To test this hypothesis, I analyzed *spp1* expression in *apc^{mcr/mcr}* mutants which exhibit constitutively active β -Catenin activity. The downregulated *spp1* expression in these mutants (Fig. 4.12) suggested that higher Wnt/ β -catenin signaling is indeed detrimental for valve maturation and Id4 could be an important player regulating this process.

From my previous findings I had established that *id4* expression is enriched in the heart endocardium (Fig. 4.1B, F) where it allows valve maturation. To test whether Id4 has a tissue autonomous function, I re-expressed *id4* under endothelial promoter *fli1* in the homozygous *id4^{-/-}* animals. This endothelial reactivation of *id4* was indeed found to be sufficient to rescue valve developmental defects, as *id4* mutants re-expressing *id4* showed improvement in expression patterns of both *spp1* and *bmp4* (Fig. 4.14). Further, I wanted to check whether Id4 functions by restricting the Wnt/ β -catenin signaling in the endocardium during valve development. To test this idea, I expressed a construct encoding Id4-2A-GFP under *fli1* promoter and used GFP expression under same promoter as experimental control. This experimental strategy revealed that co-expression of Id4 – GFP but not GFP alone was able to decrease the TCF reporter activity cell-autonomously and in a dose dependent manner (Fig. 4.13), further confirming that Id4 activity in the AVC endocardium is crucial to regulate Wnt/ β -catenin signaling. An interesting scenario here is that *id4* mutants have high TCF reporter activity and previous data suggests that high Wnt/ β -catenin signaling is associated with high *bmp4* expression (Verhoeven et al., 2011). Now if we look at this together with fact that Id4 functions downstream of Bmp, it can be suggested that high Wnt/ β -catenin levels can

autoregulate through a negative feedback via Bmp mediated Id4 induction. This can also be an explanation for co-existence of Id4 and Wnt/ β -catenin signaling in the same cell types.

Taken together, these data highlight the importance of Id4 as an integral part of the cardiac Wnt-Bmp signaling axis, where it works downstream of Bmp signals as a cell-autonomous regulator of the Wnt/ β -catenin activity. This regulation of the Wnt signaling is crucial for proper valve maturation. However, the adult *id4*^{-/-} mutants are viable indicating that other genes, including other *id* family members compensate for loss of Id4 and support valve maturation. Recent findings suggest that Id4 can function as a suppressor of p38MAPK activity (Dong et al., 2011), a kinase which can stimulate Wnt signaling by phosphorylating and inactivating the endogenous Wnt inhibitor GSK3beta (Thornton et al., 2008). These data point towards a possible mechanism by which Id4 can regulate Wnt activity to promote valve development.

6. Conclusion

In conclusion, my data identifies *Id4* as a novel player in cardiac Wnt-Bmp signaling axis. Here I show for the first time that *id4* is expressed during heart development, and is important for proper functioning of cardiac valves as *id4*^{-/-} hearts show retrograde blood flow at the AV canal under pressure overload conditions. Additionally, I show the evidence that *Id4* regulates cardiac valve development and maturation in response to Bmp signals by restricting Wnt/ β -Catenin activity in the endocardium of developing AV canal.

However, the mechanism by which *Id4* restricts Wnt signaling remains open at this point, future studies should shed light on the exact mode of action of *Id4* in cardiac development and disease.

6.1 Proposed Model

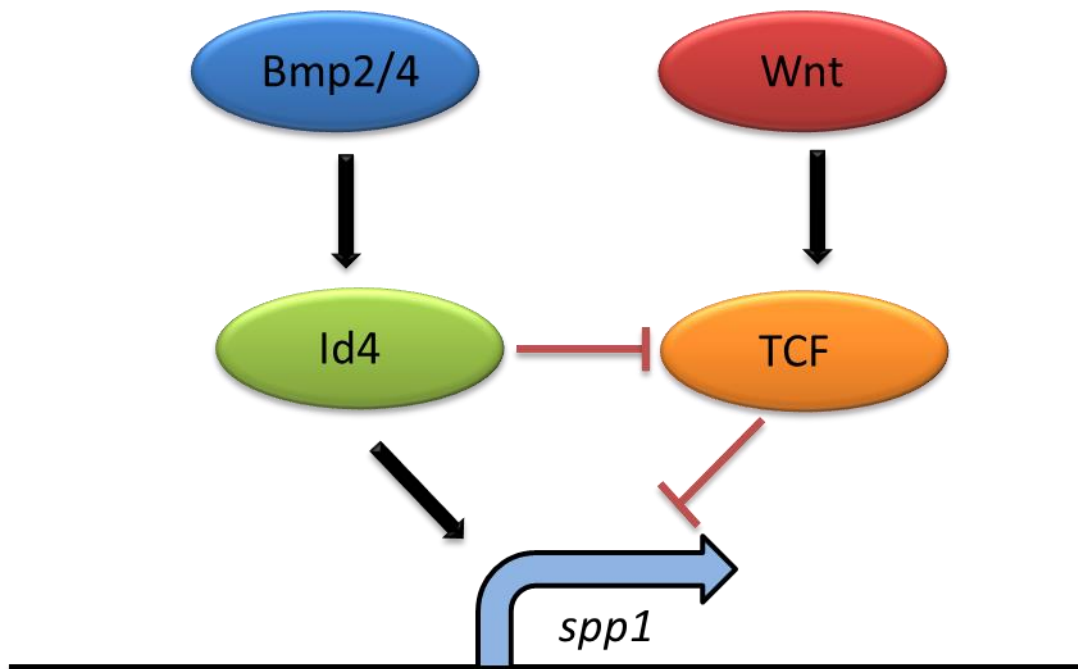


Figure 6.1. *Id4* functions downstream of Bmp signaling to restrict TCF function for proper valve development and maturation. Figure reprinted with permission from Ahuja et. al, Dev. Biol. 2016; 412(1): 71-82.

I GERMAN SUMMARY

Zusammenfassung

Id4 agiert in der Signalkaskade unterhalb von Bmp um die Funktion von TCF in endokardialen Zellen während der Herzklappenbildung zu begrenzen.

Einführung

Die Entwicklung und Strukturierung des Wirbeltier-Herzens aus seinen mesodermalen Vorläuferzellen ist ein streng regulierter und evolutionär konservierter Prozess (Stainier, 2001; Rosenthal and Harvey, 2010). Nach ihrer Spezifikation innerhalb des vorderen Splanchnopleura (Seitenplattenmesoderm), migrieren Herzvorläuferzellen in Richtung der Mittellinie (paraxial), wo sie einen primitiven Herzschauch bilden (Yelon et al., 1999; Berdougo et al., 2003). Danach vollzieht der Herzschauch eine Reihe von morphogenetischen Veränderungen. Diese münden in der Bildung der individuellen, durch den Atrioventrikulären-Kanal (atrioventricular canal - AVC) getrennten, Herzkammern. Im Anschluss wird die Migration innerhalb des AVC's angesiedelter endokardialer Zellen in die Herzgallerte durch räumlich begrenzte Signale des AVC's induziert. Diese formen spezialisierte Strukturen, die man als Endokardkissen bezeichnet (Harrelson et al., 2004; Plageman and Yutzey, 2004; Ma et al., 2005). Diese differenzieren sich aus und vergrößern sich Schritt für Schritt um sich später zu Mitralk- und Trikuspidalklappe zu entwickeln.

Der größte Teil unseres Wissens über die Funktion der an der AVC Ausbildung beteiligten Signalwege stammt aus Analysen verschiedener Modellorganismen wie der Maus, dem Huhn und dem Zebrafisch. Von zentraler Bedeutung für die AVC Strukturierung sind zentrale morphogenetische Signalwege wie BMP, Notch und Wnt/ β -Catenin (Hurlstone et al., 2003; Timmerman et al., 2004; Ma et al., 2005). Während der frühen Bildung des Herzschauchs sind all diese Signalwege im gesamten Herzen aktiv. Im Gegensatz dazu, ist während der Spezifizierung und Ausdifferenzierung der AVC's ihre Aktivität räumlich nur auf diese Struktur begrenzt. Eine elegante Studie zeigt, dass Wnt/ β -Catenin Signalübertragung essentiell ist für die Differenzierung des atrioventrikulären Leitungssystems und dabei in der Signalkaskade oberhalb von Tbx3 aktiv ist. Die Studie verwendet dabei ein Allel von β -Catenin (Ctnnb1), welches seine Funktion in Adhärenzverbindungen beibehält, dem aber die

Wnt-Signal Effektor Eigenschaften fehlen (Gillers et al., 2015). Eine zweite Studie berichtet über die Aktivität von Wnt oberhalb von Bmp und der Verhinderung des Ausreifens der Herzklappen bei übermäßiger Wnt Signalübertragung (Verhoeven et al., 2011).

Im Zebrafisch bildet sich ein kontraktile linearer Herzschlauch ab 24 Stunden nach der Befruchtung. Ab 48 Stunden nach der Befruchtung kann man die Spezifikation des AVC beobachten wenn die Expression myokardialer Markergene wie *bmp4*, *cspg2a* und *tbx2b* sich nur noch auf das AVC beschränkt (Bartman et al., 2004; Chi et al., 2008; Walsh and Stainier, 2001). Während des gleichen Zeitraums beschränkt sich die Expression von endokardialen AVC Markergenen wie z.B. *notch1b* und *has2* (zunächst im Herzkammer Endokard exprimiert) auf die AV-Grenze (Bartman et al., 2004; Smith et al., 2011; Walsh and Stainier, 2001). Darüber hinaus ist die Expression von *alcam* in kubischen, das AVC auskleidende, Endokardzellen, im Gegensatz zu negativen plattenepithelialen Endokardialzellen der Herzkammern, ein Kennzeichen der AVC Entwicklung (Beis et al., 2005). Bei atrioventrikulären Septumdefekten (AVSD) handelt es sich um die häufigste Form angeborener Herzfehler. Die Tatsache, dass Anomalien aller Mechanismen die das Ausbilden des AVC's steuern zu AVSD's führen, betont, wie wichtig das Verständnis der molekularen Signalwege dieser Prozesse ist. Die räumlich/zeitliche Beschränkung der Signalübertragung auf das AVC und die mögliche Interaktion verschiedener Signalwege ist noch weitgehend unverstanden. Folglich ist es wichtig, die zugrunde liegenden molekularen Details der AVC Strukturierung und der Herzklappenentwicklung zu verstehen, um Erkenntnisse zur Ätiologie von Herzklappenerkrankungen zu gewinnen. Der Zebrafisch eignet sich besonders gut, um den Prozess der Herzentwicklung einschließlich der AVC Strukturierung und der Funktion der Herzklappen zu untersuchen, da es möglich ist, die Prozesse in Echtzeit abzubilden (Beis et al., 2005; Scherz et al., 2008).

In diesem Bericht beschreiben ich zum ersten Mal die Rolle von Id4 bei der Regulierung der Entwicklung und Funktion des AVC's. Id4 gehört zur Id-Proteinfamilie. Es handelt sich um bHLH Faktoren, die bHLH Transkriptionsfaktoren negativ regulieren und denen eine DNA Bindestelle fehlt. Um die Expression von Zielgenen zu regulieren und wirksam an DNA binden zu können, formen bHLH Transkriptionsfaktoren Dimere mit anderen ubiquitär exprimierten bHLH Faktoren (Massari and Murre, 2000). Typischerweise kann diese Interaktion in Gegenwart eines id-Proteins inhibiert werden. Um die DNA Bindung von

bHLH Transkriptionsfaktoren zu verhindern, heterodimerisieren *id*-Faktoren mit diesen kompetitiv (Benezra et al., 1990). Frühere Berichte legen nahe, daß ID4 die Verzweigungsmorphogenese und Apoptose von Maus-Brustzellen durch Unterdrücken der p38/MAPK-Aktivität reguliert (Dong et al., 2011). Weiterhin wurde gezeigt, dass ID4 mesenchymale Stammzellendifferenzierung steuert indem diese in Richtung Osteoblasten anstelle von Adipozyten gelenkt werden (Tokuzawa et al., 2010). In diesem Zusammenhang setzt ID4 HES1 aus HES1-HEY2 frei, was zu einer Stabilisierung von RUNX2 führt, und erhöht dadurch seine Transkriptionsaktivität. Darüber hinaus zeigen Mäuse ohne *Id4* langsamer proliferierende neuronale Vorläuferzellen und ein kleineres Gehirn im Vergleich zu wildtypischen Wurfgeschwistern (Yun et al., 2004). Zusammengefasst erweitert diese Studie unser Wissen über die Funktion von ID4, jedoch bleibt seine Rolle in der Herzentwicklung weiter unklar.

In dieser Studie erbringe ich den Nachweis, dass *Id4* ein entscheidender Mediator der Interaktion zwischen dem Wnt- und Bmp-Signalweg während der AVC Entwicklung ist und der Verlust von *Id4* eine verbesserte Wnt/ β -Catenin Signalübertragung und Defekte in der Herzklappen Ausreifung bewirkt.

Um die Funktion von *Id4* während der Herzentwicklung besser zu verstehen, habe ich folgende spezifische Ziele entworfen:

- **Ziel 1:** Bestimmen der räumlich/zeitlichen Expressionsmuster von *id4* während der Herzentwicklung.
- **Ziel 2:** Verstehen der Funktion von *Id4* durch das Etablieren einer loss-of-function Mutante mit Hilfe der TALEN Technologie.
- **Ziel 3:** Erfassen der Signalkaskade in der *id4* eine Rolle spielt und der potenziellen Interaktionen zwischen Molekülen oder anderen Kaskaden während der Herzentwicklung.

Ergebnisse und Diskussion

***id4* ist im Atrioventrikulären Kanal des sich entwickelnden Herzen und im adulten Vorhof expremiert**

Um den zeitlichen und räumlichen Verlauf der Expression von *id4* zu erfassen, wurden whole mount In-situ-Hybridisierung sowohl auf kompletten Embryonen als auch adulten Herzen durchgeführt. 52 Stunden nach Befruchtung (hpf) ist das Gen *id4* sowohl im Gehirn als auch im Auge des Zebrafährblings stark expremiert, ein Befund der sich mit Studien in Mausembryonen deckt. Zusätzlich haben meine Studien jedoch eine bisher nicht veröffentlichte Expression von *id4* im embryonalen Herzen detektiert. 52 hpf ist die kardiale Expression von *id4* im Atrioventrikulären Kanal (AVC) konzentriert (Ergebnis durch unabhängige Experimente meiner Kollaboratorin Dogra, D. bestätigt). *id4* bleibt von diesem Zeitpunkt an bis ins adulte Herz expremiert. In diesem beschränkt sich die Expression von *id4* nicht alleine auf den AVC sondern erstreckt sich, im Gegensatz zur embryonalen Expression, zusätzlich auf die Vorkammer (Atrium). Diese Ergebnisse wurden durch quantitative PCR Methoden (qRT-PCR) überprüft. Die Ergebnisse dieser Experimente bestätigen die Ergebnisse der Hybridisierungstechniken und messen zudem einen 125fachen Expressionsunterschied zwischen dem Atrium und der Kammer (Ventrikel). Um zu testen welches kardiale Gewebe *id4* im Herzen expremiert, wurden die RNA-Hybridisierungsexperimente in einem mutanten Hintergrund wiederholt. Hierzu wurde die *clo* Mutante verwendet, welche kein Endokardium entwickelt (Stainier et al., 1995). Die *id4* Sonde detektiert in dieser Mutante keine kardiale Expression, ein Ergebnis das vorschlägt, dass *id4* im Endokardium expremiert ist.

***id4* Mutanten sind überempfindlich gegenüber kardialen Stress welcher zu retrogradem Blutfluss führt und zeigen eine fehlerhafte Regulierung von Entwicklungsgenen des Herzens.**

Um die Funktion von *id4* während der Entwicklung zu untersuchen, wurde mittels revers-genetischer Methoden eine Leserasterverschiebung in *id4* induziert (5bp Deletion, *id4^{bns18}*), die ,mutmaßlich, zu einem Verlust der Genfunktion führt. Überraschenderweise sind homozygote *id4^{bns18}* Tiere phänotypisch von ihren wildtypischen Geschwistern nicht zu unterscheiden, wachsen normal und erreichen ein fertiles Stadium was eventuell auf eine gewisse Redundanz mit anderen Genen der *id* Familie schließen lässt. Es ließ sich aber

feststellen, dass *id4^{bns18}* homozygote Tiere unter verstärkter Herzlast (Baker et al., 1997) dazu neigen retrograden Blutfluss zu entwickeln, ein Zeichen für eine potentiell vorliegende Klappeninsuffizienz. Um Entwicklungsdefekte der Herzklappen näher zu untersuchen wurden verschiedene Entwicklungsmarker des Atrioventrikulären Kanals näher untersucht.

Mittels In-situ-Hybridisierung und immunhistologischer Verfahren wurden die Expressionsmuster der myokardialen Gene *bmp4*, *tbx2b*, *cspg2a* und der endokardialen Gene *spp1*, *has2* und Alcam untersucht. Während einige der Marker wie *tbx2b* und *has2* keine Veränderungen zeigten, konnte bei anderen eine signifikante Veränderung in homozygoten *id4^{bns18}* Tieren festgestellt werden. *bmp4* und *cspg2a* sind anfänglich bei etwa 37 hpf im gesamten Herz exprimiert, bevor sich ihre Expression bei etwa 48 hpf auf den AVC reduziert (Walsh and Stainier, 2001). Im Gegensatz dazu verbleibt die Expression von *bmp4* expandiert und erstreckt sich über das gesamte Ventrikel und den AVC. Die Expression von *cspg2a* ist ebenfalls expandiert und umfasst den AVC sowie Teile des Atriums und den venösen Pol des Herzens. Diese Expansion weist auf eine Expansion des AVC Kanals hin. Konsistent mit diesen Erkenntnissen konnte ich eine erhöhte Zahl an Alcam positiven Zellen im AVC bei 52 und 77 hpf detektieren welche jeweils 22% und 40% betrug. Interessanter weise konnte ich in den *id4^{bns18}* Mutanten gleichzeitig eine signifikante Reduktion der Expression von *spp1* feststellen, ein Marker für die Differenzierung des Endokardiums während der Bildung der Herzklappen. Zusammenfassend weisen diese Daten darauf hin, dass *id4* Funktion bei der Reduzierung des Bmp Signalwegs zukommt.

Id4 Vermittelt Bmp Signale welche zur Induktion von *spp1* notwendig sind.

Die reduzierte *spp1* Expression und ektopische Expression von *bmp4* in *id4^{bns18}* Mutanten weist darauf hin, dass *id4* oberhalb von *bmp4* und *spp1* wirkt. Vorliegende Studien hingegen kommen zu dem Schluss das *id4* unterhalb des Bmp Signalwegs wirkt (Ishibashi and Inui, 2014; Tokuzawa et al., 2010). Daher wurde getestet, ob diese Signalkaskade in den Zellen des Herzens grundlegend anders verläuft, indem eine konditionale Überaktivierung des Bmp Signalwegs gewählt wurde welche über den gleichen Rezeptor verläuft (Hager-Theodorides et al., 2002; Miyazono et al., 2010). Eine Induktion des Bmp Signalwegs mittels einer transgenen Linie des Zebrafischlings *Tg(hsp70l:bmp2b)^{fr13}* (Chocron et al., 2007) zeigte eine Induktion der Gene *id4* und *spp1*, was bestätigt, dass sowohl *spp1* als auch *id4* Zielgene dieses Signalwegs sind. Um zu testen, ob die Induktion von *spp1* über *id4* verläuft, wurde des Weiteren getestet ob eine konditionale Bmp Überaktivierung via Id4 zu einer Induktion von

spp1 führt. Hierzu wurde das Experiment in homozygoten *id4^{bns18}* Mutanten wiederholt. Interessanterweise ist dieses der Fall und *spp1* lässt sich in Abwesenheit von funktionalem *id4* nicht durch Bmp induzieren. Dies führt zu der Erkenntnis, dass Id4 ein zentraler Vermittler des Bmp Signalwegs ist.

Id4 hat eine inhibitorische Wirkung auf den Wnt Signalweg und endocardiale Reexpression ist ausreichend um Herzklappen-Reifung in *id4* Mutanten zu induzieren.

Id4 Mutanten zeigen eine ektopische Expression von *bmp4*, ein Phänotyp der in vorherigen Studien mit dem Wnt Signalweg in Verbindung gebracht wurde (Verhoeven et al., 2011). Daher besteht die Möglichkeit das Id4 ebenfalls eine Funktion in diesem Signalweg hat indem es die Aktivität von Wnt innerhalb des Herzens reduziert. Um diese Hypothese zu überprüfen, wurde die Aktivität des Wnt Signalwegs in den Herzen von *id4^{bns18}* mutanten Tieren getestet. Erreicht wurde dieses durch eine Kreuzung des *id4^{bns18}* Alleles in den Hintergrund einer bereits verfügbaren Wnt Reporterline *Tg(7xTCF-Xla.Siam:nlsmCherry)^{ia5}* (Moro et al., 2012), welche das Binden von TCF durch die Aktivierung eines Kernlokalisierenden mCherry anzeigt. In diesem Experiment ließ sich bei 77 hpf ein signifikanter Anstieg der Zahl der Wnt positiven Zellen im Endokardium beider Seiten des AVC feststellen. Um den Effekt einer erhöhten Wnt Aktivität auf die Reifung der sich bildenden Herzklappen zu überprüfen benutzte ich eine weitere Mutante, *apc*. *Apc* ist ein Negativregulator des Wnt Signalwegs, ein Verlust von *apc* führt daher zu einer Überaktivierung. In-situ-Hybridisierung für das Gen *spp1* zeigte auf, dass genau jener Effekt der in der *id4* Mutante beobachtet werden konnte auch in der *apc* Mutante zu einer signifikanten Reduktion von *spp1* führte. Der negative Effekt von *id4* auf die Aktivität von Wnt wurde daraufhin klonal noch einmal genauer bestimmt. Hierzu wurde ein Id4-2A-GFP Konstrukt unter einen Endothel spezifischen Promoter kloniert und durch DNA Injektionen klonal in einzelnen Zellen des Endokards exprimiert und die Aktivität durch die Expression von mCherry in der Wnt Reporter Linie bestimmt. Interessanterweise zeigte sich, dass die Aktivität von Wnt sich Dosis abhängig mit dem Anstieg von GFP verringerte.

Zusammengenommen zeigen diese Daten auf, dass Id4 ein Negativregulator von Wnt ist und eine erhöhte Wnt Aktivität in den *id4^{bns18}* kausal für den Verlust an *spp1* Expression und einer Reifung der Herzklappen ist. Dafür spricht auch, dass eine artifizielle, transgene Reexpression von *id4* in Endothelzellen alleine in der Lage ist den Reifungsmarker *spp1* in *id4^{bns18}* wieder herzustellen.

Zusammenfassung und Ausblick

Zusammenfassend etablieren diese Daten *id4* als eine neue Komponente der kardialen Wnt-Bmp Signalachse. Id4 wirkt hier als ein Zell autonomer Regulator des Wnt Signalwegs in endokardialen Zellen in Abhängigkeit von Bmp Signalen. Dieses Justieren der Wnt Bmp Signalachse ist von Wichtigkeit bei der Entwicklung und Reifung der Herzklappen, auch wenn die Lebensfähigkeit der homozygoten *id4* Mutanten darauf hinweist, dass *id4* nicht alleine an diesen Prozessen beteiligt sein kann. Id4 wurde kürzlich als ein negativ Regulator der Aktivität von p38MAPK (Dong et al., 2011) identifiziert, einer Kinase welche nachweislich Wnt Signale durch die Phosphorylierung und Inaktivierung des Wnt Supressors GSK3beta moduliert (Thornton et al., 2008). Diese Ergebnisse deuten auf eine potentiellen Mechanismus hin auf welche Weise Id-Proteine im Allgemeinen und Id4 im Speziellen die Aktivität von Wnt unterdrücken könnten. Weitere Forschung in dieser Richtung wird die Funktion von Id Proteinen in der Herzentwicklung und ihre Rolle bei der Entstehung von Krankheiten ausleuchten.

II ENGLISH SUMMARY

Id4 functions downstream of Bmp signaling to restrict TCF function in endocardial cells during atrioventricular valve development

Introduction

The vertebrate heart development is a critically regulated process. It starts very early in the development with specification of cardiac progenitors which migrate to form the linear heart tube (Yelon et al., 1999; Berdougo et al., 2003). This heart tube undergoes a series of looping and ballooning processes which lead to formation of distinct heart chambers and an AVC (Atrioventricular Canal). Specialized structures known as the endocardial cushions form in the AVC which give rise to the heart valves between the atrium and the ventricle (Harrelson et al., 2004; Plageman and Yutzey, 2004). Some key molecular networks like Bmp, Wnt and Notch have been previously reported to contribute to valve development but how they work in coordination with each other or a potential cross talk between them remains largely unknown (Hurlstone et al., 2003; Timmerman et al., 2004; Ma et al., 2005).

Correct patterning of AVC requires precise expression of various marker genes at the AVC. For instance, during zebrafish valve development, the AVC gets specified when the molecular markers like *bmp4*, *cspg2a*, *tbx2b* (myocardial) and *notch1b*, *has2* (endocardial) initially expressed in the whole ventricle (at 37hpf), become restricted to AV(Atrioventricular) boundary by 48 hpf (Bartman et al., 2004; Chi et al., 2008; Smith et al., 2011; Walsh and Stainier, 2001). In addition to these, the expression of cell junction marker Alcam by cuboidal endocardial cells of the AVC is also an important milestone for valve development (Beis et al., 2005).

Genetic anomalies affecting cardiac development can lead to congenital heart defects, amongst which valve related disorders are reported to be quite prevalent (Fahed et al., 2013). Valvular prolapse is one of the major outcomes of such malformations leading to retrograde blood flow and consequently heart has to exert more pressure to pump the regurgitating blood. Thus it is important to understand valve development to have a deeper insight towards

disease. In this regard, I describe for the first time the role of *id4* in regulating valve development and function.

Id4 belongs to *Id* family of proteins which are dominant negative regulators of bHLH (basic Helix Loop Helix) factors (Benezra et al., 1990; Massari and Murre, 2000). It lacks a classical DNA binding domain but has a HLH domain with which it binds to other bHLH factors and prevents their DNA binding. Previously reported data from mice studies shows that *Id4* is expressed in mammary cap cells, myoepithelial cells and a subset of luminal epithelial cells. The *Id4*^{-/-} mice mammary cells show reduced ductal elongation, branching morphogenesis and increased apoptosis due to increase p38 MAPK activity (Dong et al., 2011). Furthermore, in another study it was shown that *Id4* controls mesenchymal stem cell differentiation by driving them towards osteoblasts instead of adipocytes (Tokuzawa et al., 2010). For this purpose, it releases HES1 from HES1-HEY2 complexes. HES1, then stabilizes RUNX2, thus increasing its transcriptional activity leading to enhanced osteoblast specific gene expression. Neuronal development is another phenomenon which requires *ID4* function. The *Id4* null mice have smaller brain size and slower proliferation of neural precursor cells as compared to their the wildtype littermates (Yun et al., 2004). Although these studies have increased our knowledge about *Id4* function, none of them have reported its expression and role in the heart development.

Here, with the help of zebrafish, I show that *Id4* is a crucial mediator of *Bmp* signaling and restricts *Wnt* signaling during heart valve development.

Results and Discussion

To understand the function of *id4* during cardiac development, I began first with understanding its expression pattern. During early developmental stage 52 hpf, I observed the *id4* expression in brain and eye of the embryo (Fig. 4.1A). This observation is consistent with previously reported mouse data. Interestingly, I also observed its expression in the embryonic AVC at 52 hpf which is not reported previously (Fig. 4.1A, C; result independently validated by collaborator Dogra, D.). To assess in which layer of the heart is *id4* expressed, I performed in situ hybridization for *id4* in *cloche* mutant, which is an established mutant in the field of zebrafish for the fact that it lacks endothelium (Stainier et al., 1995). A lack of staining in *cloche* mutant helped me conclude that *id4* is enriched in endocardial layer of the

heart (Fig. 4.1B). In order to validate its expression in the adult heart, I performed in situ hybridization for *id4* in adult heart followed by sectioning it. In this case, I observed staining at the luminal side of the heart tissue, further confirming that *id4* appears to be present in the endocardium of the heart (Fig. 4.1 D', F).

To figure out the function of *id4*, I performed TALEN mutagenesis by targeting TALEN arms to region encoding HLH domain of Id4 (Fig. 4.2A). Post mutagenesis I recovered a 5 bp deletion allele (*id4^{bns18}*) that leads to premature stop codon leading to formation truncated protein with presumably no function (Fig. 4.3A, B). Due to lack of an apparent morphological defect in *id4* mutants (Fig. 4.3D, E), I stressed the embryos by exposing them to 37°C for 1 hour at 48hpf, to increase the heart rate. Post cardiac stress, I could observe retrograde flow in *id4* mutant larvae at 77 hpf which indicated aberrant AVC development in those larvae (Fig. 4.4). To gain a better molecular insight to this defect, I performed in situ hybridization of various AVC marker genes at 52 hpf (Fig. 4.5). At this stage, while two marker genes *tbx2b* and *has2* appeared unaffected, the other three namely *bmp4*, *cspg2a* and *spp1* showed altered expression pattern in *id4* mutants. While both *bmp4* and *cspg2a* expression domains were expanded beyond AV boundary, the *spp1* expression was severely downregulated in *id4* mutants. Consistent with the expanded expression domains of *bmp4* and *cspg2a*, the number of Alcam positive AV endocardial cells were also increased in *id4* mutants. This increase was approximately around 25% and 40% at 52 hpf (Fig. 4.6) and 77 hpf (Fig. 4.7) respectively in both superior and inferior aspect of the AVC.

As *bmp4* was mis-expressed in *id4* mutants, I explored the Bmp signaling further using a conditional Bmp overexpression line *Tg(hsp70l:bmp2b)^{fr13}* (Chocron et al., 2007) that expresses Bmp2b under heat shock promoter. Post heat shock, there was a robust upregulation in expression of both *id4* (Fig. 4.8A, B) and *spp1* (Fig. 4.8C, D) in brain and heart of the embryos at 52 hpf. When *spp1* expression was analyzed post heat shock in *id4* mutant background, it was still found to be downregulated indicating that Id4 mediates Bmp signaling leading to *spp1* expression (Fig. 4.10B).

To characterize the mutant phenotype better, I analyzed *id4* mutants in Wnt reporter background *Tg(7xTCF-Xla.Siam:nlsmCherry)^{ia5}* that reports active Wnt signaling by showing nuclear mCherry fluorescence. A quantification of Wnt positive nuclei at 77 hpf at the AVC revealed more mCherry reporting nuclei in *id4* mutants, indicating that *id4* mutants have higher Wnt signaling (Fig. 4.11). To ascertain whether higher Wnt signaling is detrimental for

AVC development I analyzed the expression of *spp1* in *apc* mutants (have constitutively active Wnt signaling). Lack of *spp1* expression in these mutants at 52 hpf (Fig. 4.12), confirmed that higher Wnt signaling can negatively regulate valve development and can be causal to defects seen in *id4* mutants. To understand if Id4 functions by restricting Wnt signaling in the developing AVC, I co-expressed Id4-GFP in the endothelial cells of *Tg(7xTCF-Xla.Siam:nlsMCherry)^{ia5}* and used just GFP expression as control. While GFP expression had no effects on Wnt signaling, the Id4-GFP co-expression downregulated active Wnt signaling in a dose dependent manner in the AVC of the larvae (Fig. 4.13). From this observation, I could conclude that Id4 appears to function by restricting Wnt signaling in the developing valves.

Having established that Id4 can restrict Wnt signaling, I wanted to assess whether selectively re-expressing *id4* in the endocardium can rescue developmental defects seen in *id4^{-/-}*. To achieve this, I generated an *id4^{-/-}* that can supply germ line clones carrying *Tg(fli1:id4-2A-mCherry)* and crossed it to *id4^{-/-}*. The *id4* re-expressing *id4^{-/-}* obtained from this cross indeed showed better expression patterns of *bmp4* and *spp1* which were much closer to wt expression patterns and unlike their *id4^{-/-}* siblings (Fig. 4.14).

Taken together, these data establish Id4 as a crucial player that mediates the crosstalk between Bmp and Wnt signaling pathways in the developing AVC.

Conclusion

In conclusion, I describe here a novel function of Id4 in the developing AVC where it can restrict the Wnt pathway in response to Bmp signals. This regulation is important as *id4^{-/-}* develop immature valves that are unable to maintain uni-directional blood flow under stress and have mis-regulated valve developmental markers. A possible explanation for Id4 mediated regulation of Wnt signaling could be that Id4 is reported to suppress p38MAPK activity (Dong et al., 2011) which itself can inactivate endogenous Wnt inhibitor GSK3beta (Thornton et al., 2008) and consequently upregulate Wnt activity. So in this case, in the absence of Id4, this cascade might get activated and increase Wnt signaling which can inhibit valve development.

III REFERENCES

Alfieri, C.M., Cheek, J., Chakraborty, S., Yutzey, K.E., 2010. Wnt signaling in heart valve development and osteogenic gene induction. *Dev. Biol.* 338, 127–35.

Auman, H.J., Coleman, H., Riley, H.E., Olale, F., Tsai, H.-J.J., Yelon, D., 2007. Functional modulation of cardiac form through regionally confined cell shape changes. *PLoS Biol.* 5, e53.

Baker, K., Warren, K.S., Yellen, G., Fishman, M.C., 1997. Defective “pacemaker” current (I_h) in a zebrafish mutant with a slow heart rate. *Proc. Natl. Acad. Sci. U.S.A.* 94, 4554–9.

Bartman, T., Walsh, E.C., Wen, K.-K.K., McKane, M., Ren, J., Alexander, J., Rubenstein, P.A., Stainier, D.Y., 2004. Early myocardial function affects endocardial cushion development in zebrafish. *PLoS Biol.* 2, E129.

Beis, D., Bartman, T., Jin, S.-W.W., Scott, I.C., D’Amico, L.A., Ober, E.A., Verkade, H., Frantsve, J., Field, H.A., Wehman, A., Baier, H., Tallafuss, A., Bally-Cuif, L., Chen, J.-N.N., Stainier, D.Y., Jungblut, B., 2005. Genetic and cellular analyses of zebrafish atrioventricular cushion and valve development. *Development* 132, 4193–204.

Benezra, R., Davis, R.L., Lockshon, D., Turner, D.L., Weintraub, H., 1990. The protein Id: a negative regulator of helix-loop-helix DNA binding proteins. *Cell* 61, 49–59.

Berdougo, E., Coleman, H., Lee, D.H., Stainier, D.Y., Yelon, D., 2003. Mutation of weak atrium/atrial myosin heavy chain disrupts atrial function and influences ventricular morphogenesis in zebrafish. *Development* 130, 6121–9.

Bruneau, B.G., 2008. The developmental genetics of congenital heart disease. *Nature* 451, 943–8.

Cai, C.-L.L., Martin, J.C., Sun, Y., Cui, L., Wang, L., Ouyang, K., Yang, L., Bu, L., Liang, X., Zhang, X., Stallcup, W.B., Denton, C.P., McCulloch, A., Chen, J., Evans, S.M., 2008. A myocardial lineage derives from Tbx18 epicardial cells. *Nature* 454, 104–8.

Camenisch, T.D., Molin, D.G.G., Person, A., Runyan, R.B., Gittenberger-de Groot, A.C., McDonald, J.A., Klewer, S.E., 2002. Temporal and distinct TGFbeta ligand requirements during mouse and avian endocardial cushion morphogenesis. *Dev. Biol.* 248, 170–81.

- Camenisch, T.D., Schroeder, J.A., Bradley, J., Klewer, S.E., McDonald, J.A., 2002. Heart-valve mesenchyme formation is dependent on hyaluronan-augmented activation of ErbB2-ErbB3 receptors. *Nat. Med.* 8, 850–5.
- Camenisch, T.D., Spicer, A.P., Brehm-Gibson, T., Biesterfeldt, J., Augustine, M.L., Calabro, A., Kubalak, S., Klewer, S.E., McDonald, J.A., 2000. Disruption of hyaluronan synthase-2 abrogates normal cardiac morphogenesis and hyaluronan-mediated transformation of epithelium to mesenchyme. *J. Clin. Invest.* 106, 349–60.
- Cermak, T., Doyle, E.L., Christian, M., Wang, L., Zhang, Y., Schmidt, C., Baller, J.A., Somia, N.V., Bogdanove, A.J., Voytas, D.F., 2011. Efficient design and assembly of custom TALEN and other TAL effector-based constructs for DNA targeting. *Nucleic Acids Res.* 39, e82.
- Chaudhary, J., Johnson, J., Kim, G., Skinner, M.K., 2001. Hormonal regulation and differential actions of the helix-loop-helix transcriptional inhibitors of differentiation (Id1, Id2, Id3, and Id4) in Sertoli cells. *Endocrinology* 142, 1727–36.
- Chi, N.C., Shaw, R.M., Val, S. De, Kang, G., Jan, L.Y., Black, B.L., Stainier, D.Y., 2008. Foxn4 directly regulates *tbx2b* expression and atrioventricular canal formation. *Genes Dev.* 22, 734–9.
- Chocron, S., Verhoeven, M.C., Rentzsch, F., Hammerschmidt, M., Bakkers, J., 2007. Zebrafish *Bmp4* regulates left-right asymmetry at two distinct developmental time points. *Dev. Biol.* 305, 577–88.
- Christoffels, V.M., Habets, P.E., Franco, D., Campione, M., Jong, F. de, Lamers, W.H., Bao, Z.Z., Palmer, S., Biben, C., Harvey, R.P., Moorman, A.F., 2000. Chamber formation and morphogenesis in the developing mammalian heart. *Dev. Biol.* 223, 266–78.
- Covassin, L.D., Villefranc, J.A., Kacergis, M.C., Weinstein, B.M., Lawson, N.D., 2006. Distinct genetic interactions between multiple *Vegf* receptors are required for development of different blood vessel types in zebrafish. *Proc. Natl. Acad. Sci. U.S.A.* 103, 6554–9.
- Dong, J., Huang, S., Caikovski, M., Ji, S., McGrath, A., Custorio, M.G., Creighton, C.J., Maliakkal, P., Bogoslovskaja, E., Du, Z., Zhang, X., Lewis, M.T., Sablitzky, F., Brisken, C., Li, Y., 2011. ID4 regulates mammary gland development by suppressing p38MAPK activity. *Development* 138, 5247–56.

- Délot, E.C.C., 2003. Control of endocardial cushion and cardiac valve maturation by BMP signaling pathways. *Mol. Genet. Metab.* 80, 27–35.
- Fahed, A.C., Gelb, B.D., Seidman, J.G., Seidman, C.E., 2013. Genetics of congenital heart disease: the glass half empty. *Circ. Res.* 112, 707–20.
- Fishman, M.C., Chien, K.R., 1997. Fashioning the vertebrate heart: earliest embryonic decisions. *Development* 124, 2099–117.
- Fortini, M.E., Artavanis-Tsakonas, S., 1994. The suppressor of hairless protein participates in notch receptor signaling. *Cell* 79, 273–82.
- Galvin, K.M., Donovan, M.J., Lynch, C.A., Meyer, R.I., Paul, R.J., Lorenz, J.N., Fairchild-Huntress, V., Dixon, K.L., Dunmore, J.H., Gimbrone, M.A., Falb, D., Huszar, D., 2000. A role for smad6 in development and homeostasis of the cardiovascular system. *Nat. Genet.* 24, 171–4.
- Garg, V., Muth, A.N., Ransom, J.F., Schluterman, M.K., Barnes, R., King, I.N., Grossfeld, P.D., Srivastava, D., 2005. Mutations in NOTCH1 cause aortic valve disease. *Nature* 437, 270–4.
- Gillers, B.S., Chiplunkar, A., Aly, H., Valenta, T., Basler, K., Christoffels, V.M., Efimov, I.R., Boukens, B.J., Rentschler, S., 2015. Canonical wnt signaling regulates atrioventricular junction programming and electrophysiological properties. *Circ. Res.* 116, 398–406.
- Gise, A. von, Pu, W.T., 2012. Endocardial and epicardial epithelial to mesenchymal transitions in heart development and disease. *Circ. Res.* 110, 1628–45.
- Gitler, A.D., Lu, M.M., Jiang, Y.Q., Epstein, J.A., Gruber, P.J., 2003. Molecular markers of cardiac endocardial cushion development. *Dev. Dyn.* 228, 643–50.
- Hager-Theodorides, A.L., Outram, S.V., Shah, D.K., Sacedon, R., Shrimpton, R.E., Vicente, A., Varas, A., Crompton, T., 2002. Bone morphogenetic protein 2/4 signaling regulates early thymocyte differentiation. *J. Immunol.* 169, 5496–504.

- Harrelson, Z., Kelly, R.G., Goldin, S.N., Gibson-Brown, J.J., Bollag, R.J., Silver, L.M., Papaioannou, V.E., 2004. Tbx2 is essential for patterning the atrioventricular canal and for morphogenesis of the outflow tract during heart development. *Development* 131, 5041–52.
- Henderson, D.J., Copp, A.J., 1998. Versican expression is associated with chamber specification, septation, and valvulogenesis in the developing mouse heart. *Circ. Res.* 83, 523–32.
- Hinton, R.B., Lincoln, J., Deutsch, G.H., Osinska, H., Manning, P.B., Benson, D.W., Yutzey, K.E., 2006. Extracellular matrix remodeling and organization in developing and diseased aortic valves. *Circ. Res.* 98, 1431–8.
- Hoffman, J.I., 2013. The global burden of congenital heart disease. *Cardiovasc J Afr* 24, 141–5.
- Hurlstone, A.F., Haramis, A.-P.G.P., Wienholds, E., Begthel, H., Korving, J., Eeden, F. Van, Cuppen, E., Zivkovic, D., Plasterk, R.H., Clevers, H., 2003. The Wnt/beta-catenin pathway regulates cardiac valve formation. *Nature* 425, 633–7.
- Ishibashi, O., Inui, T., 2014. Identification of endoglin-dependent BMP-2-induced genes in the murine periodontal ligament cell line PDL-L2. *J Mol Signal* 9, 5.
- Jiao, K., Kulesa, H., Tompkins, K., Zhou, Y., Batts, L., Baldwin, H.S., Hogan, B.L., 2003. An essential role of Bmp4 in the atrioventricular septation of the mouse heart. *Genes Dev.* 17, 2362–7.
- Kashiwada, T., Fukuhara, S., Terai, K., Tanaka, T., Wakayama, Y., Ando, K., Nakajima, H., Fukui, H., Yuge, S., Saito, Y., Gemma, A., Mochizuki, N., 2015. β -Catenin-dependent transcription is central to Bmp-mediated formation of venous vessels. *Development* 142, 497–509.
- Keegan, B.R., Meyer, D., Yelon, D., 2004. Organization of cardiac chamber progenitors in the zebrafish blastula. *Development* 131, 3081–91.
- Kern, C.B., Norris, R.A., Thompson, R.P., Argraves, W.S., Fairey, S.E., Reyes, L., Hoffman, S., Markwald, R.R., Mjaatvedt, C.H., 2007. Versican proteolysis mediates myocardial regression during outflow tract development. *Dev. Dyn.* 236, 671–83.

- Kern, C.B., Twal, W.O., Mjaatvedt, C.H., Fairey, S.E., Toole, B.P., Iruela-Arispe, M.L., Argraves, W.S., 2006. Proteolytic cleavage of versican during cardiac cushion morphogenesis. *Dev. Dyn.* 235, 2238–47.
- Kim, R.Y., Robertson, E.J., Solloway, M.J., 2001. Bmp6 and Bmp7 are required for cushion formation and septation in the developing mouse heart. *Dev. Biol.* 235, 449–66.
- Kohda, D., Morton, C.J., Parkar, A.A., Hatanaka, H., Inagaki, F.M., Campbell, I.D., Day, A.J., 1996. Solution structure of the link module: a hyaluronan-binding domain involved in extracellular matrix stability and cell migration. *Cell* 86, 767–75.
- Kokubo, H., Tomita-Miyagawa, S., Hamada, Y., Saga, Y., 2007. Hesr1 and Hesr2 regulate atrioventricular boundary formation in the developing heart through the repression of Tbx2. *Development* 134, 747–55.
- Krug, E.L., Rezaee, M., Isokawa, K., Turner, D.K., Litke, L.L., Wunsch, A.M., Bain, J.L., Riley, D.A., Capehart, A.A., Markwald, R.R., 1995. Transformation of cardiac endothelium into cushion mesenchyme is dependent on ES/130: temporal, spatial, and functional studies in the early chick embryo. *Cell. Mol. Biol. Res.* 41, 263–77.
- Lange, F.J. de, Moorman, A.F., Anderson, R.H., Männer, J., Soufan, A.T., Gier-de Vries, C. de, Schneider, M.D., Webb, S., Hoff, M.J. van den, Christoffels, V.M., 2004. Lineage and morphogenetic analysis of the cardiac valves. *Circ. Res.* 95, 645–54.
- Lee, R.K., Stainier, D.Y., Weinstein, B.M., Fishman, M.C., 1994. Cardiovascular development in the zebrafish. II. Endocardial progenitors are sequestered within the heart field. *Development* 120, 3361–6.
- Liebner, S., Cattelino, A., Gallini, R., Rudini, N., Iurlaro, M., Piccolo, S., Dejana, E., 2004. Beta-catenin is required for endothelial-mesenchymal transformation during heart cushion development in the mouse. *J. Cell Biol.* 166, 359–67.
- Lincoln, J., Alfieri, C.M., Yutzey, K.E., 2004. Development of heart valve leaflets and supporting apparatus in chicken and mouse embryos. *Dev. Dyn.* 230, 239–50.
- Lockhart, M., Wirrig, E., Phelps, A., Wessels, A., 2011. Extracellular matrix and heart development. *Birth Defects Res. Part A Clin. Mol. Teratol.* 91, 535–50.

- Luna-Zurita, L., Prados, B., Grego-Bessa, J., Luxán, G., Monte, G. del, Benguría, A., Adams, R.H., Pérez-Pomares, J.M.M., Pompa, J.L.L. de la, 2010. Integration of a Notch-dependent mesenchymal gene program and Bmp2-driven cell invasiveness regulates murine cardiac valve formation. *J. Clin. Invest.* 120, 3493–507.
- Lyons, K.M., Pelton, R.W., Hogan, B.L., 1990. Organogenesis and pattern formation in the mouse: RNA distribution patterns suggest a role for bone morphogenetic protein-2A (BMP-2A). *Development* 109, 833–44.
- Ma, L., Lu, M.-F.F., Schwartz, R.J., Martin, J.F., 2005. Bmp2 is essential for cardiac cushion epithelial-mesenchymal transition and myocardial patterning. *Development* 132, 5601–11.
- MacGrogan, D., Luna-Zurita, L., Pompa, J.L.L. de la, 2011. Notch signaling in cardiac valve development and disease. *Birth Defects Res. Part A Clin. Mol. Teratol.* 91, 449–59.
- Martinsen, B.J., 2005. Reference guide to the stages of chick heart embryology. *Dev. Dyn.* 233, 1217–37.
- Massari, M.E., Murre, C., 2000. Helix-loop-helix proteins: regulators of transcription in eucaryotic organisms. *Mol. Cell. Biol.* 20, 429–40.
- McCulley, D.J., Kang, J.-O.O., Martin, J.F., Black, B.L., 2008. BMP4 is required in the anterior heart field and its derivatives for endocardial cushion remodeling, outflow tract septation, and semilunar valve development. *Dev. Dyn.* 237, 3200–9.
- Miyazono, K., Kamiya, Y., Morikawa, M., 2010. Bone morphogenetic protein receptors and signal transduction. *J. Biochem.* 147, 35–51.
- Mjaatvedt, C.H., Yamamura, H., Capehart, A.A., Turner, D., Markwald, R.R., 1998. The *Cspg2* gene, disrupted in the *hdf* mutant, is required for right cardiac chamber and endocardial cushion formation. *Dev. Biol.* 202, 56–66.
- Monte, G. Del, Grego-Bessa, J., González-Rajal, A., Bolós, V., La Pompa, J.L.L. De, 2007. Monitoring Notch1 activity in development: evidence for a feedback regulatory loop. *Dev. Dyn.* 236, 2594–614.
- Moorman, 2003. Development Of The Heart: (1) Formation Of The Cardiac Chambers And Arterial Trunks. *Heart* 89, 806–814.

- Moro, E., Ozhan-Kizil, G., Mongera, A., Beis, D., Wierzbicki, C., Young, R.M., Bournele, D., Domenichini, A., Valdivia, L.E., Lum, L., Chen, C., Amatruda, J.F., Tiso, N., Weidinger, G., Argenton, F., 2012. In vivo Wnt signaling tracing through a transgenic biosensor fish reveals novel activity domains. *Dev. Biol.* 366, 327–40.
- Moskowitz, I.P., Wang, J., Peterson, M.A., Pu, W.T., Mackinnon, A.C., Oxburgh, L., Chu, G.C., Sarkar, M., Berul, C., Smoot, L., Robertson, E.J., Schwartz, R., Seidman, J.G., Seidman, C.E., 2011. Transcription factor genes Smad4 and Gata4 cooperatively regulate cardiac valve development. [corrected]. *Proc. Natl. Acad. Sci. U.S.A.* 108, 4006–11.
- Murad, J.M., Place, C.S., Ran, C., Hekmatyar, S.K., Watson, N.P., Kauppinen, R.A., Israel, M.A., 2010. Inhibitor of DNA binding 4 (ID4) regulation of adipocyte differentiation and adipose tissue formation in mice. *J. Biol. Chem.* 285, 24164–73.
- Nakajima, Y., Yamagishi, T., Hokari, S., Nakamura, H., 2000. Mechanisms involved in valvuloseptal endocardial cushion formation in early cardiogenesis: roles of transforming growth factor (TGF)-beta and bone morphogenetic protein (BMP). *Anat. Rec.* 258, 119–27.
- Neely, M.D., Litt, M.J., Tidball, A.M., Li, G.G., Aboud, A.A., Hopkins, C.R., Chamberlin, R., Hong, C.C., Ess, K.C., Bowman, A.B., 2012. DMH1, a highly selective small molecule BMP inhibitor promotes neurogenesis of hiPSCs: comparison of PAX6 and SOX1 expression during neural induction. *ACS Chem Neurosci* 3, 482–91.
- Ninov, N., Borius, M., Stainier, D.Y., 2012. Different levels of Notch signaling regulate quiescence, renewal and differentiation in pancreatic endocrine progenitors. *Development* 139, 1557–67.
- Ober, E.A., Verkade, H., Field, H.A., Stainier, D.Y., 2006. Mesodermal Wnt2b signalling positively regulates liver specification. *Nature* 442, 688–91.
- Peal, D.S., Burns, C.G., Macrae, C.A., Milan, D., 2009. Chondroitin sulfate expression is required for cardiac atrioventricular canal formation. *Dev. Dyn.* 238, 3103–10.
- Person, A.D., Garriock, R.J., Krieg, P.A., Runyan, R.B., Klewer, S.E., 2005. Frzb modulates Wnt-9a-mediated beta-catenin signaling during avian atrioventricular cardiac cushion development. *Dev. Biol.* 278, 35–48.

- Plageman, T.F., Yutzey, K.E., 2004. Differential expression and function of Tbx5 and Tbx20 in cardiac development. *J. Biol. Chem.* 279, 19026–34.
- Ramachandra, C.J., Mehta, A., Guo, K.W., Wong, P., Tan, J.L., Shim, W., 2015. Molecular pathogenesis of Marfan syndrome. *Int. J. Cardiol.* 187, 585–91.
- Robinson, P.N., Booms, P., Katzke, S., Ladewig, M., Neumann, L., Palz, M., Pregla, R., Tiecke, F., Rosenberg, T., 2002. Mutations of FBN1 and genotype-phenotype correlations in Marfan syndrome and related fibrillinopathies. *Hum. Mutat.* 20, 153–61.
- Rosenthal, N., Harvey, R.P., 2010. Heart Development and Regeneration (Academic Press, San Diego)
- Scherz, P.J., Huisken, J., Sahai-Hernandez, P., Stainier, D.Y., 2008. High-speed imaging of developing heart valves reveals interplay of morphogenesis and function. *Development* 135, 1179–87.
- Schoen, F.J., 2008. Evolving concepts of cardiac valve dynamics: the continuum of development, functional structure, pathobiology, and tissue engineering. *Circulation* 118, 1864–80.
- Schoenebeck, J.J., Keegan, B.R., Yelon, D., 2007. Vessel and blood specification override cardiac potential in anterior mesoderm. *Dev. Cell* 13, 254–67.
- Schroeder, J.A., Jackson, L.F., Lee, D.C., Camenisch, T.D., 2003. Form and function of developing heart valves: coordination by extracellular matrix and growth factor signaling. *J. Mol. Med.* 81, 392–403.
- Sharma, P., Chinaranagari, S., Patel, D., Carey, J., Chaudhary, J., 2012. Epigenetic inactivation of inhibitor of differentiation 4 (Id4) correlates with prostate cancer. *Cancer Med* 1, 176–186.
- Sharma, P., Knowell, A.E., Chinaranagari, S., Komaragiri, S., Nagappan, P., Patel, D., Havrda, M.C., Chaudhary, J., 2013. Id4 deficiency attenuates prostate development and promotes PIN-like lesions by regulating androgen receptor activity and expression of NKX3.1 and PTEN. *Mol. Cancer* 12, 67.

- Shirai, M., Imanaka-Yoshida, K., Schneider, M.D., Schwartz, R.J., Morisaki, T., 2009. T-box 2, a mediator of Bmp-Smad signaling, induced hyaluronan synthase 2 and Tgfbeta2 expression and endocardial cushion formation. *Proc. Natl. Acad. Sci. U.S.A.* 106, 18604–9.
- Sinning, A.R., 1997. Partial purification of HLAMP-1 provides direct evidence for the multicomponent nature of the particulate matrix associated with cardiac mesenchyme formation. *J. Cell. Biochem.* 66, 112–22.
- Smith, K.A., Lagendijk, A.K., Courtney, A.D., Chen, H., Paterson, S., Hogan, B.M., Wicking, C., Bakkers, J., 2011. Transmembrane protein 2 (Tmem2) is required to regionally restrict atrioventricular canal boundary and endocardial cushion development. *Development* 138, 4193–8.
- Somi, S., Buffing, A.A., Moorman, A.F., Den Hoff, M.J. Van, 2004. Dynamic patterns of expression of BMP isoforms 2, 4, 5, 6, and 7 during chicken heart development. *Anat Rec A Discov Mol Cell Evol Biol* 279, 636–51.
- Song, L., Fässler, R., Mishina, Y., Jiao, K., Baldwin, H.S., 2007. Essential functions of Alk3 during AV cushion morphogenesis in mouse embryonic hearts. *Dev. Biol.* 301, 276–86.
- Srivastava, D., 2006. Making or breaking the heart: from lineage determination to morphogenesis. *Cell* 126, 1037–48.
- Stainier, D.Y., 2001. Zebrafish genetics and vertebrate heart formation. *Nat. Rev. Genet.* 2, 39–48.
- Stainier, D.Y., Lee, R.K., Fishman, M.C., 1993. Cardiovascular development in the zebrafish. I. Myocardial fate map and heart tube formation. *Development* 119, 31–40.
- Stainier, D.Y., Weinstein, B.M., Detrich, H.W., Zon, L.I., Fishman, M.C., 1995. Cloche, an early acting zebrafish gene, is required by both the endothelial and hematopoietic lineages. *Development* 121, 3141–50.
- Tartaglia, M., Gelb, B.D., 2005. Noonan syndrome and related disorders: genetics and pathogenesis. *Annu Rev Genomics Hum Genet* 6, 45–68.
- Tartaglia, M., Mehler, E.L., Goldberg, R., Zampino, G., Brunner, H.G., Kremer, H., Burgt, I., van der, Crosby, A.H., Ion, A., Jeffery, S., Kalidas, K., Patton, M.A., Kucherlapati, R.S.,

- Gelb, B.D., 2001. Mutations in PTPN11, encoding the protein tyrosine phosphatase SHP-2, cause Noonan syndrome. *Nat. Genet.* 29, 465–8.
- Thornton, T.M., Pedraza-Alva, G., Deng, B., Wood, C.D., Aronshtam, A., Clements, J.L., Sabio, G., Davis, R.J., Matthews, D.E., Doble, B., Rincon, M., 2008. Phosphorylation by p38 MAPK as an alternative pathway for GSK3beta inactivation. *Science* 320, 667–70.
- Timmerman, L.A., Grego-Bessa, J., Raya, A., Bertrán, E., Pérez-Pomares, J.M.M., Díez, J., Aranda, S., Palomo, S., McCormick, F., Izpisua-Belmonte, J.C., Pompa, J.L.L. de la, 2004. Notch promotes epithelial-mesenchymal transition during cardiac development and oncogenic transformation. *Genes Dev.* 18, 99–115.
- Tokuzawa, Y., Yagi, K., Yamashita, Y., Nakachi, Y., Nikaido, I., Bono, H., Ninomiya, Y., Kanesaki-Yatsuka, Y., Akita, M., Motegi, H., Wakana, S., Noda, T., Sablitzky, F., Arai, S., Kurokawa, R., Fukuda, T., Katagiri, T., Schönbach, C., Suda, T., Mizuno, Y., Okazaki, Y., 2010. Id4, a new candidate gene for senile osteoporosis, acts as a molecular switch promoting osteoblast differentiation. *PLoS Genet.* 6, e1001019.
- Verhoeven, M.C., Haase, C., Christoffels, V.M., Weidinger, G., Bakkers, J., 2011. Wnt signaling regulates atrioventricular canal formation upstream of BMP and Tbx2. *Birth Defects Res. Part A Clin. Mol. Teratol.* 91, 435–40.
- Walsh, E.C., Stainier, D.Y., 2001. UDP-glucose dehydrogenase required for cardiac valve formation in zebrafish. *Science* 293, 1670–3.
- Wang, J., Sridurongrit, S., Dudas, M., Thomas, P., Nagy, A., Schneider, M.D., Epstein, J.A., Kaartinen, V., 2005. Atrioventricular cushion transformation is mediated by ALK2 in the developing mouse heart. *Dev. Biol.* 286, 299–310.
- Wang, Y., Wu, B., Chamberlain, A., Lui, W., Koirala, P., Susztak, K., Klein, D., Taylor, V., Zhou, B., 2013. Endocardial to Myocardial Notch-Wnt-Bmp Axis Regulates Early Heart Valve Development. *PLoS ONE* 8.
- Westerfield, M., 2000. *The Zebrafish Book*. A Guide for the Laboratory Use of Zebrafish (*Danio rerio*), 4th Edition. University of Oregon Press, Eugene
- Wight, T.N., 2002. Versican: a versatile extracellular matrix proteoglycan in cell biology. *Curr. Opin. Cell Biol.* 14, 617–23.

- Wiley, D.M., Kim, J.-D.D., Hao, J., Hong, C.C., Bautch, V.L., Jin, S.-W.W., 2011. Distinct signalling pathways regulate sprouting angiogenesis from the dorsal aorta and the axial vein. *Nat. Cell Biol.* 13, 686–92.
- Yamagishi, T., Ando, K., Nakamura, H., 2009. Roles of TGFbeta and BMP during valvulo-septal endocardial cushion formation. *Anat Sci Int* 84, 77–87.
- Yelon, D., 2001. Cardiac patterning and morphogenesis in zebrafish. *Dev. Dyn.* 222, 552–63.
- Yelon, D., Horne, S.A., Stainier, D.Y., 1999. Restricted expression of cardiac myosin genes reveals regulated aspects of heart tube assembly in zebrafish. *Dev. Biol.* 214, 23–37.
- Yelon, D., Ticho, B., Halpern, M.E., Ruvinsky, I., Ho, R.K., Silver, L.M., Stainier, D.Y., 2000. The bHLH transcription factor *hand2* plays parallel roles in zebrafish heart and pectoral fin development. *Development* 127, 2573–82.
- Yun, K., Mantani, A., Garel, S., Rubenstein, J., Israel, M., 2004. *Id4* regulates neural progenitor proliferation and differentiation in vivo. *Development* 131, 5441–5448.
- Zhou, B., Ma, Q., Rajagopal, S., Wu, S.M., Domian, I., Rivera-Feliciano, J., Jiang, D., Gise, A. von, Ikeda, S., Chien, K.R., Pu, W.T., 2008. Epicardial progenitors contribute to the cardiomyocyte lineage in the developing heart. *Nature* 454, 109–13.

ACKNOWLEDGEMENTS

I would like to take this opportunity to thank all my colleagues and friends whose contribution has been immense during the course of my Ph.D.

I take the honor to thank Prof. Dr. Didier Stainier for giving me the opportunity to pursue Ph.D. in his laboratory. I highly regard his constant guidance and critical suggestions that channelized my work in the correct direction.

I would like to extend warm regards to Dr. Sven Reischauer for direct supervision. I would like to thank him for his honest feedbacks, constant support and encouragement during my Ph.D project.

I would like to express my gratitude to my colleagues and friends for their help, invaluable inputs and sharing happy moments in and outside the lab: Raoul Freitas, Chinmoy Patra, Almary Guerra, Ayele Taddese, Vanesa Jimenez, Sophie Ramas, Claudia Carlantoni, Javad Rasouli, Ziba Jaberansari, Jenny Pestel, Claudia Gerri, Michele Marass, Pourya Sarvari, Brijesh Kumar, Sri Teja Mullapudi, Jason Lai, Filomena Ricciardi, Anoop Cherian, Sabine Fischer, Radhan Ramadass, Hans-Martin Maischein, Nana Fukuda, Ryuichi Fukuda, Hyun-Taek Kim, Sharon Meaney-Gardian and in particular Deepika Dogra.

I am also grateful to Dr. Benno Jungblut for teaching me the basic concepts and fundamentals of all the zebrafish work that I have learned till date.

Finally, I would like to thank my family who has always stood beside me through thick and thin and always motivated me to move ahead in life.

Curriculum Vitae

Suchit Ahuja

Liebigstr.12, 61231 Bad Nauheim, Germany
+49-17661385781, suchit.ahuja@mpi-bn.mpg.de, suchitahuja1987@gmail.com

Personal Details

Place of Birth New Delhi, India

Date of Birth 30 June 1987

Languages

Full Proficiency English, Hindi

Limited Proficiency German

Education

Early 2016
(Expected) **PhD, Developmental Genetics**
Laboratory of Prof. Didier Stainier
Max Planck Institute for Heart and Lung Research, Bad Nauheim
Germany.

June 2011 **B.Tech-M.Tech (Biotechnology), 81%**
Jaypee Institute of Information Technology University, NOIDA, India.

Research Experience

05/2013-12/2015 PhD, Developmental Genetics
Max Planck Institute for Heart and Lung Research, Germany

- Studied Atrio-Ventricular Canal / Heart Development in great detail.
- Created several mutants using TALEN and CRISPR/CAS technology.
- Characterized Heart Valve Developmental disorders in '*id4*' loss-of-function mutant by high resolution Spinning Disc/Confocal microscopy, genetic overexpression studies and spatiotemporal expression analysis of AV Canal marker genes by in situ hybridization.

11/2011-04/2013 Research Fellow, Laterality cues guiding Heart Development using Zebrafish
Laboratory of Dr. Benno Jungblut
Max Planck Institute for Heart and Lung Research, Germany

- Studied various developmental events contributing to the asymmetric organ placement in vertebrates.
- Characterized the role of enzyme soluble epoxide hydrolase in maintaining heart laterality by studying its loss-of-function morphant using high resolution confocal microscopy, biochemical assays and various chemical treatments.

07/2010-06/2011

M.Tech Thesis

Jaypee Institute of Information Technology University, NOIDA, India

- Studied the effect of oxidative stress induced cardiac hypertrophy in H9C2 cardiac cell line by various molecular biology and biochemistry assays.

07/2009-06/2010

B.Tech Thesis

Jaypee Institute of Information Technology University, NOIDA, India

- Characterized various molecular events underlying norepinephrine induced cardiac hypertrophy by different molecular biology techniques and potential of curcumin in circumventing induction of hypertrophy.

06/2009-07/2009

Summer Internship

Indian Institute of Integrative Medicine, Jammu, India

- Evaluated different synthetic compounds for their anti-cancer potential on various cancer cell lines by studying cell apoptosis markers.

Technical Skills

- **High Resolution Microscopy** Confocal (LSM 700, LSM 780, LSM 800), Spinning Disk
- **In Vivo Genetic Manipulations** Mutagenesis : TALEN, CRISPR/CAS9, Morpholino Knockdowns, Tissue Specific gene overexpression, Transgenic animal generation
- **Spatio-Temporal Gene Expression Analysis** In situ Hybridization (Chromogenic and Fluorescent)
- **Molecular Biology** RT-PCR, qPCR, Molecular Cloning, Plasmid Isolation
- **Biochemistry** Western Blot, Immunohistochemistry

- **Zebrafish Injections** Embryo Microinjections, Adult I.P injections
- **Image Processing** ImageJ, Imaris, Adobe Photoshop, Adobe Illustrator
- **Data Analysis and Statistics** Graph Pad Prism, MS Excel, Online Bioinformatics tools

Achievements and Certifications

- Certificate course on Laboratory Animals according to FELASA (Federation of European Laboratory Animal Science Associations) conducted by IMPRS-HLR. (Nov 2014).
- Accomplished the graduate program of International Max Planck Research School for Heart and Lung Research (IMPRS-HLR) that comprised of lecture series, methods seminars, soft skills, progress reports and annual retreats (Nov 2014).
- Awarded International Max Planck Research School Fellowship (Nov 2011).
- Secured 2nd position in Technical Paper Presentation at cognizance, technical fest of Indian Institute of Technology, Roorkee on the topic “Cardio-protective properties of curcumin in reversal of hypertrophy”. (March 2010).

Publications

- **Ahuja S**, Dogra D, Stainier DY, Reischauer S. Id4 functions downstream of Bmp signaling to restrict TCF function in endocardial cells during atrioventricular valve development. *Dev. Biol.* 2016; 412(1): 71-82.
- **Ahuja S**, Kohli S, Krishnan S, Dogra D, Sharma D, Rani V. Curcumin: a potential therapeutic polyphenol, prevents noradrenaline-induced hypertrophy in rat cardiac myocytes. *Journal Pharmacy and Pharmacology.* 2011 Dec;63(12):1604-12.
- Kohli S, **Ahuja S**, Rani V. Transcription factors in heart: promising therapeutic targets in cardiac hypertrophy. *Current Cardiology Reviews.* 2011 Nov;7(4):262-71.
- Shrey K, **Suchit A**, Deepika D, Shruti K, Vibha R. Air pollutants: The key stages in the pathway towards the development of cardiovascular disorders. *Environmental Toxicology Pharmacology.* 2011 Jan;31(1):1-9
- Shrey K, **Suchit A**, Nishant M, Vibha R. RNA interference: Emerging diagnostics and therapeutics tool. *Biochemical and Biophysical Research Communications.* 2009 Aug 21;386(2):273-7.

